USE OF POLYMERIC MICROFILTRATION MEMBRANES TO REMOVE MICROORGANISMS AND ORGANIC POLLUTANTS FROM PRIMARY SEWAGE EFFLUENT

by

Claude Moeng Modise

BS in Civil Engineering, University of Southern California, 1998

Submitted to the Graduate Faculty of

The School of Engineering in partial fulfillment

of the requirements for the degree of

Masters of Science in Civil Engineering

University of Pittsburgh

2003

UNIVERSITY OF PITTSBURGH

SCHOOL OF ENGINEERING

This thesis was presented

by

Claude Moeng Modise

It was defended on

April 14, 2003

and approved by

Radisav D. Vidic, Ph.D., Associate Professor
Department of Civil and Environmental Engineering

Leonard W. Casson, Ph.D., Associate Professor
Department Civil and Environmental Engineering

Thesis Advisor, Ronald D. Neufeld, Ph.D., Professor
Department Civil and Environmental Engineering

ABSTRACT

USE OF POLYMERIC MICROFILTRATION MEMBRANES TO REMOVE MICROORGANISMS AND ORGANIC POLLUTANTS FROM PRIMARY SEWAGE EFFLUENT

Claude Moeng Modise, MS

University of Pittsburgh, 2003

Combined Sewers are designed in such a way that when their design capacity is exceeded excess water from the sewers is diverted to the rivers and streams resulting in combined sewer overflow (CSO). Now, with increased Environmental Protection Agency (EPA) monitoring and stringent new river water standards, the City of Pittsburgh finds itself having to come up with measures to combat the CSO problem. One approach investigated in this research is to capture the CSO water, treat it using polymeric microfiltration membranes, send the permeate to the nearby rivers and streams while the concentrated retentate is directed back to the Wastewater Treatment Plant.

Seven polymeric microfiltration membranes ranging in size from 0.2 μm to 0.8 μm were obtained from membrane manufacturers (e.g Osmonic, PALL and Millipore) and were tested for their effectiveness in treating the combined sewer overflow. Primary effluent wastewater from Allegheny County Sanitation Authority (ALCOSAN) Wastewater Treatment Plant (WWTP) with COD values of less than 100 mg/l was assumed to resemble combined sewer overflow pretreated by a swirl separator and was used in the filtration runs. A particular membrane's effectiveness to treat CSO was measured for its ability to reduce fecal coliforms, *Escherichia coli* and *enterococci* bacteria to levels recommended by EPA. Reduction of chemical oxygen

demand and flux rate for different membranes were also investigated. Effect of membrane surface chemistry on the flux rate and on the permeate quality were investigated.

The results show that flux is proportional to pore size for membranes of the same material and same surface chemistry. Hydrophilic membranes gave higher initial flux rate than hydrophobic membranes of the same pore sizes. The steady state flux rates were about the same at all pressures and pore sizes, indicating that at steady state fouling becomes the only variable that controls flux. The membranes with pore size 0.45 μm and below were able to reduce the bacteria levels to low detection limits except for the one membrane with pore size of 0.3 μm. The membranes had varying COD removal efficiency. The results show that polymeric microfiltration membranes can be used to treat combined sewer overflow.

ACKNOWLEDGEMENTS

I am grateful to my sponsor Fraunhofer Center for Energy and Environment for their financial support and provision of equipment, without, this work could not have been undertaken. I would also like to earnestly thank my advisors Dr. Ronald D. Neufeld and Dr. Radisav D. Vidic of the University of Pittsburgh. Their insightful input and dedication has challenged and helped me see this research come to completion.

And last, but not least my heartfelt thanks goes to my wife, Samkelo Modise, without whose support and encouragement this work would not have been possible.

TABLE OF CONTENTS

LIST OF TABLES

LIST OF FIGURES

1.0 INTRODUCTION AND OVERVIEW

Combined Sewers Systems (CSS) are sewer systems designed to transport domestic sewage, industrial wastewater, and storm water to a wastewater treatment plant through a single pipe (US EPA, 2001). During heavy rainfalls or snowmelt, the water flow is too great for the combined sewer system to handle. When flooding occurs, the sewer system is designed to send excess water to nearby streams, rivers, lakes, or other surface water locations resulting in combined sewer overflow (CSO) (US EPA, 2001). The discharge of the excess water into rivers and streams pollutes the receiving waters. Some of the pollutants in the combined sewer overflow include pathogens, oxygen demanding pollutants, suspended material, toxins and floatable matter (US EPA, 1994). Material presence in water compromises the required water standards in the rivers and streams and may pose health hazards both to animals and human life, which calls for the abatement of pollutants from the combined sewer overflow water (US EPA, 1994).

The CSO Control Policy, issued by EPA on April 11, 1994, established a national approach to the control of CSO discharges under the National Pollutant Discharge Elimination System (NPDES). Further regulatory response came in May 1995 with the release of the 'Combined Sewer Overflows – Guidance for Nine Minimum Controls,' and May 9, 2000 with the 'Draft – Guidance on Implementing the Water Quality-Based Provisions on the CSO Control Policy' (US EPA, 2001). The pending regulations forced the municipalities to find a feasible alternative for CSO control.

Several CSO control technologies can be employed to bring about desired water quality standards. The technologies include controlling the CSO at the source by building porous pavements to increase infiltration, separation of sewers, building of storage tanks, capturing and

disinfecting the CSO before releasing it (Metcalf & Eddy, 2003). CSO can also be treated to reuse standards by conventional methods such as biological treatment followed by coagulation, flocculation, clarification, multimedia filtration, ion exchange, etc. (Metcalf & Eddy, 2003). With the growing awareness of membrane technology and the reduction in the costs of membranes, membrane technology may become a viable option in treating CSO (Parameshwaran et al., 2001). Membrane filtration has a number of advantages over conventional biological processes (e.g reduced or removal of pathogens, suspended solids and organic and inorganic pollutants (Gan, 1994)).

This study was conducted to evaluate the applicability of microfiltration in treating municipal wastewater or CSO to levels where the treated water can be safely disposed of into the nearby rivers and streams. The wastewater would have to go through a swirl separator first to remove grit and big pieces of material before taking it through microfiltration. The experiments discussed herein investigate the performance of commercial polymeric membranes on the removal of substances measured as chemical oxygen demand, fecal coliforms, *Escherichia coli* and *enterococci*. The importance of the membrane physical parameters, membrane pore size and its effects on the flux performance and solids retention efficiency is investigated.

1.1 CSO Occurrences, Regulations and Standards

1.1.1 Occurrences

Figure 1 below shows regions were CSO events occur. There are 772 CSO communities with a total of 971 CSOs that are regulated by National Pollutant Discharge Elimination System (NPDES) (US EPA 2001). Combined Sewer Systems are found in 32 States and these are mostly concentrated in the North East and Great Lakes region (US EPA 2001).

Figure 1 Places where CSO events occurs (From US EPA 2001)

1.1.2 Pollutants

CSO contains several possible pollutants, including bacteria, viruses, suspended matter, solids, metals and organic pollutants. Concentrations of key pollutants from various sources are compared in Table 1 below.

Table 1 Comparison between typical pollutant concentrations in CSO and other sources (From US EPA 2001).

Contaminant Source	BOD5, mg/L	TSS, mg/L	Total N, mg/L	Total P	Fecal Coliforms, cts/100ml
Untreated Domestic Wastewater	100 – 400	100 – 350	20 – 85	4 - 15	10^7 - 10^9
Treated Wastewater-Secondary	<5 – 30	<5 – 30	15 – 25	<1 - 5	<200
Urban Runoff	10 – 250	67 – 101	0.4 - 1.0	0.7 - 1.7	10^3 - 10^7
CSO	25 – 100	150 – 400	3 – 24	1 - 10	10^5 - 10^7

The choice of a filtration process to be used is based on the size of the bacteria to be removed. Fecal coliforms, *Escherichia coli* and *enterococci* are used as indicator organism for pathogenic bacteria. Certain strain of *Escherichia coli* in wastewater can cause gastroenteritis disease thus, warranting the need to come up with water standards and regulations which will guide in curbing these pathogenic bacteria from water. These bacteria have different sizes with *Escherichia coli* having a size of 0.6-1.2 μm in width and 2-3 μm in length while *enterococci* are spherical and are about 0.5 to 4 μm in diameter (Metcalf & Eddy, 2003), therefore they fall within the rage of microfiltration pore sizes.

1.1.3 Standards and Regulations

The Environmental Protection Agency's CSO Control Policy of 1994 has provisions for developing appropriate site-specific NPDES requirements for all CSOs and requires the development of the Long Term Control Policy (LTCP). Different States that have CSO events are also supposed to develop these LTCPs to meet water quality standards. These States are supposed to revise their water quality standards to show the difficulty in achieving compliance with the current bacterial standards during wet weather (US EPA 1986). The EPA proposed new bacterial stream standards because the current standards are not adequately protecting of human life (Slack et al., 2000). These new standards are summarized in the Table 2 below.

Table 2 Summary of EPA-Recommended Bacteria criteria (From Slack et al., 2000)

	Steady State, 30-day Geometric Mean Indicator* Density (cfu/100ml)	Single Sample Maximum(cfu/100ml)			
		Designated Beach Area	Moderate Full Body Contact Recreation	Lightly Used Full Body Contact Recreation	Infrequently Used Full Body Contact Recreation
Freshwater					
Enterococci	33	61	89	108	151
E.Coli	126	235	298	406	576
Marine Water					
Enterococci	35	104	124	276	500

*Minimun of 5 samples per month

The EPA expects all states to adopt these new bacterial standards by 2003. The new criteria are based on EPA's Ambient Water Quality Criteria for Bacteria (1986), which

recommend using *Escherichia coli* and *Enterococci* as indicators for primary contact recreation (Slack et al., 2000).

Currently, there are two different water quality standards available in the state of Pennsylvania to measure the effectiveness of membrane filtration. Those standards are effluent limitations of the local wastewater treatment plant and the standards for swimming in the waters that the treated CSO will be discharged to. ALCOSAN discharges treated sewage to the Ohio River. The water discharged to the river is regulated under the NPDES Permit PA 0025984. The effluent limitations stated within that permit under Pennsylvania Code 27 Pa.B. 4360 are provided in Table 3 below:

Table 3 The effluent limitations for ALCOSAN Wastewater Treatment Plant

ALCOSAN	Average	Average
PERMIT PA 0025984	Monthly	Weekly
Discharge Parameter	Minimum	mg/L
CBOD5		
(May 1 to Oct. 31)	20	30
(Nov. 1 to Apr. 30)	25	37.5
Suspended Solids	30	45
Ammonia Nitrogen		
(May 1 to Oct. 31)	9	13.5
(Nov. 1 to Apr. 30)	25	37.5
Heptachlor Epoxide	monitor and report	
Total Resiudal Chlorine	0.5	
Fecal Coliform		
(May 1 to Oct. 31)	200/100 mL as a geometric mean	
(Nov. 1 to Apr. 30)	2,000/100 mL as a geometric mean	
Dissolved Oxygen	minimum daily average 5 mg/L, minimum 4 mg/L at ar	
pH (S.U)	not less than 6.0 nor greater than 9.0	

In addition to the limits imposed by the ALCOSAN permit, Pennsylvania water quality standards exist for public swimming and bathing places. The Pennsylvania Department of Health regulates the water quality for swimming under Title 28, Chapter 18, Part 28 of the Pennsylvania Code. The water in the bathing beaches will be considered contaminated for bathing purposes when the fecal coliforms density of a sample collected at a bathing beach exceeds 1,000 per 100 milliliters and when the fecal coliforms density in at least five consecutive samples of the water taken over not more than a 30-day period exceeds a geometric mean of 200 per 100 milliliters.

To strike a balance in treating the CSO water using polymeric membranes both the EPA bacteria criteria in Table 2, the Pennsylvania Code 27 Pa.B 4360 standards in Table 3 and the Pennsylvania water quality standards for public swimming and bathing places need to be considered.

1.2 Membrane History

The history of membrane development covers the development of polymeric membranes and ceramic membranes. Membrane development and research dates back to 1748 when Abbe Nolet described the permeation of water through a diaphragm as osmosis. Bladders of pigs, cattle or fish and sausage casings were used by early membrane investigators. A technique to prepare nitrocellulose (collodion) membranes of graded size was devised by Bechold in 1907. This technique was developed further and by the early 1930s microporous collodion membranes were commercially available and in the following 20 years microfiltration membrane technology was expanded to other polymers such as cellulose acetate. Although the elements of modern membrane science had been developed by 1960, the use of membranes was restricted to

laboratory and small specialized laboratories. Industrial usage of membranes came into effect by the 1980s and microfiltration, ultrafiltration, reverse osmosis and electrodialyses became established processes and were used in large plants. Nowadays membranes are extensively used in desalination plants, food-processing plants and in the medical field (Baker, 2000).

1.3 Description of Membrane Materials

Membranes are selective and permeable structures which let some substances or molecules pass through while preventing others from passing through. A membrane can either be thick or thin with a heterogeneous structure. The transport of substances across the membrane can be due to pressure, electric current, and concentration or a temperature difference (Baker, 2000).

Membranes can be classified as biological and synthetic. Synthetic membranes can be divided into organic membranes, (e.g. polymeric or liquid), and inorganic membranes (e.g ceramic or metal membranes). Synthetic membranes can be made from different kinds of materials of which polymers and ceramics are the most important. Synthetic polymeric membranes can be divided into hydrophobic and hydrophilic classifications. Membranes can also be classified by their structure. Structural classification is very important because it is the structure which determines separation mechanisms and membrane application. Membranes can be further classified as symmetric or asymmetric as shown in Figure 2. The symmetric membranes can be porous, cylindrical porous and homogeneous (non porous). The asymmetric membranes can be 1) porous, 2) porous with top layer and 3) composite that is consisting of a porous membrane part and a dense top layer. The top layer in asymmetric membranes is 0.1 to

0.5 µm and is supported on a porous sub layer with a thickness of about 50 to 150 µm. In composite membranes, the top layer and sub layer originate from different polymeric materials. The support layer is already an asymmetric membrane on which a thin dense layer is deposited. The asymmetric membrane gives high permeate flow due to the very thin selective top layer and a reasonable mechanical stability, resulting from the underlying porous structure (Baker, 2000 and Nenes et al, 2001).

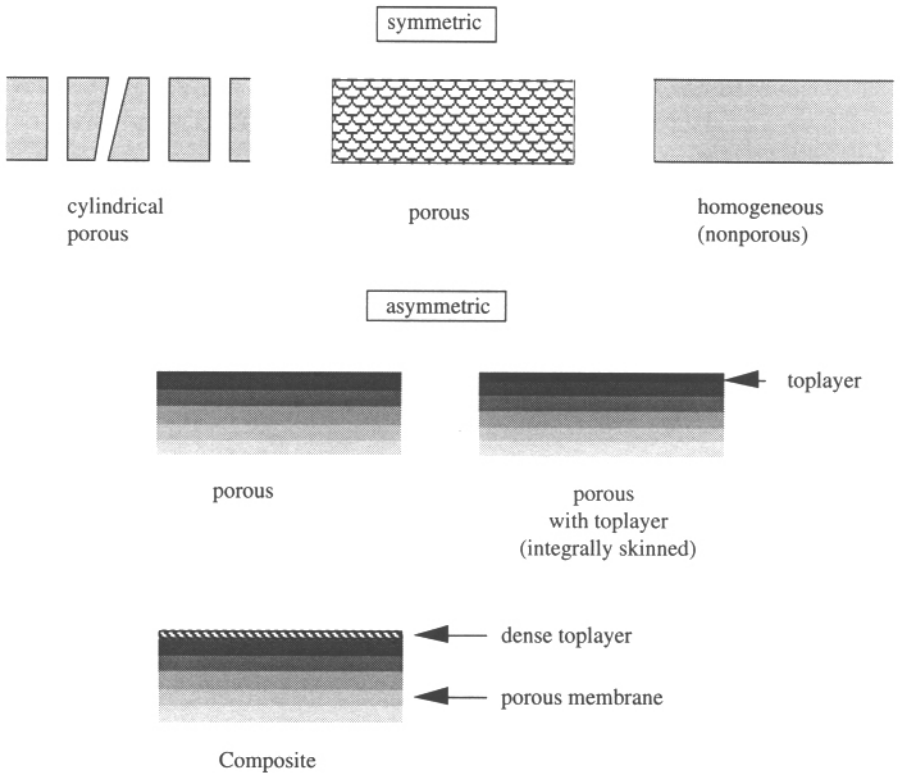

Figure 2 Schematic representation of various membrane cross-sections (From Mulder, 1991).

Various polymers and other organic materials can be used to yield hydrophobic and hydrophilic surface. Hydrophobic polymeric membranes can be made of Poly tetrafluoro ethylene (PTFE,Teflon), Poly Vinylidene fluoride (PVDF), Poly propylene (PP) and Poly ethylene(PE). Hydrophilic polymeric membranes can be made of Cellulose esters, Poly carbonate (PC), Poly sulfone/Poly (ether sulfone)(Psf/PES), Polyimide/Poly(ether imide)(PI/PEI), (aliphatic) Poly amide(PA) and Poly etherether ketone (PEEK) (Mulder, 1991).

Table 4 below lists the types of filtration processes commonly employed in practice together with typical pore sizes and operating pressures (All the processes are pressure driven).

Table 4 Types of processes, the pore size range and recommended operating pressures (From Mulder, 1991)

Process	Pore size (μm)	Transmembrane Pressure	
		Bar	psi
Reverse Osmosis	< 0.002	10 -100	145-1450
Nanofiltration	< 0.002	5.0 - 20	72.5-290
Ultrafiltration	0.001 - 0.1	1.0 – 5.0	14.5-72.5
Microfiltration	0.05 – 10	0.1 – 2.0	1.45-29

1.4 Membrane Transport Mechanisms

Membranes provide absolute barrier to particles greater than their pore size. A membrane process requires two bulk phases physically separated by a third phase, the membrane (Figure 3). The membrane phase interposed between the two-bulk phases controls the exchange of mass between the two bulk phases in a membrane process. The process allows the selective

and controlled transfer of a certain species from one bulk phase to another bulk phase separated by the membrane (Mulder, 1991).

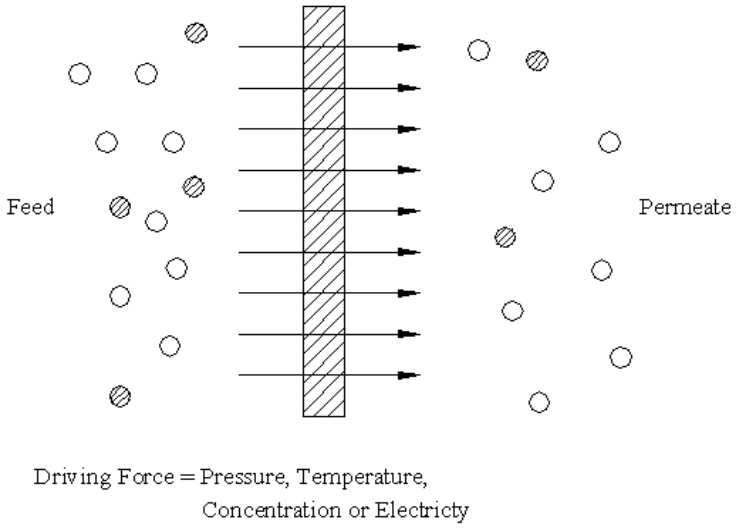

Figure 3 Schematic representation of the different phases in membrane separation

1.5 Fouling of Membranes

The resistance to mass transfer across the membrane is a resultant of the membrane and due to the layer of material that builds up on the membrane surface and inside the membrane. The buildup layer and the clogging of the pores are referred to as a fouling layer. Fouling is caused by the deposition of suspended solids and colloids, organic and inorganic foulants and biological foulants inside and on the membrane. The extent to which the membrane fouls depends on the

type of membrane and the concentration of contaminants in the feed water (Ho et al, 1992). The total resistance to flux depicted in Figure 4 is caused by several factors:

a) Membrane resistance, R_m. Membrane resistance depends on the membrane thickness, nominal pore size, pore density/porosity, pore size distribution, pore depth and tortuosity (Ho et al, 1992).
b) Resistance due to internal colloidal fouling, R_a.
c) Resistance due to the formation of highly concentrated layer adjacent to the membrane, concentration polarization, R_{cp}. "Concentration polarization is the accumulation, at the upstream surface of the membrane, of solute molecules which are rejected or retained by the course of ultra- and microfiltration." (Al –Malack et al, 1997).
d) Resistance due to the formation of the gel layer, R_g due to the increasing concentration of particles near the surface of the membrane (Al –Malack et al, 1997).
e) Resistance due to pore-blocking, R_p.

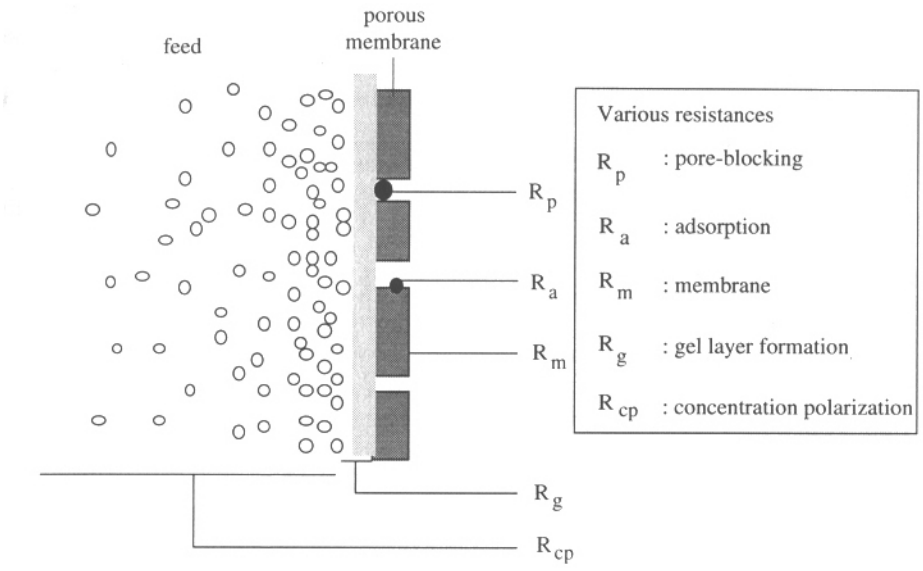

Figure 4 Overview of various types of resistance towards mass transport across a membrane in pressure driven processes (From Mulder, 1991).

Membrane resistance, ($R_m = R_{m\,(initial)} + R_a + R_p$), may increase with time since R_a and R_p increase with time of filtration run. Resistance due to cake is given by $R_c = R_{cp} + R_g$. Total resistance, ($R_t = R_m + R_c$), changes with time of the filtration run. The longer the membrane is run, the harder it is to transfer mass across the membrane. Backwashing can be used to remove the foulants and hence increase the filtration run. However, foulants can undergo irreversible changes to form cohesive solid which is more difficult to remove. Cardew notes that concentration polarization forms quickly and it is a reversible process, while gel polarization is associated with slow irreversible changes and thus contributing to more permanent fouling (Cardew et al., 1998).

1.6 Theory of Membrane Transport

Darcy's Law

When the sieving mechanism of microfiltration is dominant, a cake layer of rejected particles usually forms on the membrane surface. Darcy's law can be used to describe the pressure driven permeate flux through the cake layer and the membrane (Ho et al., 1992):

$J = (dV/dt)1/A_m = \Delta P/(\eta(R_t))$ ……..……(1)

Where, J = volumetric flux ($L/m^2 \cdot hr$)

A_m = Area of the membrane (m^2)

V = volume of the permeate (L)

t = time(s)

ΔP = change in pressure across the cake and the membrane (bar)

η = viscosity of the liquid ($N.s/m^2$)

R_t = total resistance ($1/m$) = $R_m + R_c$ …….(2)

R_m = membrane resistance

R_c = cake resistance

Membrane fouling and compaction can cause membrane resistance to increase with time. Cake resistance increases with time due to cake build up and compaction (Ho et al., 1992).

1.6.1 Transport Equations and Formation of Resistance

The flow of water through membranes can be modeled using empirical equations. The Hagen-Poiseuille or Carman-Kozeny models can be used to demonstrate this flow of water. The use of these equations depends on the shapes and sizes of the pores.

a) Hagen Poiseuille equation

The Hagen-Poiseuille equation considers that the membrane has a number of parallel cylindrical pores, which are parallel or oblique to the membrane surface. It assumes that the capillaries are uniform and clydrical.

Flux is given by,

$J = (\varepsilon_m r^2/8\eta\tau)\Delta P/\Delta X_m$ …….. (3)

Where, J = flux ($L/m^2 \cdot hr$)

ΔP = pressure difference (N/m^2)

ΔX_m = membrane thickness (m)

η = viscosity of the liquid ($N.s/m^2$)

ε_m = surface porosity = membrane void volume/total volume

$= (n_p.\pi.\ \Delta X_m.d_m^2/4)/\ (\Delta X_m.A_m)$

$= (n_p.\pi.\ d_m^2/4)/\ (A_m)$……..…….(4)

n_p = number of pores

d_m = diameter of the pores (μm)

τ = pore tortuosity (for cylindrical perpendicular pores, $\tau = 1$)

A_m = membrane area (m^2)

Membrane resistance can be determined as follows

$J = (n_p\pi (d_m/4)^2/8\Delta X_m A_m)\Delta P/\eta$, $(\tau = 1)$ ……..……(5)

$= 1/R_m(\Delta P/\eta)$

Assuming that there is no cake build up membrane resistance is

$R_m(1/ft) = 8\Delta x A_m/n_p\pi r^4$……....(6)

The equation indicates that membrane resistance is proportional to the thickness of the membrane and inversely proportional to the number of pores and the pore size to the fourth power (Ho et al., 1992).

b) Carman-Kozeny equation

For membranes which consist of closely packed spheres the flux through the membrane follows Kozeny-Carman equation.

Flux is given by,

$J = \varepsilon_m^3/(K\Delta X_m S_m^2(1-\varepsilon_m)^2)\Delta P/\eta$…….(7)

J = flux ($L/m^2 \cdot hr$)

S_m = pore internal surface area/unit volume (for cylindrical pores) (1/m)

$= 2\pi n_p d_m/A_m(1-\varepsilon)$……..…….(8)

K = Carman – Kozeny constant

ε_m = surface porosity

Membrane resistance is given by,

$R_m = K(1-\varepsilon_m)^2 S^2{}_m \Delta X_m/\varepsilon^3{}_m$ ……(9)

Where K = 2 for cylindrical pores. For other membranes K varies with membrane morphology and pore structure (Ho et al., 1992).

Cake Resistance can be estimated as follows:

For an incompressible cake the porosity and resistance are independent of the imposed pressure (Baker, 2000). Carman-Kozeny equation can be used to estimate cake resistance.

$R_c = K(1-\varepsilon_c)^2 S^2_c \Delta X_c / \varepsilon^3_c$ ……...(10)

ΔX_c = cake thickness (m)

S_c = solids surface area/unit volume of solids in the cake (1/m)

ε_c = void fraction of the cake

For rigid spherical particles of diameter, d_p, the specific surface area is $S_c = 6/\psi d_p$ (ψ=1), the void fraction, ε_c, of a randomly packed cake is approximately 0.4 and the constant K is reported to have a value of 5.0 (Ho et al., 1992).

1.7 Types of Filtration Processes

The membrane filtration process can be carried out in two types of configurations: dead-end and crossflow.

1.7.1 Dead-End

The dead-end filtration is whereby the water flow is perpendicular to the membrane surface as shown in Figure 5a. The water is pushed through the membrane by pressure. All the water that is introduced in the dead-end cell passes through as the permeate, in other words there is no rejected water. In dead-end filtration, the retained particles build up with time on the membrane surface (surface sieving) or within the membrane (depth sieving). In either case, the

particle buildup results in an increased resistance to filtration and causes the permeate flux to decline. As a result, the dead-end filtration method requires the stopping of filtration in order to clean or replace the membrane. As such, dead-end filtration is a batch operation (Ho et al., 1992).

There are two types of filtration, which can be employed in a dead-end cell; dead-end microfiltration with constant flux and dead end microfiltration with constant pressure drop. The dead end microfiltration with constant flux ensures that the permeate flux through the filter remains constant at its initial value. This filtration can be achieved by using a positive-displacement pump. As the cake build-up increases with time, the pressure drop must increase with time to maintain the constant flux. This increase in pressure ensures that the total permeate volume increases linearly with time. In dead end microfiltration with constant pressure drop, as the cake builds up with time the permeate flux decreases (Ho et al., 1992).

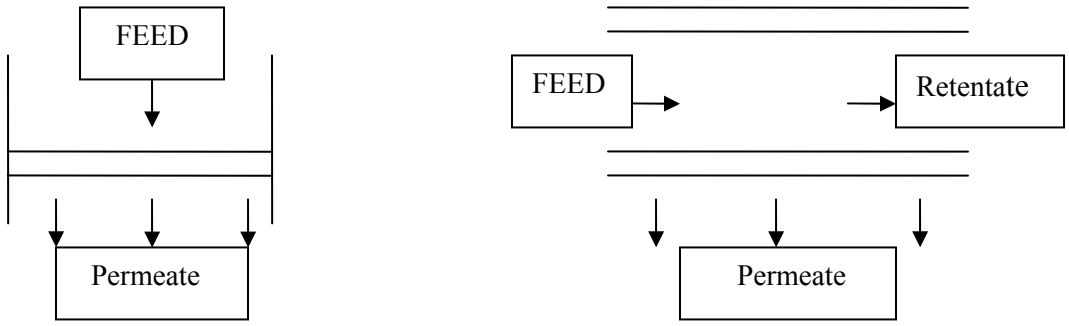

a) Dead-end Filtration b) Crossfllow Filtration

Figure 5 A representation of dead-end and crossflow filtration

1.7.2 Crossflow

In crossflow filtration the wastewater flows parallel to the water surface and water is pushed through the membrane by a pressure gradient (Figure 5b). The crossflow filtration is a continuous operation. For cross flow filtration, surface sieving is the dominant filtration mechanism. Particles buildup on the membrane surface during cross flow operation. The time required to reach a substantial buildup is less due to the flow of wastewater sweeping the particles away from the membrane surface (Baker, 2000).

1.8 Previous Work

Several studies evaluated the use of either polymeric or ceramic microfiltration membranes to treat sewage effluent, synthetic sewage and beer. Some of their findings are discussed below.

1.8.1 Flux

Gan (1999) evaluated permeate flux and solids retention efficiency of ceramic microfiltration membranes with nominal pore sizes of 0.22, 0.35 and 1.3 μm on a primary municipal sewage effluent at TMP of 1.5 bar. It was observed that the transient flux showed large variations with pore size at start up, but the difference diminished progressively with filtration time. The explanation for this kind of phenomenon was that large pore sizes are more likely to experience more severe in-pore fouling than the small pore size membranes. Another

observation was that the flux at smaller pore sizes demonstrated an earlier establishment of steady conditions than at larger pore sizes (Gan, 1999).

Gan et al. (1997) studied fouling mechanisms and flux enhancement in beer clarification by crossflow microfiltration. Tubular ceramic membranes of nominal pore sizes of 0.2, 0.5 and 1.3 μm from Ceramen were used. Flux investigation was performed using 0.11, 0.3, 0.6, 0.79 and 1.15 bar transmembrane pressure. The results showed that the flux rates below the transmembrane pressure(TMP) of 0.8 bar attained similar steady-state level after an initial and rapid decline. Contrary to expectations, the authors observed that the steady state flux was lower for TMP over 0.8 bar. A comparison of fluxes was made between 0.5 μm and 1.3 μm membranes at 1.3 bar TMP and it was observed that the 0.5 μm membrane gave a higher flux than the 1.3 μm membranes. An explanation to this phenomenon given by the authors was in-depth pore fouling. The authors noted that the smaller pores size membranes excludes much of the fine material from the membrane matrix while the bigger pore size membrane does not (Gan et al., 1997).

The effects of membrane morphology on permeate flux were investigated by Mueller et al., (1996). They examined four 0.2 μm polymeric membranes with different thickness, bulk porosity, surface porosity and surface chemistry. Filtration experiment with 0.1 g/L of bovine serum albumin (BSA) performed at TMP of 10 psig showed that cellulose acetate membrane exhibited the highest flux and the lowest flux decline, while the polyvinyldiene fluoride (PVDF) showed the lowest flux. According to the authors, the polycarbonate and cellulose acetate membranes exhibited internal fouling initially, which later became external. The polysulfone and the polyvinyldiene exhibited external fouling from the start. The authors linked the differences in behavior to the fact that the four membranes are made of different materials with

different morphology, thickness and surface characteristics, indicating that they may foul in different ways (Mueller et al., 1996).

Hong et al., (1997) observed the effects of transmembrane pressure (TMP) during crossflow filtration of colloidal suspensions. Increase in TMP resulted in rapid decline in permeate flux and they observed that the difference in permeate flux at three different TMPs declined as steady state conditions were reached. The authors suggested that the resistance to flux at steady state is to a large extent controlled by the cake layer. Similar observation was made by Asaadi et al. (1991), who suggested that the influence of the increase in TMP on steady state flux is only noticeable at low TMPs that TMP does not affect the permeate flux above a certain value.

1.8.2 Bacterial Rejection

Till et al. (1998) studied the removal of fecal coliform bacteria (FCB) from sewage effluents using microporous polymeric membranes. They used 0.45 μm and a 1.2 μm pore size membranes to filter primary and secondary effluent obtained from a wastewater treatment plant. The 0.45 μm membrane was effective in reducing the FCB from the primary effluent with initial log reduction of 4.3 at the start of the run and mean log reduction of 4.8 during the entire filtration run. This membrane was less effective for the treatment of secondary effluent. They observed an initial log reduction of 3.1 with an average of 4.1 during the entire filtration run. The 1.2 μm membrane was less effective than the 0.45 μm membrane for both primary and secondary effluent. FCB removal for the primary effluent ranged from 2.3 to 3.3 log while only 0.3 log reduction was observed during the treatment of secondary effluent. The 0.45 μm membrane also removed greater fraction of chemical oxygen demand (COD) than the 1.2 μm

membrane. Till et al. suggested that the primary effluent is capable of forming a dynamic layer on the membrane surface which enhances the removal of FCB because 1.2 μm pore size is able to reject more bacteria when treating primary effluent than when treating secondary effluent. They also concluded that the smaller pore size membrane do not benefit from any deposits onto the membrane surface.

Alonso et al. (2001) performed a comparative study on the feasibility of tertiary treatment of urban wastewater by membranes. They compared dead-end microfiltration and crossflow ultrafiltration with 0.2 μm hollow fiber membrane made of propylene and a spiral membrane made of propylene with 50000 molecular weight cutoff (MWCO). Their study showed that both processes completely eliminated total coliform, fecal coliform and fecal streptococcus bacteria (Alonso et al., 2001).

Judd et al. (2000) studied data on bacterial rejection in crossflow microfiltration of sewage. They investigated 0.2, 0.45, 0.67 and 1.2 μm polypropylene membranes for the treatment of primary and secondary effluent from a wastewater treatment plant and synthetic sewage. The synthetic sewage comprised of kaolin as suspended solids and bovine serum albumin as dissolved protein. This water was spiked with fecal coliform bacteria to produce levels similar to those recorded in sewage samples. The authors observed that the breakthrough of bacteria for all the membranes was seen at the start of the filtration run. Bacteria removal efficiency increased within the first 3 minutes to a more stable level. They also observed considerable decrease in bacterial rejection when the membrane pore size increased from 0.67 μm to 1.2 μm and suggested that the fouling layer reduces permeate flux but increases bacterial rejection (Judd et al., 2000).

1.9 Objectives of the Research

This study is part of a larger study with the goal of assessing the feasibility of using polymeric and ceramic membranes to treat CSO and discharge the permeate into the nearby rivers and streams while sending the retentate to the wastewater treatment plant. The specific project reported herein is aimed at understanding the effectiveness of polymeric membranes in reducing the indicator organisms fecal coliforms, *Escherichia coli*, *enterococci* and organic pollutants measured as COD to levels recommended by EPA. Both hydrophobic and hydrophilic polymeric membranes were used to find out their effect on the flux rate and permeate quality. The experimental studies were carried out using a dead-end cell with polymeric membranes obtained from different manufacturers (i.e Osmonics, PALL, and Millipore).

2.0 EXPERIMENTAL PROCEDURE, MATERIALS AND METHOD

2.1 Experimental Set Up

Figure 6 shows the schematic diagram of the dead-end filtration setup with constant pressure drop employed in this study. The setup has a nitrogen gas tank which provides the necessary pressure gradient needed to force the feed solution through the membrane. The holding capacity of the stirring cell is about 350 ml. The magnetic stirrer provides a high but undefined shear force needed to reduce solids cake build up on the membrane surface. The sinter metal plate provides support for the membrane. The permeate was collected in a measuring cylinder and the flux rates were calculated by measuring the time needed to obtain a predetermined permeated volume.

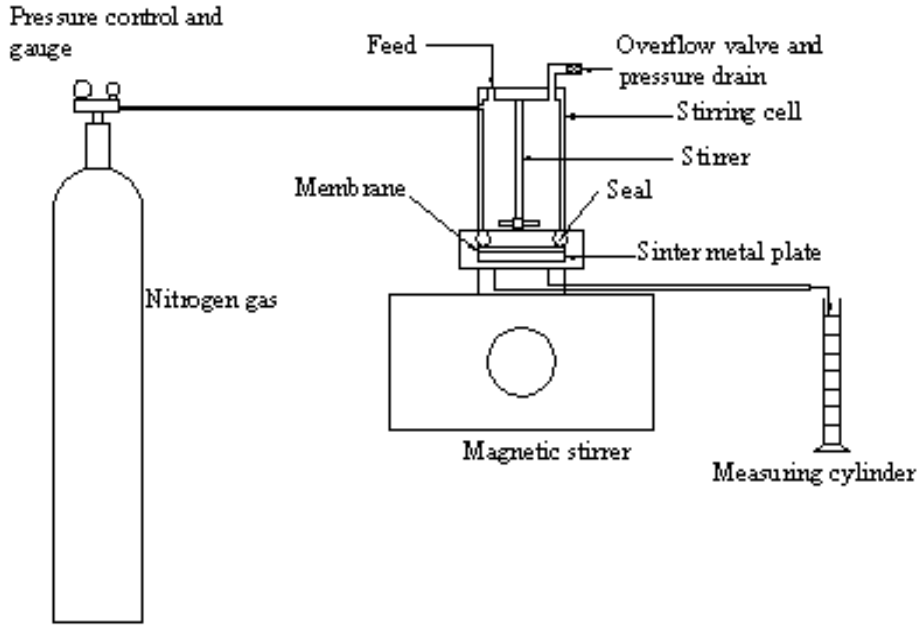

Figure 6 Experimental setup of dead end cell

2.2 Feed Water

Feed solution was a primary effluent from ALCOSAN Municipal Wastewater Treatment Plant(WWTP) in Pittsburgh, Pennsylvania. The feed solution was collected and analyzed between months of May and October 2002, which is the period during which the CSO events usually occur. The primary settled effluent was assumed to resemble the CSO which has been pretreated by a swirl separator. The COD values obtained in the lab (University of Pittsburgh) for the primary effluent ranged from 39.7 to 99.6 mg/l, suggesting that the sewage in ALCOSAN is very dilute. Table 5 compares characteristics of the CSO and the primary effluent.

Table 5 Comparison between CSO and primary effluent

	BOD_5 (mg/)	C-BOD (mg/)	COD (mg/)	TSS (mg/)	Total N (mg/)	NH_3-N (mg/)	Total P (mg/)	Fecal Coliforms[3] (col/100 mL)
CSO Range[1]								
	25-100	-	[4]260 -480	150-400	3-24	-	1-10	10^5-10^7
Primary Effluent[2]								
Min.	-	23	44	24	-	2	1	10^6
Max.	-	70	218	184	-	13	3	10^6
Avg.	-	40	125	55	-	7	2	10^6

[1] US EPA, 2001, [2] ALCOSAN Monitoring Data, [3] University of Pittsburgh Lab Data, [4]Metcalf & Eddy, 2003

2.3 Types of Membranes and their Characteristics

Several thin film composite flat sheet polymeric membranes were obtained from different manufacturers and were characterized by their pore size, water affinity, water bubble point, thickness and porosity as shown in Table 6. The membranes are of different thickness and have about similar porosity. The membranes have different surface chemistry. The bubble point pressure is the pressure needed to push a bubble of air through a wet membrane. The scanning electron microscopy is used to investigate the porous structure of a membrane. The membrane sample is placed under a scanning electron microscope and then exposed to electrons beam. The incident electrons are called primary electrons and these cause the membrane to emit electrons called secondary electrons. The secondary electrons are then sent to a detector where a micrograph of the membrane structure can be plotted (Mulder, 1991). The examples of the

micrographs of acrilyic copolymer and polyvinyldiene membranes are shown in Figure7 and Figure 8.

Table 6 Types of membranes used and their properties

Membrane	Manufacturer	Material	Water Affinity	Pore Size, µm	Membrane Thickness, µm	Water Bubble Point, bar	Porosity, %
AC+0.2	PALL	Acrilyc Co-polymer	hydrophilic	0.2	530-1050	1.72-3.45	70-80
AC+0.45	PALL	Acrilyc Co-polymer	hydrophilic	0.45	530-1050	1.10-1.79	70-80
AC-0.45	PALL	Acrilyc Co-polymer	hydrophobic	0.45	500-1020	-	70-80
AC+0.8	PALL	Acrilyc Co-polymer	hydrophilic	0.8	530-1050	0.50-0.88	70
PF+0.45	Millipore	PVDF[1]	hydrophilic	0.45	125	1.55	70
PF-0.45	Millipore	PVDF	hydrophobic	0.45	125	0.56	70
PF-0.3	Osmonics	PVDF	hydrophobic	0.3	800	1.38	-

+ = hydrophilic

- = hydrophobic

[1]PVDF = polyvinyldiene fluoride

2.3.1 PALL Versapore (Hydrophilic and Hydrophobic) Membranes

The hydrophilic membrane is called Versapore while the hydrophobic one is called Versapore R. Versapore membrane is made up of acrylic co-polymer and it is supported on a non-woven nylon. This hydrophilic membrane is coated with silicon based surfactant which acts as a wetting agent. Versapor R membrane is hydrophobic and is made up of a modified acrylic

co-polymer supported on a non-woven nylon support. These membranes are double layered and therefore they are 'composite' membranes. The pore sizes investigated are the hydrophilic 0.2, 0.45 and 0.8 μm and the hydrophobic 0.45 μm. The micrograph for both the Versapore and Versapore R membrane resembles that of Figure 7. The micrograph shows the tortuous nature of its porous structure.

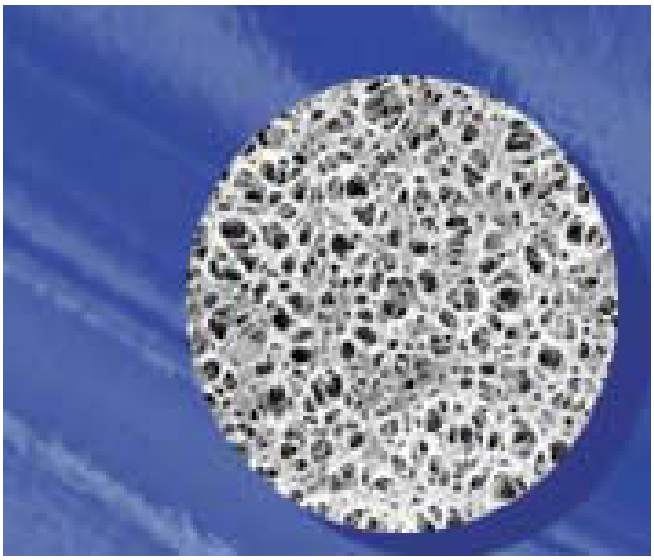

Figure 7 Micrograph of a Versapore membrane (From PALL webpage)

2.3.2 Osmonics JX 0.3 Membrane

The JX membrane is a hydrophobic membrane. It is made up of polyvinyldiene supported on polyester. The Figure 8 shows a micrograph of the polyvinyldiene (PVDF) membrane. The membrane porous structure is clearly not capillary like, but rather tortuous.

Typical uses of this membrane include removal of suspended solids, diatomaceous earth replacement and cationic ED paint removal.

2.3.3 Millipore Durapore (Hydrophilic and Hydrophobic) Membranes

The hydrophilic Durapore membrane is made of modified PVDF and the hydrophobic membrane is made up of PVDF. The membrane porous structure is clearly not capillary like, but rather tortuous as shown in Figure 8. The Durapore membrane is single layered unlike the JX membrane and Versapore membranes. The hydrophilic membrane is used in clarification of air and other gases; sterilizing filtration of protein solutions, tissue culture media, additives, antibiotics and alcohols and particulate removal. Hydrophobic membrane is used in clarification of air/gases and sterilizing filtration of gases. The pore sizes investigated are the hydrophilic 0.45 μm and the hydrophobic 0.45 μm.

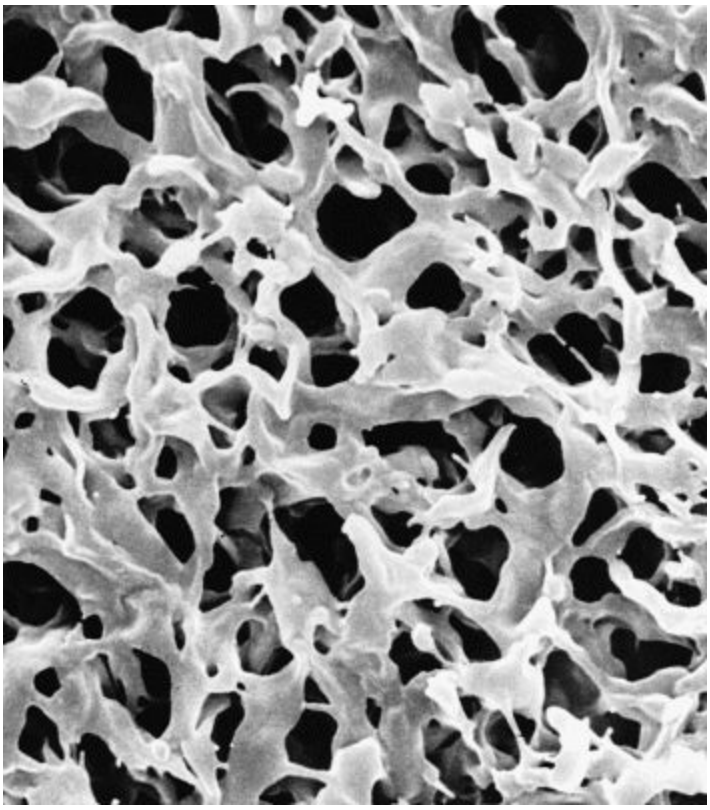

Figure 8 Micrograph of a polyvinyldiene membrane (From Millipore webpage)

2.4 Test Procedures

2.4.1 Preparation of the Membranes

All the membranes were subjected to similar preparation procedures. The membranes were cut out to discs of diameter of 68 mm so that they can fit inside the cell. They were then rinsed by passing deionized water at a pressure between 1.03 bar and 4.12 bar. The rinsing helps

get rid of any organic substances which may affect the COD readings. The rinsing also helps wet the membranes thereby making it easy for the permeate to pass though.

2.4.2 pH and Temperature

The primary effluent was collected from ALCOSAN WWTP on different dates from May 2002 to October 2002. The sample was kept at room temperature and this varied from 22 ^{o}C to 24 ^{o}C . The pH of the primary effluent sample before treatment was determined to range from 6.4 to 7.0.

2.4.3 Flux Rate

a) Primary effluent flux

The flux of each type of membrane was investigated over a period of about 10 hours at 1.03 bar and 2.06 bar. The flux was measured by timing how long it takes for certain filtrate volume to pass through the membrane. Steady state was reached during each filtration run. For this research steady state condition is defined when the time for filtering predetermined sample volume varied by less than 1%.

b) Flux due to periodic increase of pressure

The flux of each type of membrane was observed at various pressures during a single run using the same membrane sample. The starting pressure of 1.03 bar was increased to 2.06, 3.09

and 4.12 bar. The flux is monitored until steady state was reached before increasing the pressure to a higher level.

2.4.4 Collection of Samples

a) In the primary effluent flux experiment samples of the permeate were collected at the beginning of the experiment and then after every three to four hours or when steady state was reached. A total of three permeate samples are collected throughout the run.

b) In the experiment which investigated flux due to periodic increase in pressure samples were collected after steady state flux was achieved at each increase in pressure.

2.4.5 Analytical Methods

The following parameters were measured according to procedures outlined in Standard Methods: COD, Fecal coliforms, *Escherichia coli* and *Enterococci*.

a) Chemical Oxygen Demand (COD)

COD determination was carried using Hach COD Reactor, Model 16500-00. 2 ml of the unfiltered samples from the primary effluent and the permeate was placed in the Hach COD reagent vials which were heated at 150 ^{o}C for 2 hours. After cooling the vials, the percentage transmittance of the solution was measured at a wavelength of 420 nm with a Bausch and Lomb spectrophotometer and COD values were taken from Figure 9, which was obtained by standardizing the COD reagent vials using potassium hydrogen phthalate. The COD values were also compared with standard tables in the Appendix, (Table D-32, Table D-33).

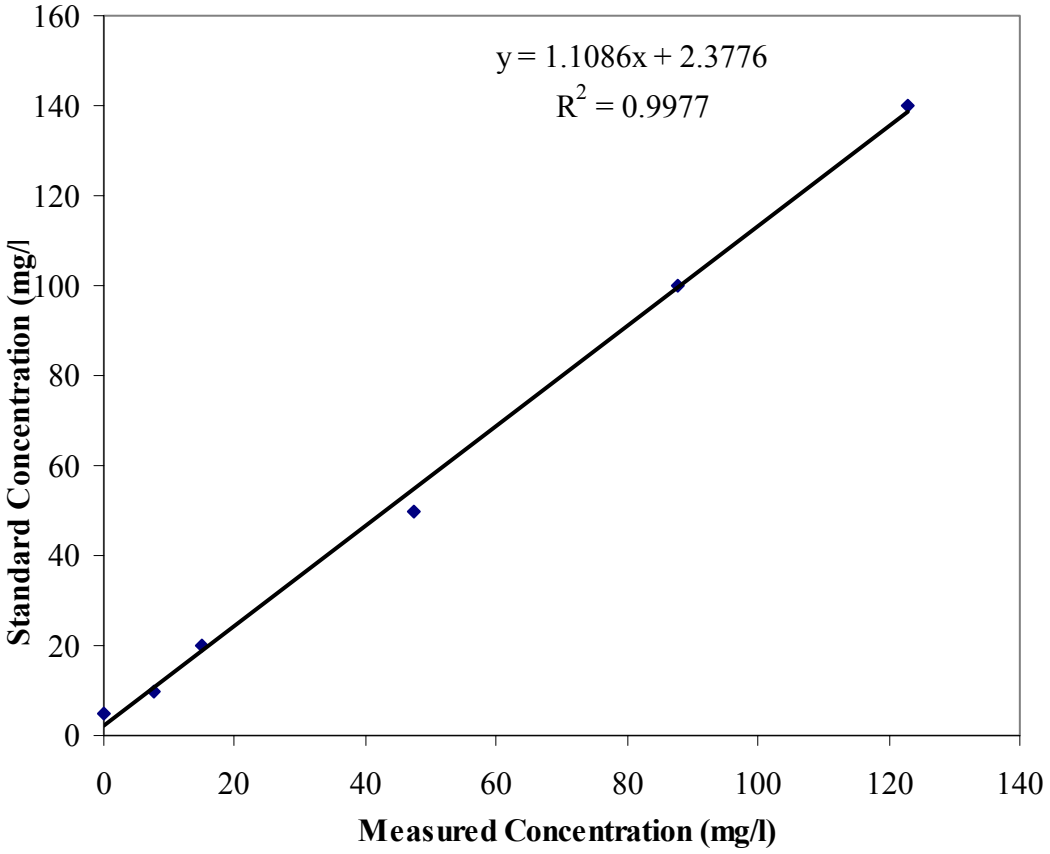

Figure 9 COD standard curve

b) Fecal coliforms Bacteria (FCB)

FCB were enumerated using the standard membrane filter technique with 0.45 µm grided filter papers. Dilutions of the samples were made using phosphate buffered dilution water. The filters were placed in petri dishes impregnated with DIFCO mFC broth. The petri dishes were then inverted and incubated at 35+/- 0.5 ^{o}C for 2 hours to acclimate the bacteria and then at 44.5 +/- 0.2 ^{o}C for 22 hours. Using this technique, colonies of fecal coliforms turn blue and non fecal coliforms and other organisms are grey and cream colored (Greenberg et al., 1992).

c) *Escherichia coli*

Escherichia coli were enumerated using the membrane filtration technique with DIFCO Bacto m-TEC agar as above. After incubation, filters were removed and placed over pads in petri dishes saturated with 2 ml urease substrate. Yellow to yellow brown colonies are indicative of *Escherichia coli* (Greenberg et al., 1992).

d) *Enterococci*

Enterococci was enumerated using the membrane filtration technique with DIFCO Bacto m- *Enterococci* Agar as above. The Petri dishes were inverted and incubated at 35+/- 0.5 ^{o}C for 24 hours. Light and dark red colonies are counted as *Enterococci* (Greenberg et al., 1992).

3.0 RESULTS AND DISCUSSION

3.1 pH and Temperature

The pH of the sewage varied between pH 6.4 to pH 7.0 indicating that the wastewater was well buffered. According to Equation 1, flux is dependent on viscosity of the liquid. Viscosity is temperature dependent, and will decrease with increase in temperature yielding a higher clean water flux. The temperature of the wastewater samples was kept as close to room temperature as possible to minimize the effects due to changes in viscosity. The wastewater temperature varied from 22 ^{o}C to 24 ^{o}C depending on the room temperature.

3.2 Fluxes and Resistance

3.2.1 Flux rates at Fixed Transmembrane Pressures

Table 7 shows initial and final fluxes of each membrane at 1.03 bar and 2.06 bar. The AC+0.2 membrane had an initial flux rate of 1966 L/m^2·hr, while the AC+0.45 and AC+0.8 membranes had initial flux rates of 6606 L/m^2·hr and 12324 L/m^2·hr respectively at 1.03 bar. The initial flux is directly related to the pore sizes for the hydrophilic membranes as shown in Figure 10. This explanation is especially true for AC+0.2, AC+0.45 and AC+0.8 which are made of the same material, same surface chemistry, and are from the same manufacturer.

The study shows that hydrophilic membranes in general have higher initial flux rates than hydrophobic membranes of the same pore size. This difference in the flux can be explained by

the membrane wetting: hydrophilic membranes are easily wetted upon the contact with water while hydrophobic membranes require time and pressure to achieve wetting.

Table 7 Initial and final flux rate for all the membranes at 1.03 bar and 2.06 bar

Membranes	Membrane thickness micrometer	Initial Flux ($L/m^2 \cdot hr$)		Final Flux ($L/m^2 \cdot hr$)	
		1.03bar	2.06bar	1.03bar	2.06bar
AC+0.2(PALL)	530-1050	1966	5505	15	13
AC+0.45(PALL)	530-1050	6606	6881	13	14
AC-0.45(PALL)	500-1020	29.3	40	8	7
AC+0.8(PALL)	530-1050	12324	23593	15	17
PF+0.45(Millipore)	125	9715	16515	15	16
PF-0.45(Millipore)	125	1032	6881	17	19
PF-0.3(Osmonics)	800	826	944	13	12

+ = hydrophilic

- = hydrophobic

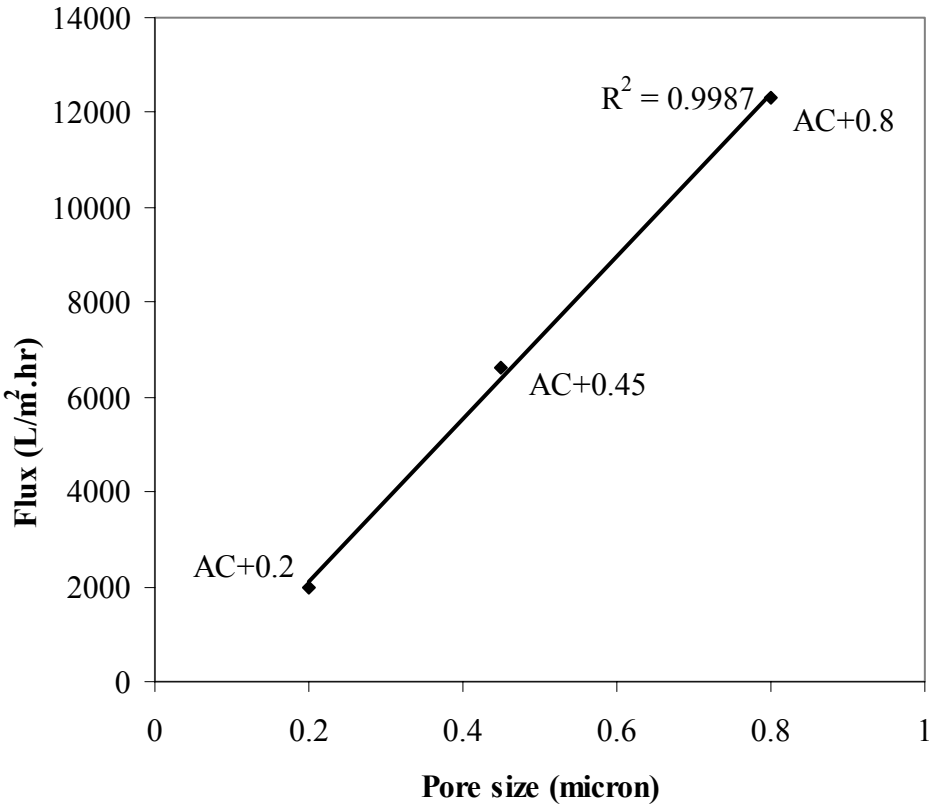

Figure 10 Variation in permeate flux with pore size at 1.03 bar for selected membranes

The AC+0.45 membrane had a lower initial flux rate (6606 L/m^2·hr) than the PF+0.45 membrane (9715 L/m^2·hr) at 1.03 bar. This difference can be explained by the difference in membrane thicknesses (530-1050 μm vs. 125 μm) that provides resistance to filtration.

The initial flux for AC+0.8 of 12324 L/m^2·hr at 1.03 bar was the highest among all membranes tested in this study. The AC-0.45 membrane had the lowest initial flux rate of 29 L/m^2·hr at 1.03 bar. The PV-0.3 membrane had a higher initial flux (826 L/m^2·hr) at 1.03 bar, than the AC-0.45 membrane, which is unexpected because it has smaller pore sizes. This behavior can be attributed to the difference in morphology and membrane material as observed by Mueller et al. (1996).

Figures 11 and 12 show a typical permeate flux during a fixed TMP experiment for the AC+0.2 membrane at 1.03 bar and 2.06 bar respectively. The permeate flux rates for AC+0.45, AC-0.45, AC+0.8, PF+0.45, PF-0.45 and PV-0.3 membranes at 1.03 bar and 2.06 are shown in the Appendix A, Figures A-27 to A-38. Noted on the graphs are the points when the samples were taken for COD and bacterial analysis. Also noted are the points when the dead-end cell was refilled with fresh primary effluent. Refilling of the stirring cell had little or no effect on the permeate flux because refilling was done before all the water in the cell ran out and there was little or no disturbance of the filtration cake. Another explanation could be that the membrane has been internally fouled or that the filtration cake is well compacted so that refilling does not affect the transient equilibrium of the filtration process.

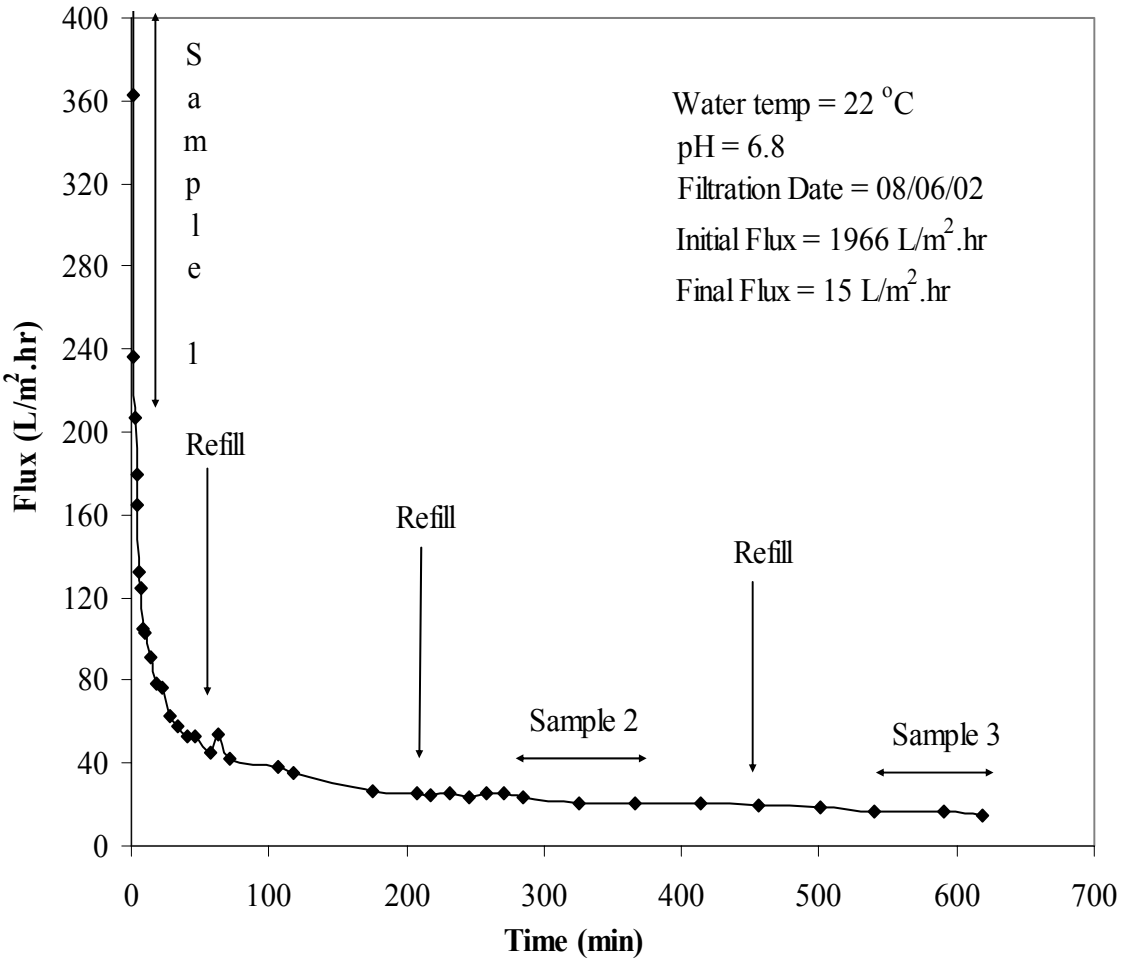

Figure 11 Variation in permeate flux for AC+0.2 membrane at 1.03 bar

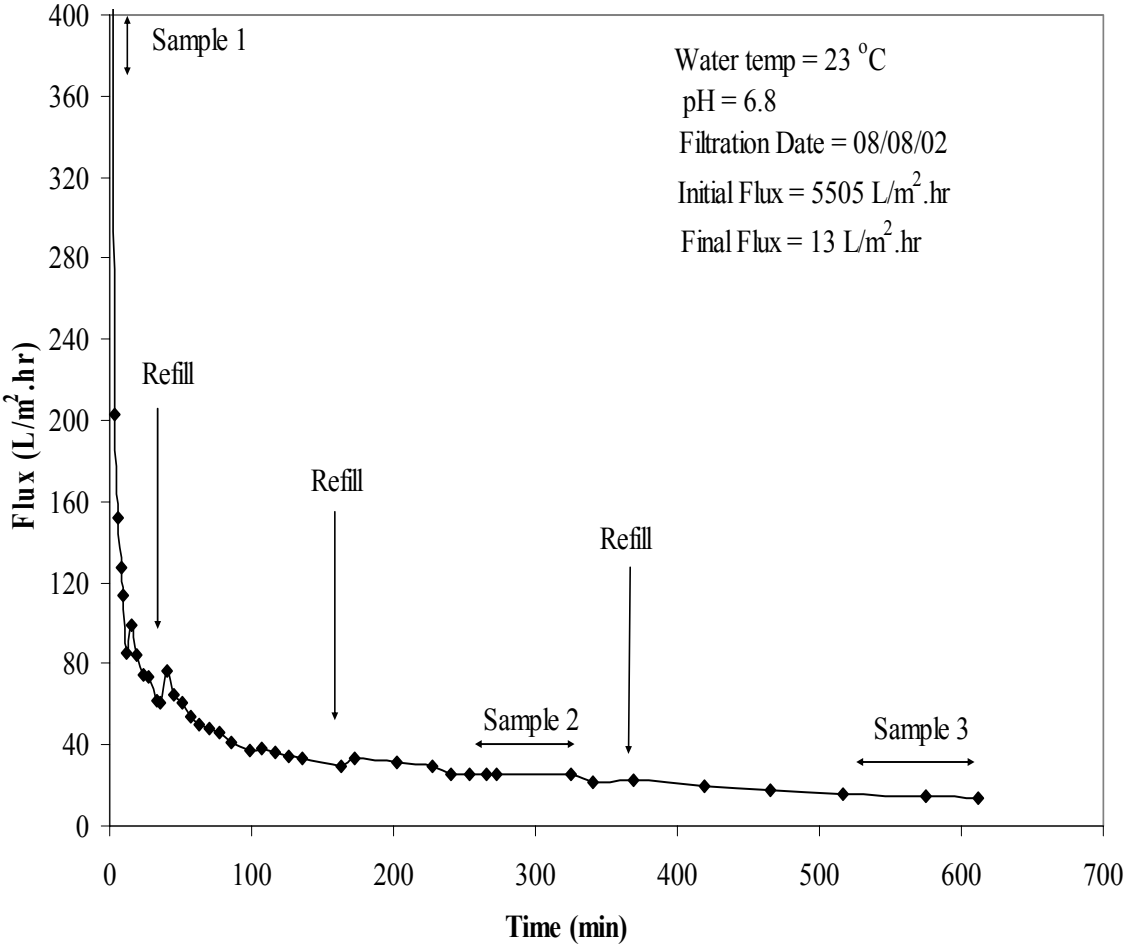

Figure 12 Variation in permeate flux for AC+0.2 membrane at 2.06 bar

Comparison of flux rates obtained at 1.03 bar and 2.06 bar on Figure 13 and 14 respectively shows that the steady state flux towards the end of the filtration run does not show any marked differences among the seven membranes tested in this study. Gan (1999) explained such behavior by the fact that membranes with large pore sizes foul faster and experience more in-pore fouling than those with smaller pores. It can therefore be hypothesized that if the particle size distribution for the primary effluent was much higher than 0.8 μm, then the steady state flux rates for the membranes would not or would take longer than ten hours to converge. The fact that all fluxes converged to a similar value fairly quickly suggests that primary effluent contains a considerable fraction of particles below 0.2 μm.

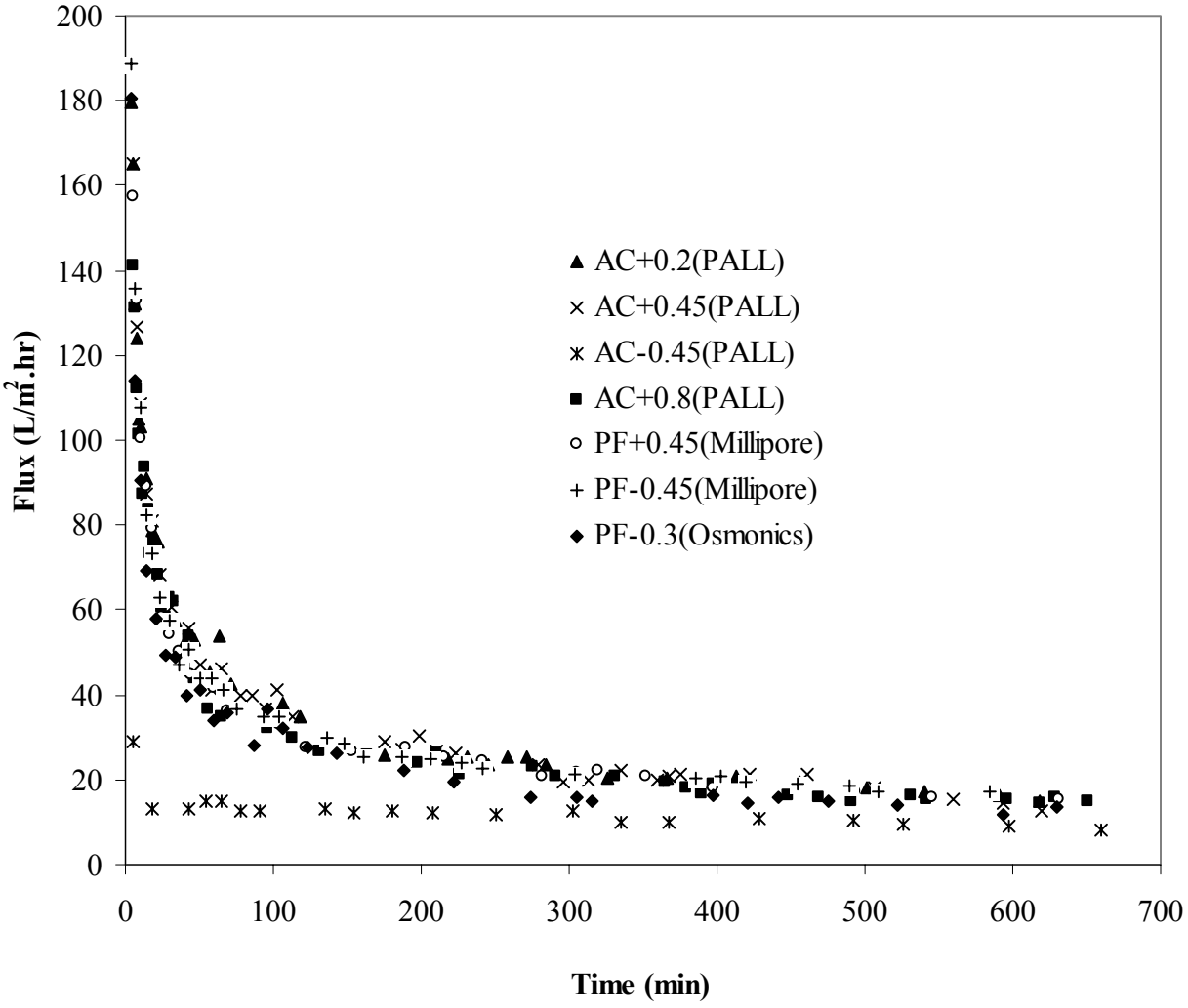

Figure 13 Comparison of permeate flux rates for different membranes at 1.03 bar

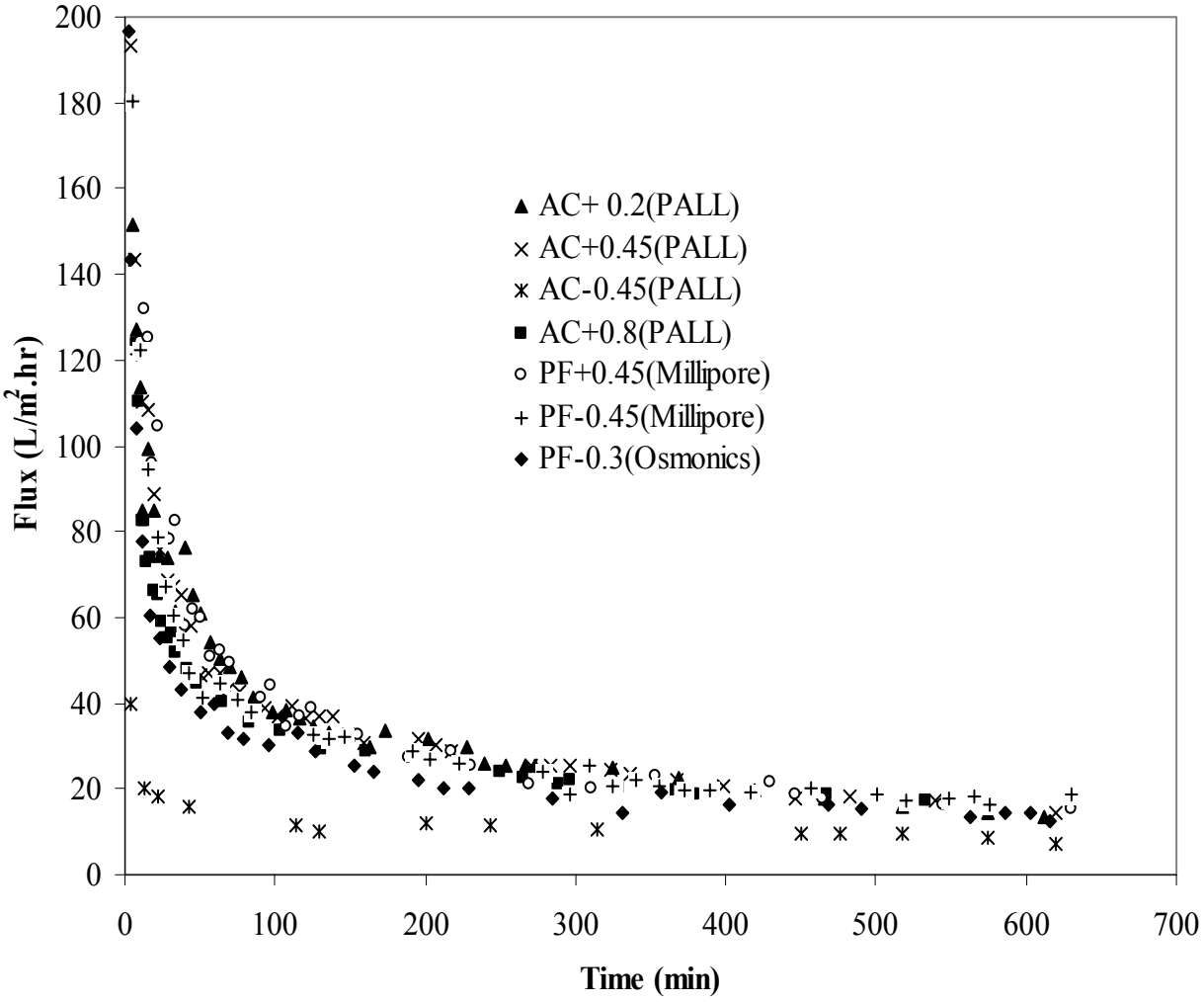

Figure 14 Comparison of permeate flux rates for different membranes at 2.06 bar

Figure 15 compares permeate flux rates for the AC+0.2, AC+0.4 and AC+0.8 membranes at 1.03 bar and 2.06 bar. The steady state permeate flux rates converged to an average of 14 $L/m^2 \cdot hr$ for the two TMPs and all pore sizes tested in this study. Such behavior suggests that fouling is the only variable that controls the steady state flux. Hong et al., (1997) and Asaadi et al., (1991) also observed that steady state flux is independent of applied pressure, a phenomenon attributable to fouling and cake layer. Three things could have caused this convergence of flux at all pressures: a) if the cake is compressible, then the higher pressure compresses the cake thus reducing its porosity which counter balances the increase in pressure, b) if the cake is incompressible, then there is a faster build up of cake at higher pressures and the resistance increases with increase in cake thickness, and c) the higher pressures may further push the trapped particles deeper into the membrane matrix thus blocking the pores and increasing the resistance.

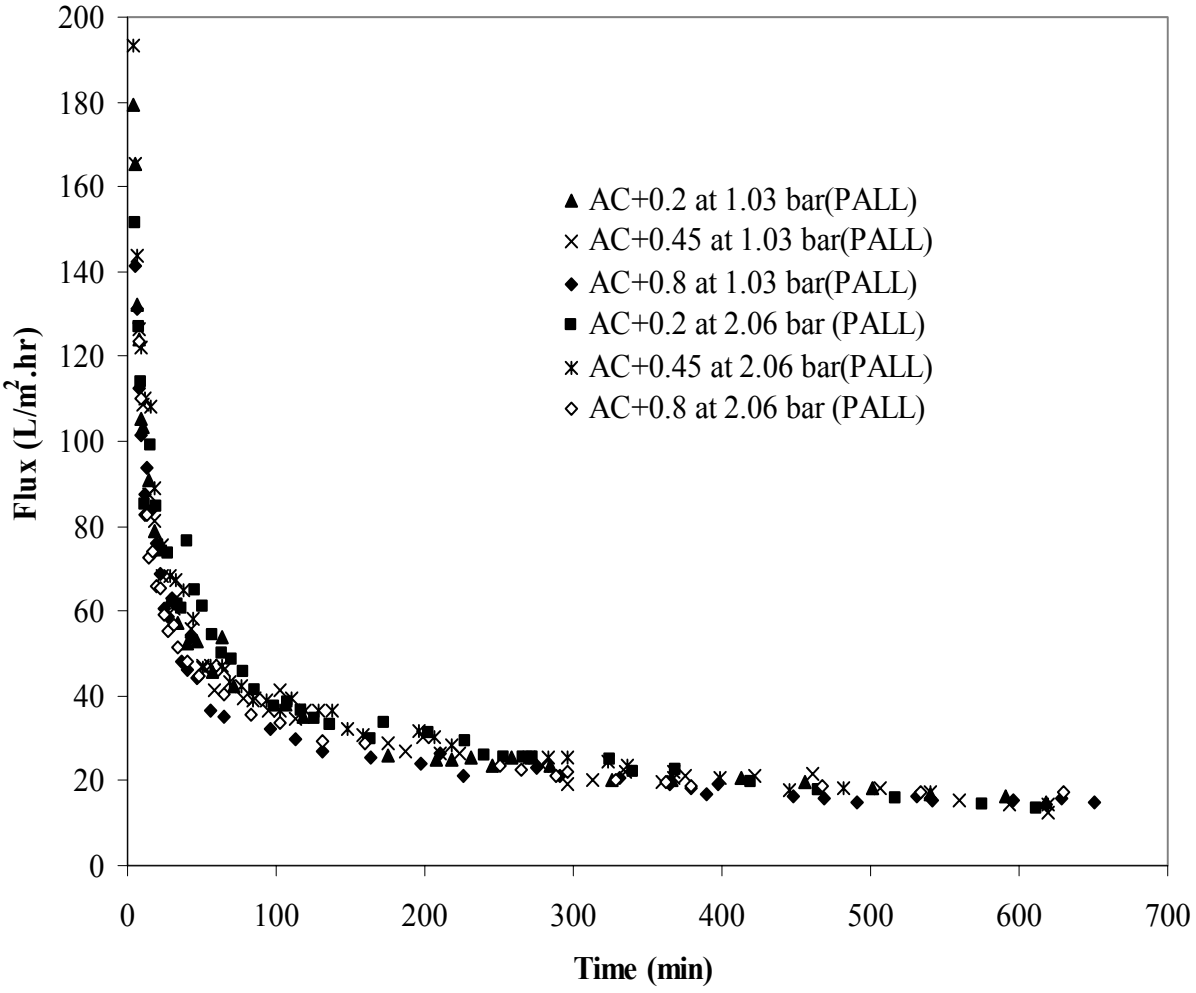

Figure 15 Comparison of fluxes for AC+0.2, AC+0.4 and AC+0.8 membranes at 1.03 bar and 2.06 bar.

3.2.2 Fluxes Due to Regular Increase in Pressure

The effect of the increasing pressure throughout the run was also investigated in this study. The starting pressure was 1.03 bar and the pressure was increased to 2.06 bar, 3.09 bar and finally to 4.12 bar after steady state conditions were reached at each pressure. All the membranes were subjected to this test. Flux was recorded throughout the filtration run and Figure 16 and 17 show the permeate flux for two of these membranes as a function of time. Indicated on the graphs are points when the pressure was increased and when the cell was refilled and when the samples for COD and bacterial analysis were taken. For the rest of the membranes the permeate flux is shown in Appendix A, Figures A-39 to A-43.

Very little change in the permeate flux due to the increase in pressure was observed for all the membranes tested in this study except for AC-0.45 membrane. This lack of the impact of pressure on the permeate flux rate is not unexpected because the membranes could be so severely fouled that the small increase in pressure cannot cause any major observable changes in the flux. Another contributing factor is that the increase in pressure may further compress the filtration cake and push more particles deeper into the membrane matrix, thus causing additional membrane fouling that counter balances increase in filtration pressure. Defrance et al., (1998) also observed that the permeate flux becomes stable and independent of the applied TMP when TMP exceeds 0.85 bar. Such behaviour explains why many filtration systems in the field are operated in constant flux mode to minimize membrane fouling.

Figure 17 illustrates unusual behavior of AC-0.45 membrane where a slight increase in flux was observed when TMP increased from 1.03 bar to 2.06 bar. However, there was a major increase in flux when the pressure was increased from 2.06 bar to 3.09 bar and then to 4.12 bar. These major increases in the flux can be attributed to the fact that the pressures below 3.09 bar

are not sufficient to overcome the membrane resistance, R_m, while the pressure between 3.09 and 4.12 bar is needed to completely wet this hydrophobic membrane. However, this increase in permeate flux is of short duration because the membrane quickly became fouled.

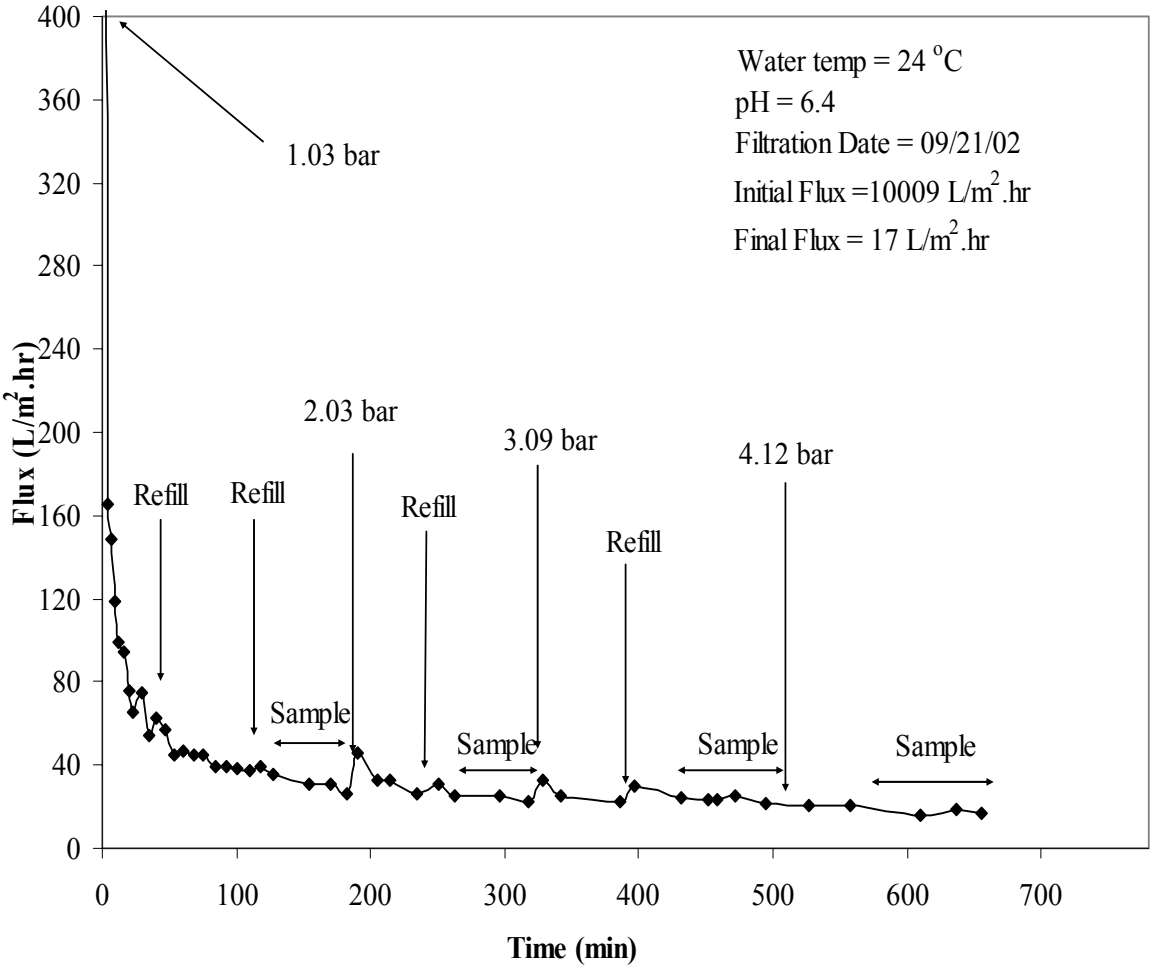

Figure 16 Variation in permeate flux for AC+0.45 membrane at various pressures

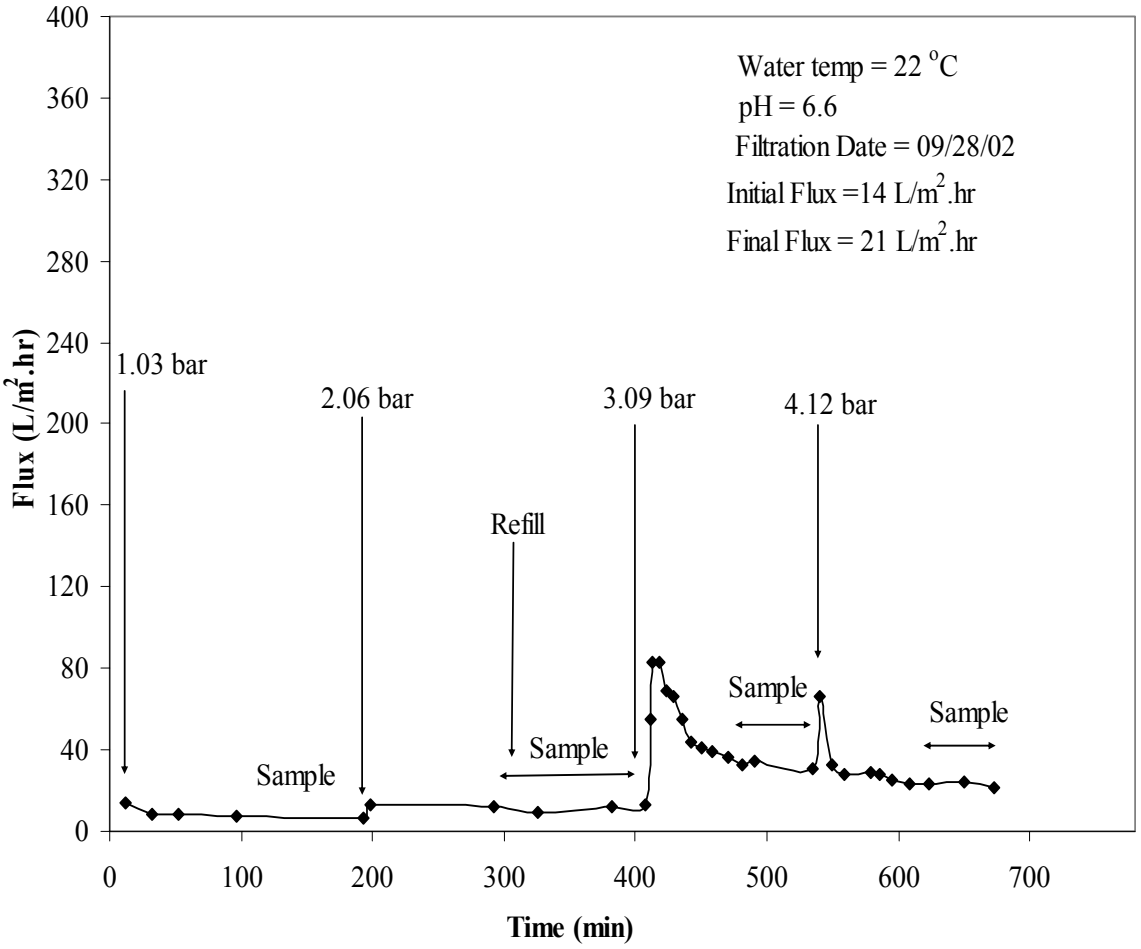

Figure 17 Variation in permeate flux for AC-0.45 membrane at various pressures

3.2.3 Comparison of Filtration Resistances at Fixed Transmembrane Pressures

Figures 18 and 19 show the total filtration resistance, R_t, of the membranes during the experiments at 1.03 bar and 2.06 bar respectively as calculated from Equation 1. As expected, total resistance increased during the filtration run due to membrane fouling. All three hydrophobic membranes (AC-0.45, PF-0.45, PF-0.3) exhibited the highest resistance to flux at the start of the run as shown by Tables 8 and 9. Since fouling did not have a chance to develop at the onset of the experiment, this phenomenon can only be attributed to the membrane resistance, R_m, resulting from the membrane surface chemistry that repels water and results in a lower flux.

Tables 8 and 9 show that the AC+0.8 membrane fouls faster than the smaller pore size membranes since it started at lower initial resistance and reached similar total resistance as other membranes after similar filtration time. The bigger pore size membranes tend to be more prone to fouling than the smaller pore size membranes because they have higher initial throughput volume that leads to increase in the amount of particulates trapped in the pore channels leading to faster membrane clogging.

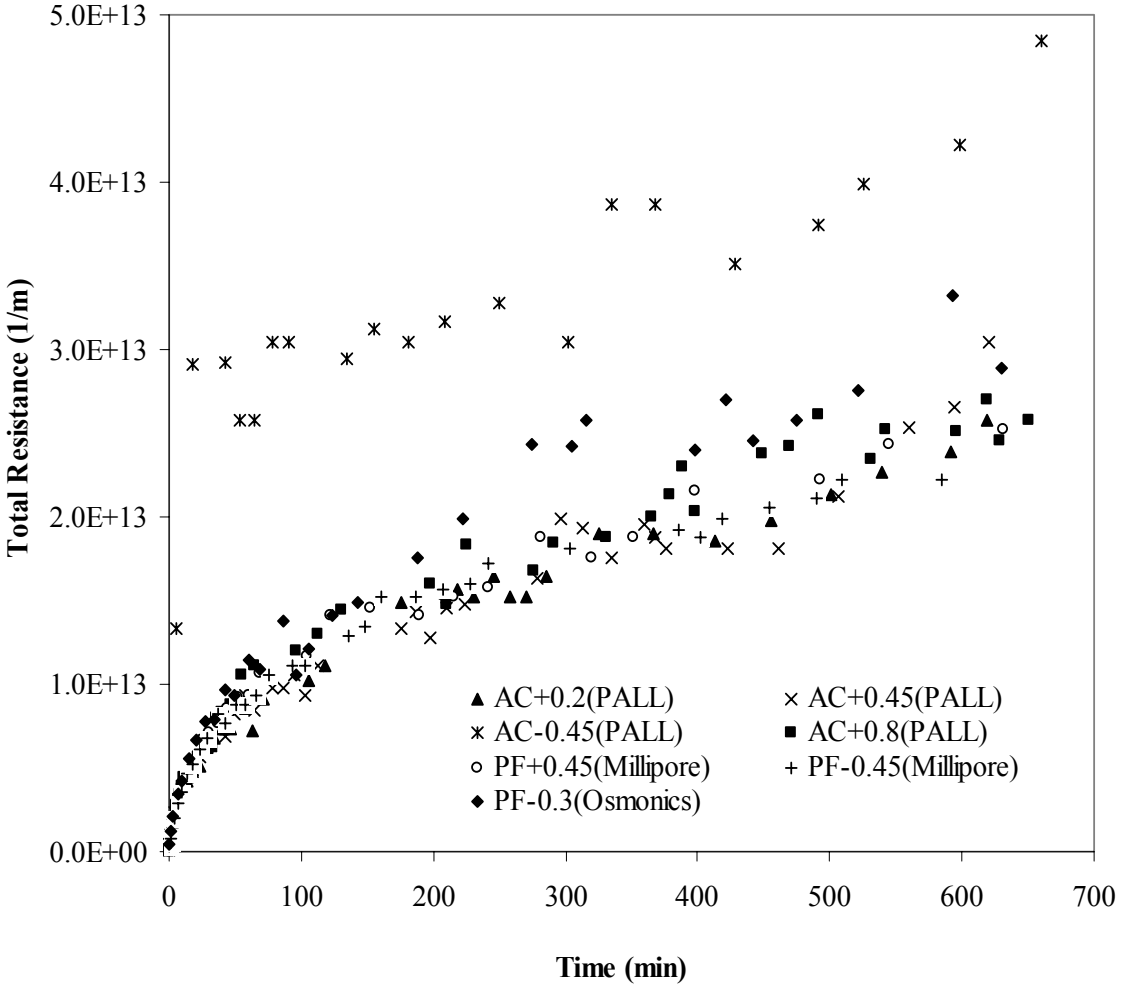

Figure 18 Total filtration resistance as a function of filtration time for different membranes operated at 1.03 bar

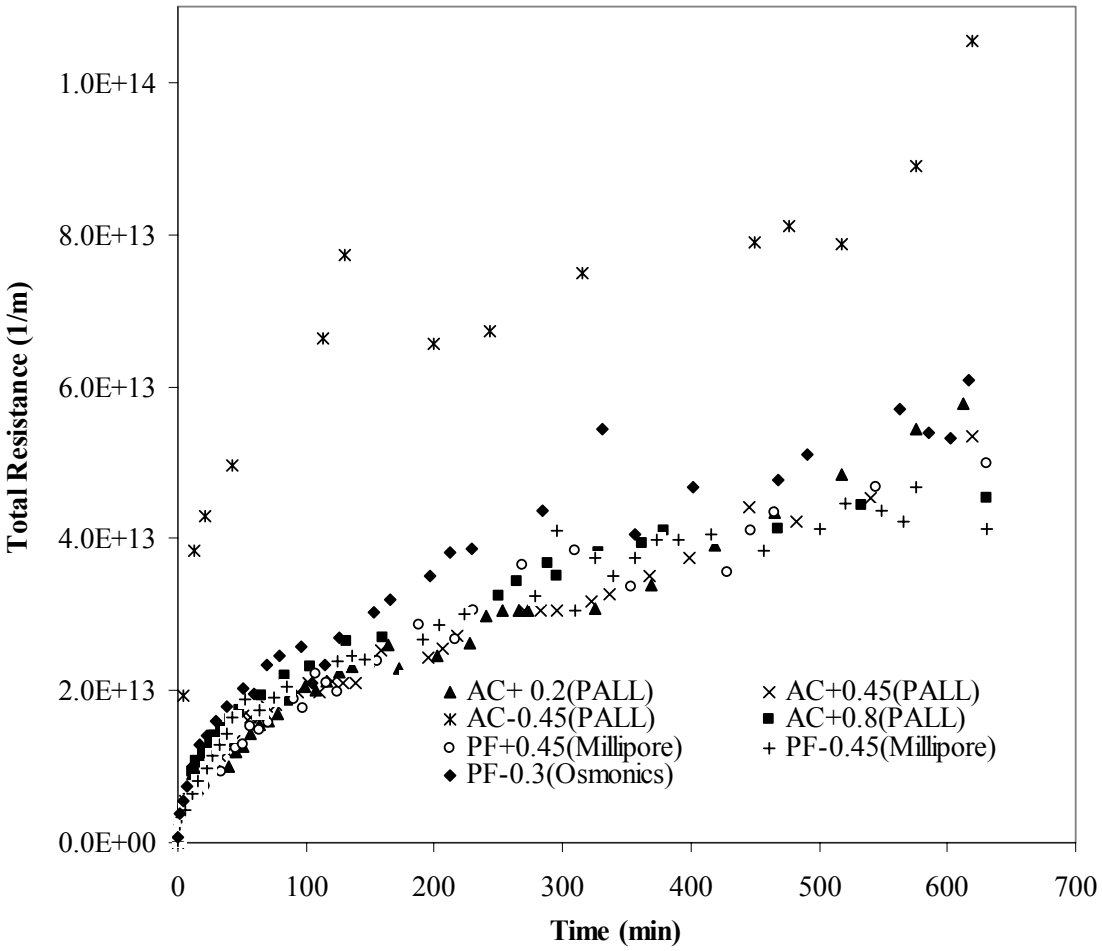

Figure 19 Total filtration resistance as a function of filtration time for different membranes operated at 2.06 bar

Table 8 Resistance, total throughput volume and total run time for each membrane at 1.03 bar

Membranes	Resistances at 1.03 bar ($1/m * 10^{10}$)		Total Run Time(min)	Throughput volume (L/m^2)
	Initial R_m	Final R_t		
AC+0.2(PALL)	20.0	2580	619	301
AC+0.45(PALL)	5.9	3050	620	306
AC-0.45(PALL)	1330.0	4840	660	124
AC+0.8(PALL)	3.1	2580	651	310
PF+0.45(Millipore)	4.0	2520	631	311
PF-0.45(Millipore)	3.8	2230	620	281
PF-0.3(Osmonics)	47.0	2890	630	233

+ = hydrophilic
- = hydrophobic
R_m = membrane resistance
R_t = total resistance

Table 9 Resistance, total throughput volume and total run time for each membrane at 2.06 bar

Membranes	Resistances at 2.06 bar ($1/m * 10^{10}$)		Total Run Time(min)	Throughput volume (L/m^2)
	Initial R_m	Final R_t		
AC+0.2(PALL)	14.1	5780	612	324
AC+0.45(PALL)	11.2	5360	620	330
AC-0.45(PALL)	1940.0	10500	620	218
AC+0.8(PALL)	3.3	453	630	329
PF+0.45(Millipore)	4.7	4980	630	339
PF-0.45(Millipore)	11.2	4120	630	326
PF-0.3(Osmonics)	82.0	6090	616	238

+ = hydrophilic
- = hydrophobic
R_m = membrane resistance
R_t = total resistance

Figures 20 and 21 suggest that there is a linear relationship between total resistance and throughput volume for all the membranes at both 1.03 bar and 2.06 bar respectively. Such behavior suggests that these membranes continue to build up solids on the surface or in the pore channels throughout the whole run. It takes some time for R_t to reach appreciable levels, and could be that the material fouling of the pores, which is a dominant mechanism takes time to develop. Also it takes longer for AC+0.8 to start building up R_t because large pores require more time to plug up, however this membrane tends to foul faster. This is a confirmation, that material fouling is the dominant resistance mechanism.

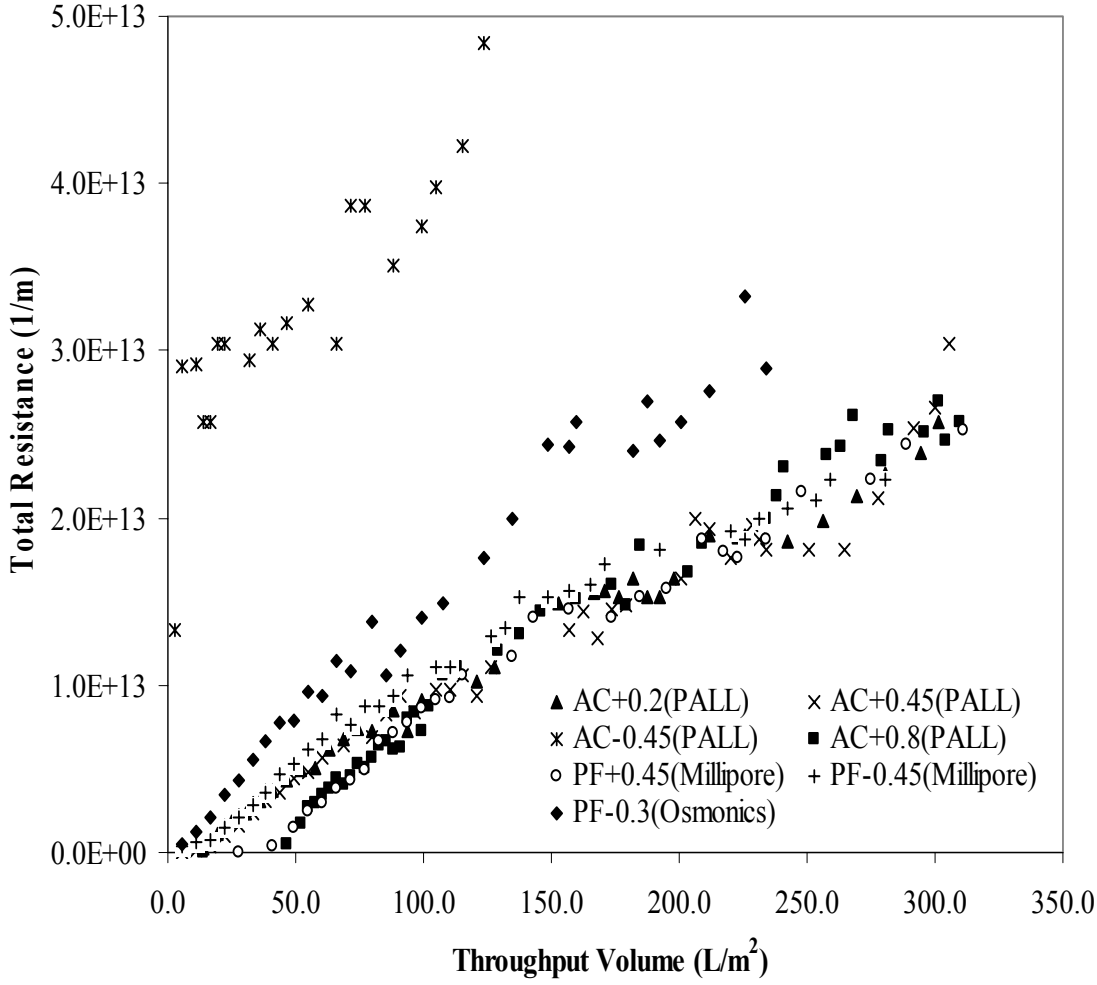

Figure 20 Total filtration as a function of throughput volume for different membranes operated at 1.03 bar

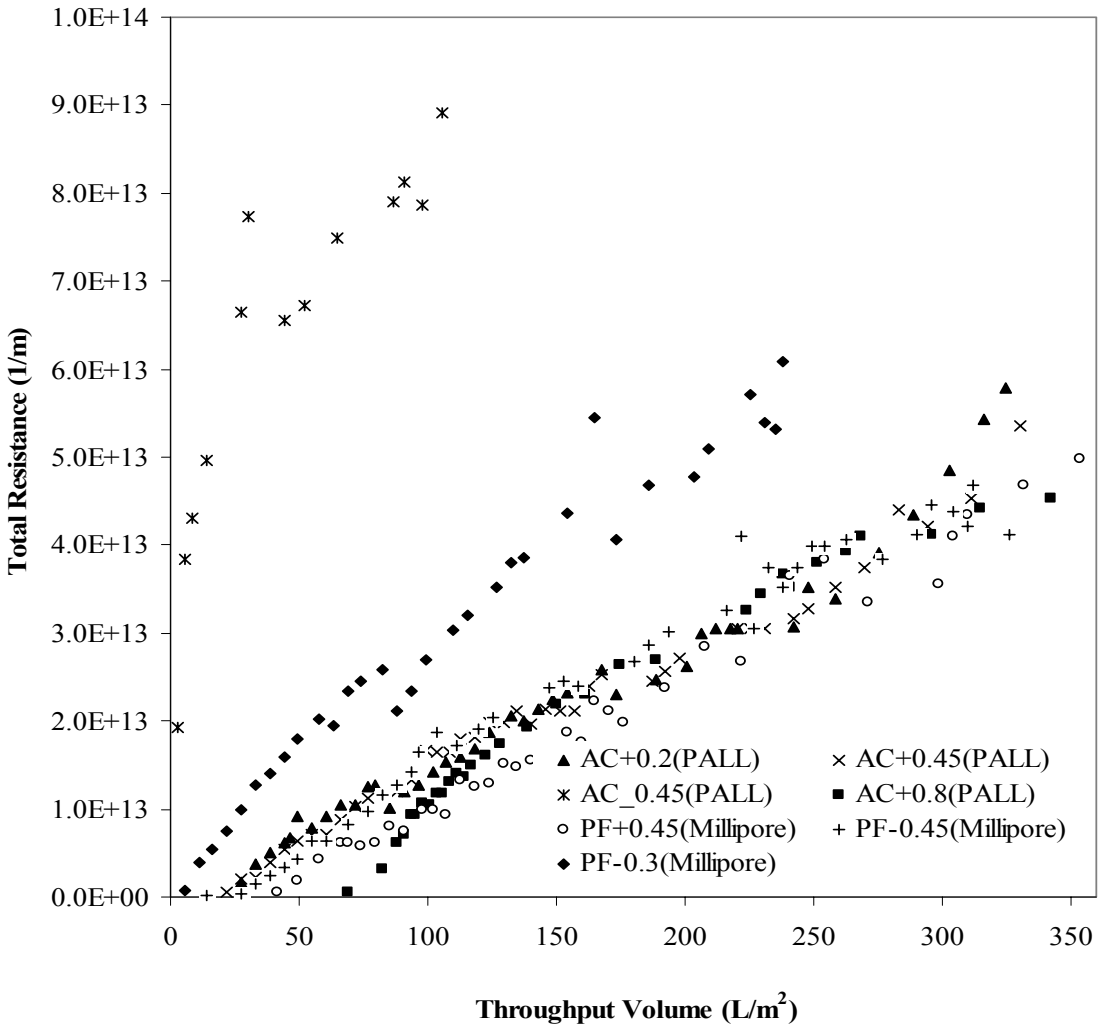

Figure 21 Total filtration as a function of throughput volume for different membranes operated at 2.06 bar

3.3 Cake Resistance and Thickness

3.3.1 Estimation of Cake Thickness Based on Equation 10

Equation 10 was used to estimate the cake thickness on the membranes. Assumptions made are that the cake is incompressible and therefore its porosity and resistance are independent of the applied pressure and also all the suspended particles remain on top of the membrane material, none goes into the membrane matrix, therefore, $R_c = R_t$ – Initial R_m. Since, porosity, K constant and S_c could not be determined in this study these were assumed. If the cake consists of randomly packed spheres then its porosity, ε is approximated to be 0.4 (Ho et al., 1992, Zeman et al., 1996, Hong et al., 1997) and the K constant is assumed to be 5 (Ho et al., 1992). S_c is given by $6/\psi d_p$, and $\psi = 1$, assuming that the particles are spherical (Ho et al., 1992). The average diameter of the suspended material was assumed to be 0.5 μm.

Figures 22 and 23 show a graph of cake thickness (the particles diameter is assumed to be 0.5 μm) plotted against throughput volume for the membranes investigated in this study at 1.03 bar and 2.06 bar respectively. The figures show an increase in cake thickness with throughput volume of the effluent filtered. There is linearity between cake thickness and throughput volume, and therefore with these assumptions fouling is proportional to throughput volume and cake resistance is proportional to cake thickness. It takes some amount of throughput volume, about 50 L/m^2, to start building appreciable amount of cake thickness for AC+0.8 and PF+0.45 membranes. This observation suggest that it takes sometime to clog these membranes' pores.

Figures 22 and 23 suggest that the hydrophobic membranes, AC-0.45, PF – 0.45 and PF-0.3 membranes have build a considerably thicker cake than other membranes which is not true because these particular membranes allow lower volume of filtrate compared to other

membranes for the same period of filtration run. The fact that these membranes allowed less water through suggest that the resistance to flux could not be due to cake resistance, but to in-pore fouling. In the microfiltration of natural organic matter, Linhua et al., (2001) observed that the rate of flux decline for hydrophobic membranes was considerably greater than for the hydrophilic membranes. They observed that in microfiltration of prefiltered water fouling of hydrophilic membranes was greatly reduced, but was not in hydrophobic membranes. This observation suggest that particle deposition was a major fouling factor for hydrophilic membranes while for hydrophobic membranes fouling was mainly due to interactions between the organic materials and the membrane. Likewise, it could be that for AC-0.45, PF-0.45 and PF-0.3 membranes the fouling is not mainly due to particle deposition, but rather due to interaction between organic matter in the primary effluent and the membranes.

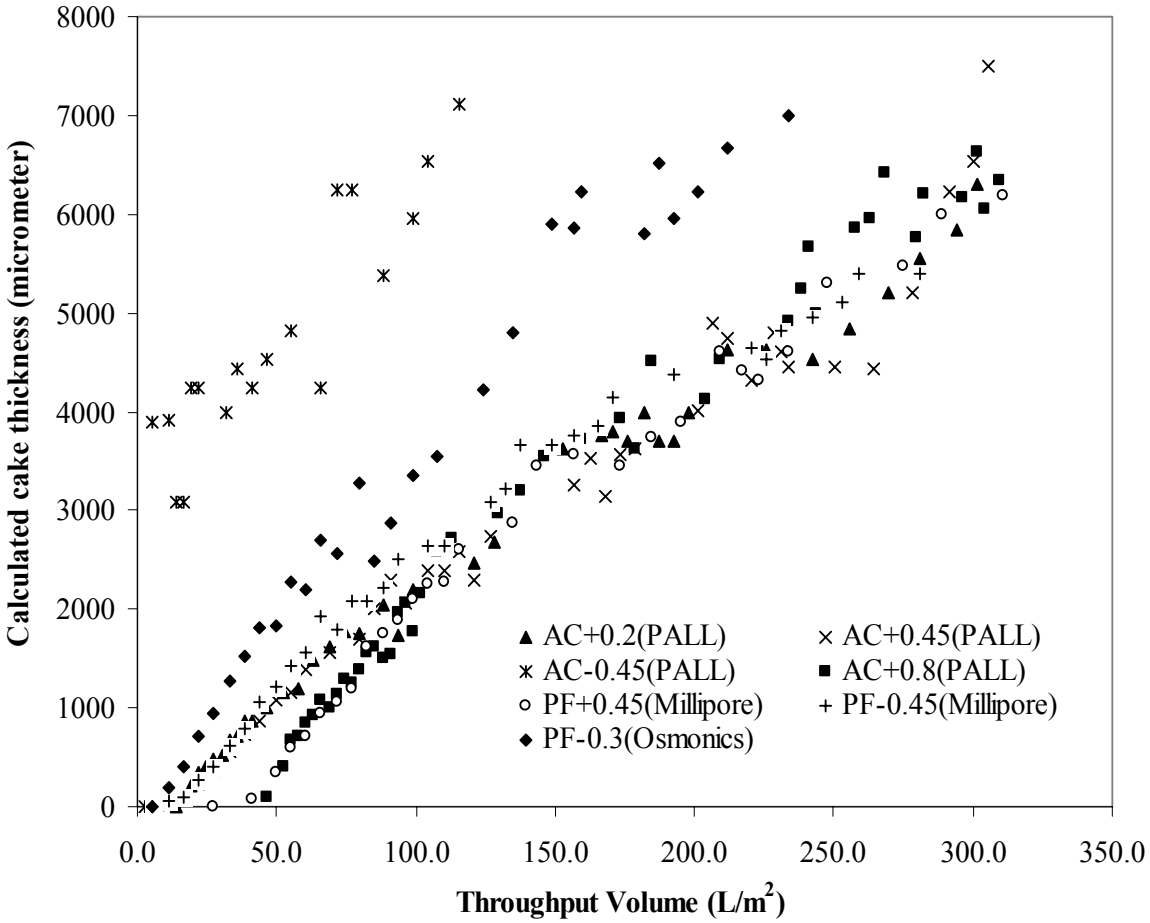

Figure 22 Calculated cake thickness (based on Equation 10) as a function of throughput volume for different membranes operated at 1.03 bar, assumes $d_p = 0.5$, $\varepsilon_c = 0.4$ and $\psi=1$

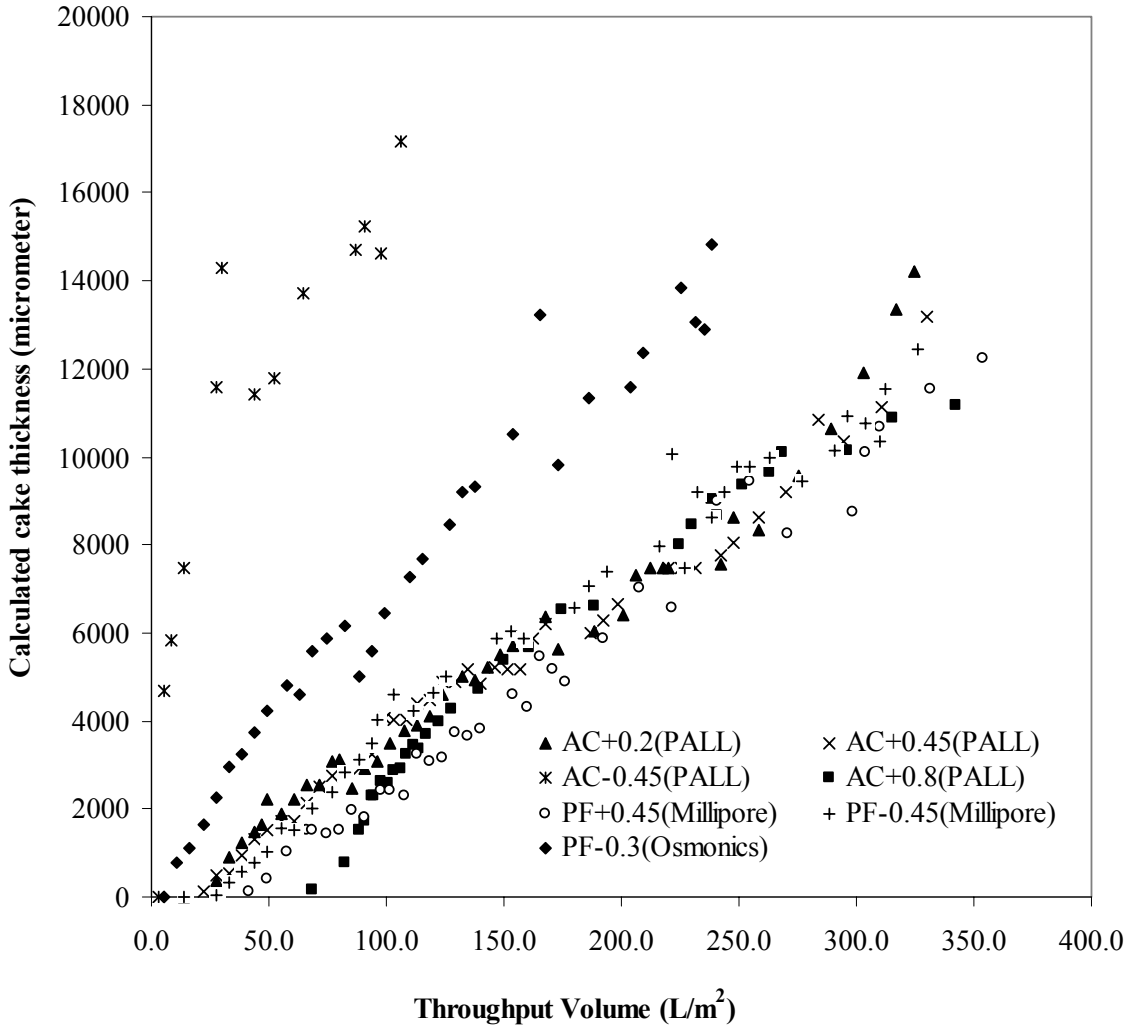

Figure 23 Calculated cake thickness (based on equation 4) as a function of throughput volume for different membranes operated at 2.06 bar, assumes d_p = 0.5, ε_c= 0.4 and ψ=1

3.3.2 Estimation of Cake Thickness Based on Suspended Solids Concentration

The concentration of the total suspended solids from ALCOSAN was an average of 52.6 mg/l. The volatile suspended solids range from 75-80% of the total suspended solids (Gary Yakub, ALCOSAN). The density of the primary effluent solids was assumed to be 1 g/cm^3 (Zeman et al., 1996 and Metcalf and Eddy 2003). If all the suspended solids get trapped on the surface of the membranes then Figures 24 and 25 represent the cake formation on the surface of the membranes with respect to time at 1.03 bar and 2.06 bar respectively. The assumption made is that deposition and buildup of the suspended solids on the membranes has got nothing to do with the membrane structure, but rather it is only dependent on the amount of throughput volume. Figure 24 and 25 show that the three hydrophobic membranes are developing the cake less fast than the rest of the membranes a phenomenon attributable to the fact that they are letting less water pass through. The difference in cake build up for the hydrophilic membranes is quite substantial at the beginning, but the differences diminish towards the end of the filtration run indicating that for these membranes cake thickness is about the same. Figure 26 is a mass balance showing that the build up of cake layer for all the membranes is directly proportional to the throughput volume.

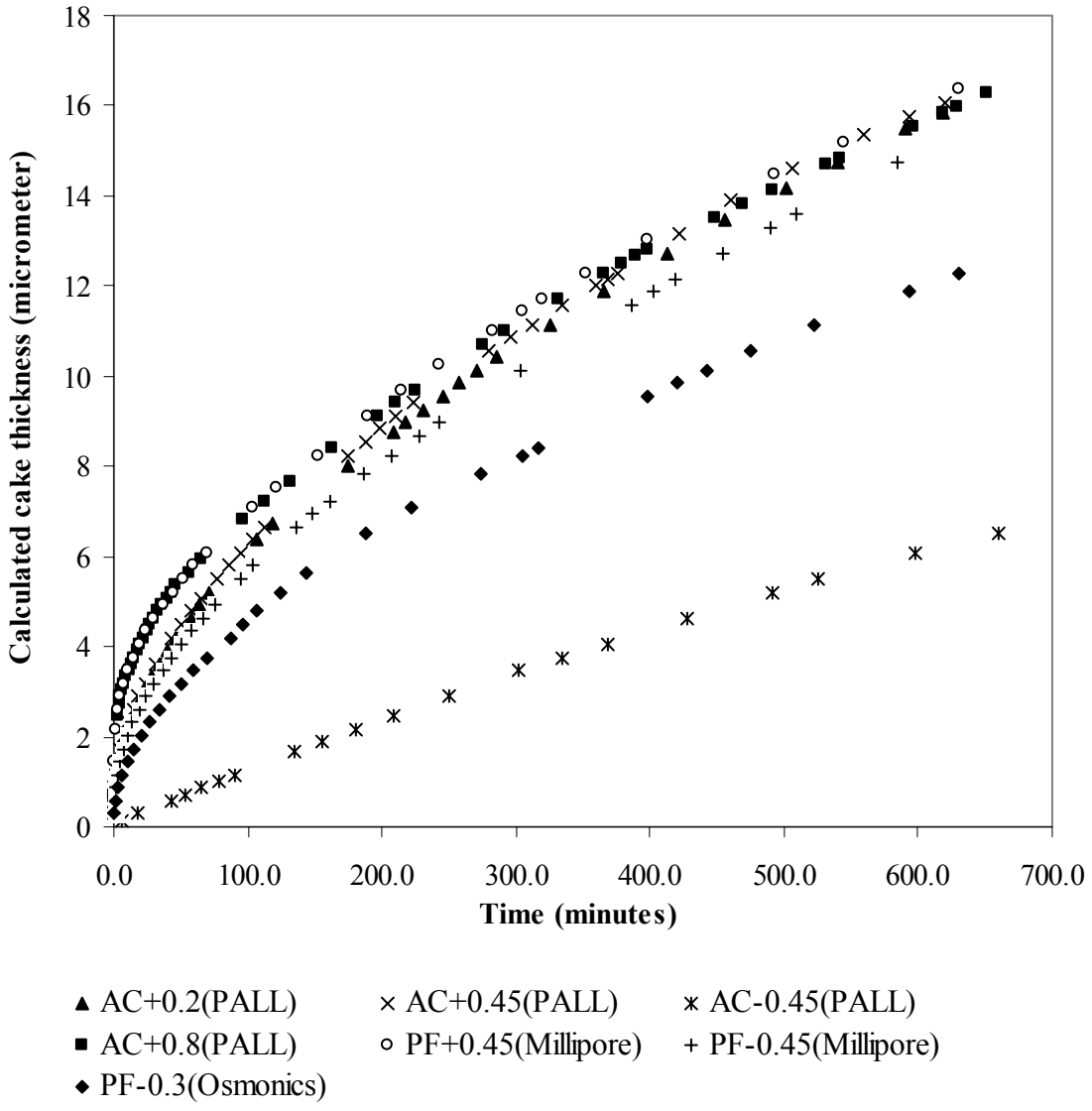

Figure 24 Calculated maximum possible cake thickness (based on suspended solids concentration) as a function of time for different membranes operated at 1.03 bar

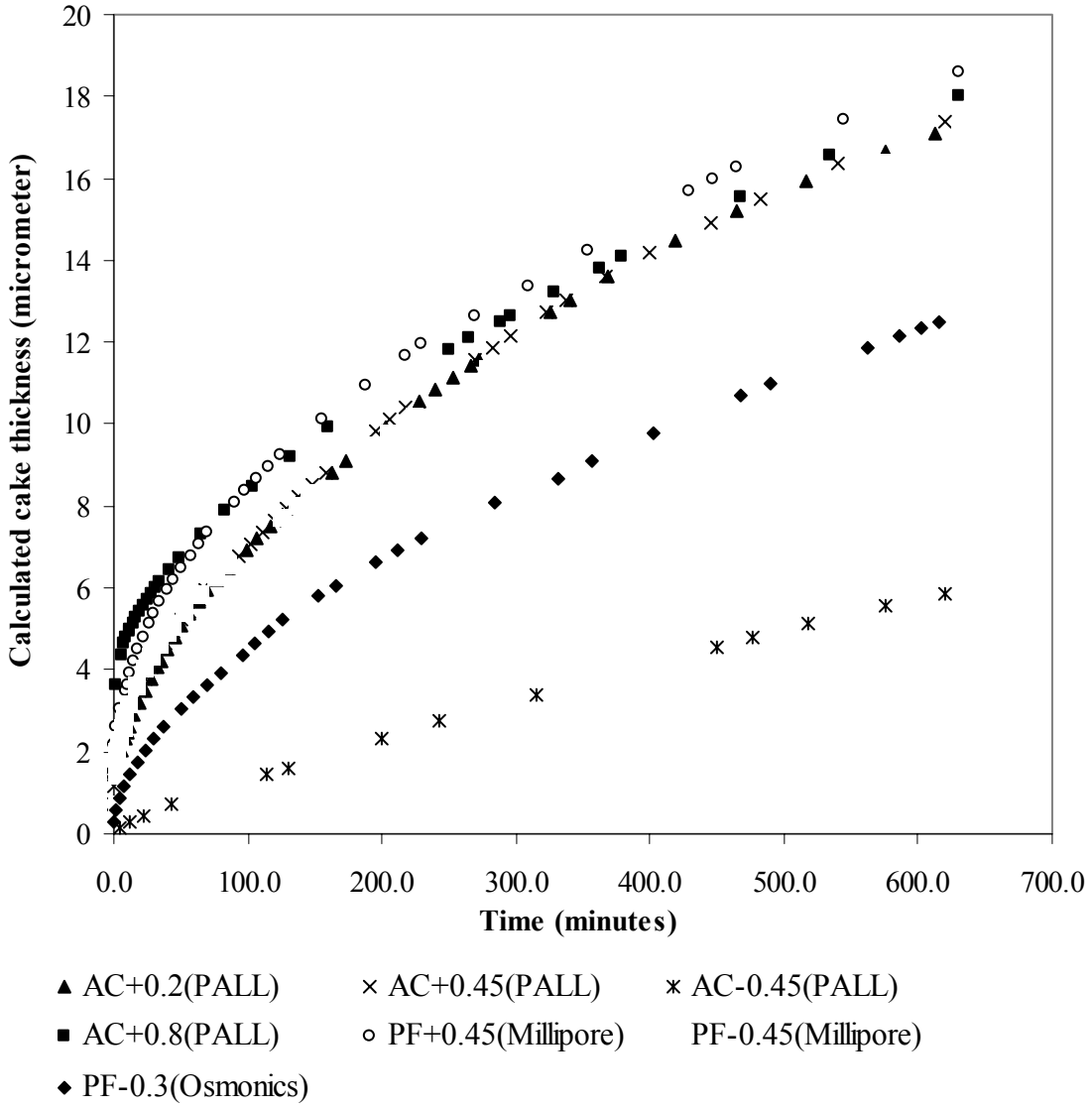

Figure 25 Calculated maximum possible cake thickness (based on suspended solids concentration) as a function of time for different membranes operated at 2.06 bar

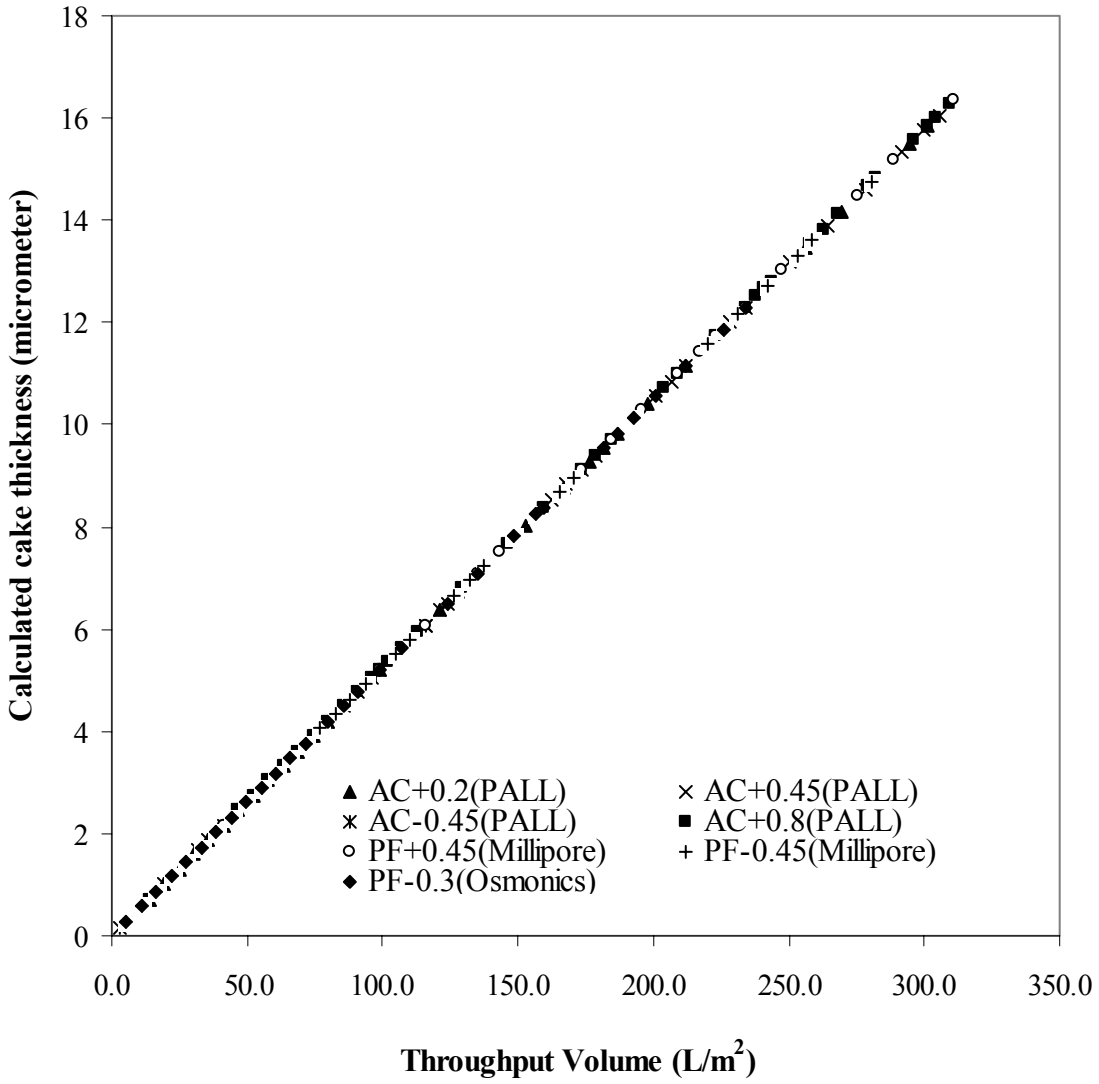

Figure 26 Calculated mass balance showing maximum possible cake thickness (based on suspended solids concentration) as a function of throughput volume for different membranes operated at 1.03 bar

3.3.3 Comparison of Cake Thickness When ψ = 1 and ψ = 0.1

Tables 10 and 11 show cake thickness based on Equation 10 for each membrane at 1.03 bar when ψ is assumed to be 1 and 0.1 respectively. Table C-28 and -29 show cake thickness when pressure = 2.06 bar. The average suspended particles diameter are assumed to be 0.1, 0.5 and 1 μm, and $\varepsilon_c = 0.4$. The tables also show calculated cake thickness based on the suspended solids concentration. The tables (Tabel 10 and C-28) suggest that an increase in the diameter of the suspended particles and increase in applied pressure can result in increase in the cake thickness. This cake thickness is needed to bring about the obtained cake resistance, R_c.

The choice of spherecity greatly affects the size of the cake thickness. The particle size distribution is not known, however Zeman et al., (1996) suggests that the average particle size of particles that deposit on the microfiltration membranes is 1 μm. If 1 μm diameter is representative of the average particle diameter, then the cake thickness is still high even when ψ = 0.1. For 1 μm particle diameter, values of ψ need to be lower than 0.1 for the cake thickness due to Equation 10 to match that due to suspended solids concentration. The assumed porosity may not be a true representative of the porosity of the primary effluent cake. However, if these assumed values (ψ = 0.1, K= 5, $\varepsilon_c = 0.4$, $d_p = 1$) are a close representative, then the high build up of resistance during filtration may not be mainly due to the cake, but rather to in-pore fouling. The hydrophobic membranes could not have developed such high cake thickness because they allowed less throughput volume to filter through than other membranes. This suggests that interactions between the organic particles and the membrane material could offer this high resistance (Section 3.3.1). For the hydrophilic membranes, which have a higher throughput volume, the resultant resistance may be due to the blocking of the pores and other factors like interaction between volatile suspended solids (organic) and the membrane, in other words the

chemistry between organic substances and the membrane material may favor in-pore fouling. If the cake thickness is the main contributor of resistance and the assumptions made are true then the Carmarn-Kozeny equation could be a good model of what happens during microfiltration of primary effluent, and could mean that higher cake thicknesses are needed for the encountered cake resistances. On the contrary if the assumptions are representative and the cake is the main form of resistance to flow then Carman-Kozeny does not give a good correlation between the predicted sewage cake thickness and that due suspended solids concentration.

Table 10 Cake thickness and cake resistance for each membrane at 1.03 bar for average suspended particles diameter of 0.1, 0.5 and 1 μm when ψ = 1

Membranes	Final R_c at 1.03bar ($1/m * 10^{10}$)	Final [1]ΔX_c(μm) for various particle diameter, d_p (μm)			[2]ΔX_c, μm
		0.1	0.5	1	
AC+0.2(PALL)	2560.0	[3]252.0	6303.0	25212.0	15.8
AC+0.45(PALL)	3044.0	300.0	7492.0	29968.0	16.1
AC-0.45(PALL)	3510.0	346.0	8659.0	34637.0	6.5
AC+0.8(PALL)	2577.0	254.0	6364.0	25375.0	16.3
PF+0.45(Millipore)	2516.0	248.0	6197.0	24790.0	16.4
PF-0.45(Millipore)	2192.0	216.0	5393.0	21572.0	14.8
PF-0.3(Osmonics)	2843.0	280.0	7006.0	28064.0	12.3

[1]ΔX_c= calculated cake thickness based on Equation 10, K = 5, ε = 0.4

[2]ΔX_c= maximum possible cake thickness based on a mass balance for suspended solids concentration

[3]Refer to Appendix C for the example of calculations

Table 11 Cake thickness and cake resistance for each membrane at 1.03 bar for average suspended particles diameter of 0.1, 0.5 and 1 μm when ψ = 0.1

Membranes	Final R_c at 1.03bar ($1/m * 10^{10}$)	Final $^1\Delta X_c$(μm) for various particle diameter, d_p (μm)			$^2\Delta X_c$, μm
		0.1	0.5	1	
AC+0.2(PALL)	2560.0	^{3}2.5	63.0	252.1	15.8
AC+0.45(PALL)	3044.0	3.0	74.9	299.7	16.1
AC-0.45(PALL)	3510.0	3.5	86.6	346.4	6.5
AC+0.8(PALL)	2577.0	2.5	63.4	253.8	16.3
PF+0.45(Millipore)	2516.0	2.5	62.0	247.9	16.4
PF-0.45(Millipore)	2192.0	2.2	53.9	215.7	14.8
PF-0.3(Osmonics)	2843.0	2.8	70.1	280.6	12.3

$^1\Delta X_c$= calculated cake thickness based on Equation 10, K = 5, ε = 0.4
$^2\Delta X_c$= maximum possible cake thickness based on a mass balance for suspended solids concentration
^{3}Refer to Appendix C for the example of calculations

3.3.4 Estimated Cake Porosity Based on the Total Suspended Solids Concentration

Tables 12 and 13 estimate porosity by setting cake thickness, ΔX_c (Equation 10) equal to maximum possible cake thickness ($^1\Delta X_c$) based on a mass balance for suspended solids concentration. The porosity values are based on ψ = 1 and 0.1 at 1.03 bar. Table C-30 and C-31 show porosity values when pressure is 2.06 bar. The cake thicknesses due to suspended solids concentration at the two pressures (Table 12 and 13 versus Table C-30 and C-31) are pretty close suggesting that the cake could be compressible. This could explain why the flux converges to the same value at all pressures (Section 3.2.1) and pore size because higher pressures compress the cake thus decreasing its porosity (Vyas et al., 2000). The porosity of the cake is higher when ψ = 0.1. It is likely that the average diameter of the particles which get trapped on the membrane

surface is 1 μm (Zeman et al., 1996). For the particle diameter of 1 μm the values of porosity are lower than the porosity of clay (0.3 – 0.5) (Barnes, 1995). Vyas et al., (2000) observed that the steady state porosity of lactalbumin particles during crossflow microfiltration was 0.2. They observed that there was no significant effect of TMP on the steady state porosity of the cake.

If the particle diameter of 1 μm is representative and the cake porosity cannot be lower than 0.3 (porosity of clay) then the lower porosity values obtained in this analysis suggest that the compressibility of the cake cannot fully explain the significant total resistance to the flow through thin-film composite membranes in dead-end filtration mode. It is more likely that the heterogeneous solids present in this wastewater are causing internal fouling of the membrane pores. Such conclusion is supported by the fact that membranes with larger pores (e.g., AC+0.8 in Section 3.2.3) exhibited significant delay in resistance build up because the internal fouling is delayed by the easier passage of suspended solids through larger pores. The hydrophobic membranes especially AC-0.45 membrane could not have developed a cake faster enough to have a porosity lower than other membranes. This suggests that this low porosity cannot be due to the compressibility of the cake but rather to other factors (Section 3.3.1). As explained in Section 3.3.3 the assumption made for porosity, particle size, K constant and spherecity may not be representative of the real values and therefore Carman-Kozeny may not be a good model for dead-end microfiltration of primary sewage effluent.

Changing porosity, spherecity and other constants in Carman-Kozeny equation gives various values of porosity and cake thickness. True values of porosity, particle size distribution and the spherecity are needed to better understand the causes of major form of fouling. The determination of what could be the major form of fouling between cake thickness and in-pore fouling is beyond the scope of this research.

Table 12 Required cake porosity at TMP of 1.03 bar when ψ = 1

Membrane	Final R_c at ($1/m * 10^{10}$)	[1]ΔX_c (µm)	Porosity, ε_c		
			Diameter of Cake Solids, d_p (µm)		
			0.1	0.5	1
AC+0.2	2560	15.8	0.193	0.072	0.047
AC+0.45	3044	16.1	0.185	0.069	0.043
AC-0.45	3510	6.5	0.136	0.049	0.032
AC+0.8	2577	16.3	0.195	0.073	0.047
PF+0.45	2516	16.4	0.196	0.074	0.047
PF-0.45	2192	14.8	0.198	0.075	0.048
PF-0.3	2843	12.3	0.174	0.065	0.042

[1]ΔX_c= calculated cake thickness based on Equation 10, K = 5

Table 13 Required cake porosity at TMP of 1.03 bar when ψ = 0.1

Membrane	Final R_c at ($1/m * 10^{10}$)	[1]ΔX_c (µm)	Porosity, ε_c		
			Diameter of Cake Solids (µm)		
			0.1	0.5	1
AC+0.2	2560	15.8	0.580	0.284	0.193
AC+0.45	3044	16.1	0.565	0.272	0.185
AC-0.45	3510	6.5	0.460	0.203	0.136
AC+0.8	2577	16.3	0.583	0.285	0.195
PF+0.45	2516	16.4	0.586	0.288	0.196
PF-0.45	2192	14.8	0.589	0.290	0.198
PF-0.3	2843	12.3	0.545	0.258	0.174

[1]ΔX_c= calculated cake thickness based on Equation 10, K = 5

3.4 Permeate Quality

Tables B-21 to B-27 in Appendix B show the COD and bacterial rejections of each membrane.

3.4.1 Bacterial Rejection

All the membranes were evaluated in three filtration runs; a) filtration at fixed pressure of 1.03 bar, b) filtration at fixed pressure of 2.06 bar and c) filtration at increasing pressure. Three permeate samples were collected at both 1.03 bar and 2.06 bar filtration runs and four samples were collected during the filtration run at increasing pressures. All the samples were then tested for fecal coliforms, *Escherichia coli* and *enterococci* counts.

The experimental results shown in Table 14, 15 and 16 reveal that AC+0.2, AC+0.45, AC-0.45, PF+0.45 and PF-0.45 membranes achieved complete bacterial rejection at fixed TMPs of 1.03 bar and 2.06 bar. These membranes offer complete barrier to the passage of the fecal coliform, *Escherichia coli* and *enterococci* as shown by low detection limits. Samples 1 and 3 indicated on Table 14, 15 and 16 were collected at the beginning and end of the filtration run, respectively. The fact that 0 cfu/100ml was recorded at the beginning of the run suggests that the membrane structure itself offers the barrier to the passage of bacteria. Such an observation is expected because the test organisms range in size from 0.5 μm to 4 μm (Metcalf and Eddy, 2003).

Table 14 Permeate quality in terms of fecal coliforms colonies (cfu/100ml) at 1.03 bar and 2.06 bar

Membranes	Fecal coliforms colonies(cfu/100ml) Unfiltered primary effluent sample = 3.2×10^6 cfu/100ml					
	1.03 bar			2.06 bar		
	[1]Sample 1	[2]Sample 2	[3]Sample 3	[1]Sample 1	[2]Sample 2	[3]Sample 3
AC+0.2(PALL)	0	0	0	0	0	0
AC+0.45(PALL)	0	0	0	0	0	0
AC-0.45(PALL)	0	0	0	0	0	0
AC+0.8(PALL)	4.1×10^5	3.1×10^4	1.7×10^4	4.2×10^5	5.7×10^4	4.0×10^4
PF+0.45(Millipore)	0	0	0	0	0	0
PF-0.45(Millipore)	0	0	0	0	0	0
PF-0.3(Osmonics)	331	30	10	700	17	0

[1]Sample 1= beginning, [2]Sample 2 = middle and [3]Sample 3 = end of a ten hour filtration run

Table 15 Permeate quality in terms of *E coli* colonies (cfu/100ml) at 1.03 bar and 2.06 bar

Membranes	*E coli* colonies(cfu/100ml) Unfiltered primary effluent sample = 2.4×10^6 cfu/100ml					
	1.03 bar			2.06 bar		
	[1]Sample 1	[2]Sample 2	[3]Sample 3	[1]Sample 1	[2]Sample 2	[3]Sample 3
AC+0.2(PALL)	0	0	0	0	0	0
AC+0.45(PALL)	0	0	0	0	0	0
AC-0.45(PALL)	0	0	0	0	0	0
AC+0.8(PALL)	2.4×10^5	3.1×10^4	1.7×10^4	2.1×10^5	2.6×10^4	2.5×10^4
PF+0.45(Millipore)	0	0	0	0	0	0
PF-0.45(Millipore)	0	0	0	0	0	0
PF-0.3(Osmonics)	0	0	0	0	0	0

[1]Sample 1= beginning, [2]Sample 2 = middle and [3]Sample 3 = end of a ten hour filtration run

Table 16 Permeate quality in terms of *enterococci* colonies (cfu/100ml) at 1.03 bar and 2.06 bar

Membranes	***Enterococci* colonies(cfu/100ml)** Unfiltered primary effluent sample = $1.5x10^5$ cfu/100ml					
	1.03 bar			**2.06 bar**		
	[1]Sample 1	**[2]Sample 2**	**[3]Sample 3**	**[1]Sample 1**	**[2]Sample 2**	**[3]Sample 3**
AC+0.2(PALL)	0	0	0	0	0	0
AC+0.45(PALL)	0	0	0	0	0	0
AC-0.45(PALL)	0	0	0	0	0	0
AC+0.8(PALL)	$8.3x10^4$	360	302	$5.3x10^3$	800	532
PF+0.45(Millipore)	0	0	0	0	0	0
PF-0.45(Millipore)	0	0	0	0	0	0
PF-0.3(Osmonics)	10	0	0	20	0	0

[1]Sample 1= beginning, [2]Sample 2 = middle and [3]Sample 3 = end of a ten hour filtration run

However, the PF-0.3 membrane did not offer complete barrier to the passage of the bacteria as shown in Tables 14, 15 and 16. The permeate has an initial fecal coliforms colony count of 331 per 100ml for the 1.03 bar filtration run and of 700 for the 2.06 bar indicating that higher pressure was able to force more bacteria through this membrane. This breakthrough in fecal coliforms diminished progressively throughout the runs resulting in very low colony counts at the end of the filtration runs. The same behavior was also observed for *E coli* and *enterococci* (Table 14 and 16) with high colony counts in the permeate at the start, lower in the middle and much lower at the end of the filtration run. The main concern with experimental results with the PF-0.3 membrane was that it allowed bacterial passage into the permeate even though it is supposed to have smaller pores than the 0.45 μm membranes investigated in this study. To ensure that there were no leakage between the membrane and the rubber O-ring the membrane was replaced by a sheet of impervious plastic and subjected to the same pressure. The test

showed that the plastic completely stopped flow of water from the cell. Therefore the bacterial counts recorded in the permeate are due to passage through the membrane only. One possible explanation is that this particular membrane had a very wide pore size distribution and contained some pores that are much bigger than 0.3 μm.

The AC+0.8 membrane allowed high initial breakthrough of fecal coliforms, *enterococci* and *Escherichia coli* bacteria for the 1.03 bar and 2.06 bar filtration runs and these colony counts in the permeate diminished progressively with the filtration run for both pressures. The diminishing colony counts in the permeate may be attributable to the fact that the filtration cake that is building up on the membrane surface and the clogging of the pores that otherwise cause membrane fouling is also helping to reduce passage of bacteria. Till et al., (1998) observed that the buildup of material on the surface of the membrane helps to stop bacteria from passing through. The colony counts are higher for the 2.06 bar filtration run an indication that pressure increases the number of colonies in the permeate.

The steady state colony counts for the filtration runs at increasing pressure are quite low for the first samples at 1.03 bar for all the membranes as shown in Tables 17, 18 and 19 because the flux had already reached steady state at the time of sampling and hence the filtration cake was already in place. For the PF-0.3 membrane colony counts of 32 cfu/100ml for fecal coliform were recorded at 1.03 bar. Colony counts at 2.06 bar dropped to 0 cfu/100ml then reached 10 cfu/100ml at 3.09 bar and 4.12 bar. Similar behavior was observed for *E. coli* (Table 18 and 19), while analysis for *enterococci* resulted in low detection limits. For the AC+0.8 membrane at different pressures, the colonies counts for fecal coliforms, *Escherichia coli* and *enterococci* increased in the permeate with an increase in pressure. The results suggest that for bigger pore size membranes pressure increases the amount of bacteria in the permeate.

Table 17 Steady State permeate quality in terms of fecal coliforms colonies (cfu/100ml) at various pressures.

Membranes	Fecal coliforms colonies(cfu/100ml) Samples at various pressures			
	1.03 bar	2.06 bar	3.09 bar	4.12 bar
AC+0.2(PALL)	0	0	0	0
AC+0.45(PALL)	0	0	0	0
AC-0.45(PALL)	0	0	0	0
AC+0.8(PALL)	$5.2x10^4$	$9.1x10^4$	$1.3x10^5$	$5.0x10^5$
PF+0.45(Millipore)	0	0	0	0
PF-0.45(Millipore)	0	0	0	0
PF-0.3(Osmonics)	32	0	10	10

Table 18 Steady State permeate quality in terms of *E coli* colonies (cfu/100ml) at various pressures.

Membranes	*E coli* colonies(cfu/100ml) Samples at various pressures			
	1.03 bar	2.06 bar	3.09 bar	4.12 bar
AC+0.2(PALL)	0	0	0	0
AC+0.45(PALL)	0	0	0	0
AC-0.45(PALL)	0	0	0	0
AC+0.8(PALL)	$1.3x10^4$	$3.3x10^4$	$3.8x10^4$	$5.0x10^4$
PF+0.45(Millipore)	0	0	0	0
PF-0.45(Millipore)	0	0	0	0
PF-0.3(Osmonics)	0	0	10	10

Table 19 Steady State permeate quality in terms of *enterococci* colonies (cfu/100ml) at various pressures.

Mebranes	*Enterococci* colonies(cfu/100ml) Samples at various pressures			
	1.03 bar	2.06 bar	3.09 bar	4.12 bar
AC+0.2(PALL)	0	0	0	0
AC+0.45(PALL)	0	0	0	0
AC-0.45(PALL)	0	0	0	0
AC+0.8(PALL)	228	355	826	992
PF+0.45(Millipore)	0	0	0	0
PF-0.45(Millipore)	0	0	0	0
PF-0.3(Osmonics)	0	0	0	0

3.4.2 COD

Table 20 summarizes COD percentage rejections by the membranes tested in this study. The COD test was done on the same sample as in bacterial analysis. There is increased rejection of COD, though very small, with extended filtration runs. These small rejections suggest that most of the COD could be soluble and hence passing through. The initial condition of the primary effluent sample could have an impact on the COD values of the permeate. The fact that the primary effluent was sampled on different dates makes it impossible to make reasonable comparisons of COD rejections of each membrane. Wastewater samples with higher suspended matter would have larger contribution to the creation of the filtration cake on the membrane, thus improving the filtration mechanism. The AC+0.8 and AC+0.45 membranes have some of the lowest rejection values. Table B-21 to B-27 show that the initial COD values are different from date to date.

Table 20 Percentage COD rejection ($COD_{particulate}/COD_{total}$) by various membranes during filtration run

Pressure Bar	Sample	AC+ 0.2	AC+ 0.45	AC- 0.45	AC+ 0.8	PF+ 0.45	PF- 0.45	PF- 0.3
	1	57	23	31	28	55	50	32
1.03	2	58	27	35	28	69	51	36
	3	58	37	40	31	69	51	38
	1	57	23	29	25	66	56	36
2.06	2	57	32	38	28	69	61	38
	3	58	37	40	28	69	61	40
Various								
1.03	1	57	23	38	25	69	59	32
2.06	2	58	23	40	28	69	59	36
3.09	3	58	42	40	28	72	64	36
4.12	4	58	42	42	25	72	64	38

4.0 SUMMARY AND CONCLUSIONS

The study examined the use of microfiltration membranes in treating combined sewer overflow. Primary effluent water from ALCOSAN WWTP was used to simulate the combined sewer overflow.

Specific objectives of the study included:

a) To correlate membrane flux with membrane type and volumetric throughput.

b) To investigate the impact of surface chemistry (hydrophobic versus hydrophilic membranes) on flux rate.

c) To investigate the impact of pressure on permeate quality and flux

d) To evaluate if microfiltration can be used to remove fecal coliforms, *Escherichia coli*, *enterococci* and COD from the CSO.

e) To evaluate what membrane pore size and membrane type gives the best removal of bacteria and COD.

Membranes from Osmonics, PALL and Millipore were subjected to flux experiments at 15psi, 30psi and to various increments of pressures during a filtration run. The permeate samples were obtained and analyzed for COD and bacteria.

The following conclusions can be drawn from the test results:

1) Initial flux rates are directly related to the pore sizes for membranes with similar material, similar surface chemistry but different pore size. Hydrophilic membranes generally have higher initial fluxes than hydrophobic membranes. Based on the analysis of the cake resistance, cake thickness and porosity it was impossible to determine what could be the major form of fouling. The determination of what could

be the major form of fouling between cake thickness and in-pore fouling is beyond the scope of this research.

2) The steady state flux rates are independent of pressure and pore sizes therefore fouling becomes the only variable that controls flux rate at steady state.
3) Fouling layer reduces flux rate but increases bacterial rejection. Bacterial rejection increased with time for the AC+0.8 membrane and the PF-0.3 membrane.
4) Microfiltration membranes can be used to reduce fecal coliforms, *Escherichia coli*, *enterococci* and COD in the CSO water to non detectable limits. Not all membranes were able to completely filter out the bacteria. The AC+0.8 membrane and the PF-0.3 membrane failed to reduce the bacteria to 0 cfu/100ml. The AC+0.2, AC+0.45, AC-0.45, PF+0.45 and PF-0.45 membranes proved to be very effective in removing bacteria as evidenced by non detectable limits of bacteria (0 cfu/100ml) in the permeate and at all test conditions. These results meet EPA-recommended bacteria criteria (33 cfu/100ml for *enterococci* and 126 cfu/100ml for *E. coli* for steady state 30-day geometric mean). The results also meet the effluent limitations for ALCOSAN WWTP (200 cfu/100ml as a geometric mean for fecal coliforms for the period between May first and October thirty first).
5) All the membranes gave some COD removal efficiency with AC+0.45 membrane and AC+0.2 membranes giving the highest removal efficiency.
6) There is need for carrying out intensive tests on membranes before field application. This need is made apparent by the fact that some membranes gave results which were contrary to expectations. For instance, all 0.45 μm membranes provided a complete barrier for microorganisms and it would be safe to hypothesize that all membranes

with pore size small than this would likewise provide complete barrier. However, this was not the case because the PF-0.3 did not provide permeate free of microorganisms.

7) The choice of a membrane to be used in the field should be based on the membrane which completely removes bacteria. The design of a membrane treatment plant is based on steady state flux rate. Most of the membranes tested in this study gave similar flux rates towards the end of the filtration run. Assuming that the CSO event occurs for a period of about ten hours and that the membrane filtration plant is run throughout the occurrence of the CSO then AC+0.2, AC+0.45, AC-0.45, PF-0.45, and PF+0.45 would make the best choice for this treatment plant. If the initial fluxes were to be used in the design PF+0.45 membrane would be the overall best membrane as it gave higher initial fluxes.

5.0 FUTURE RESEARCH NEEDS

The analysis of the data has raised several questions which could not be answered in this research. The assumptions made on the behavior of the cake (spherecity, porosity, particle diameter, and compressibility of the cake) proved to be unsatisfactory.

- Further research has to be done on the porosity, spherecity, particle diameter and on other properties of a filtration sewage cake. Other models of flow through porous media need to be investigated.
- There is need to find out an effective cake thickness which would give a noticeable measurable cake resistance. The effect of volatile suspended solids and proteins that deposit on the membrane surface needs to be determined.
- Fouling adversely affects permeate flux and therefore this poses further research needs to curb fouling. Effect of changing the surface chemistry on the permeate flux need to be investigated.
- Effect of backpulsing the clogged up polymeric membranes needs to be looked into.
- Application costs of dead end filtration in the field need to be investigated.

APPENDIX A

Variation in Permeate Flux at Fixed TMPs and at Various Pressures

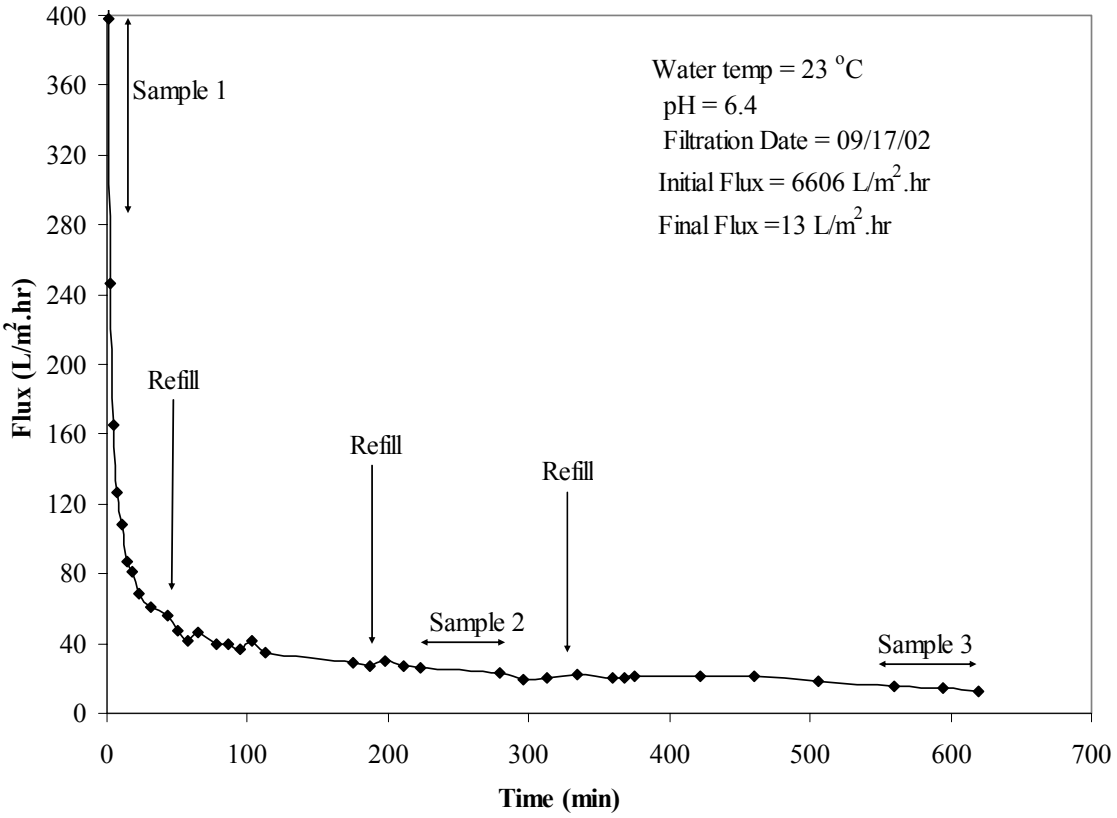

Figure A-27 Variation in permeate flux for AC+0.45 membrane at 1.03 bar

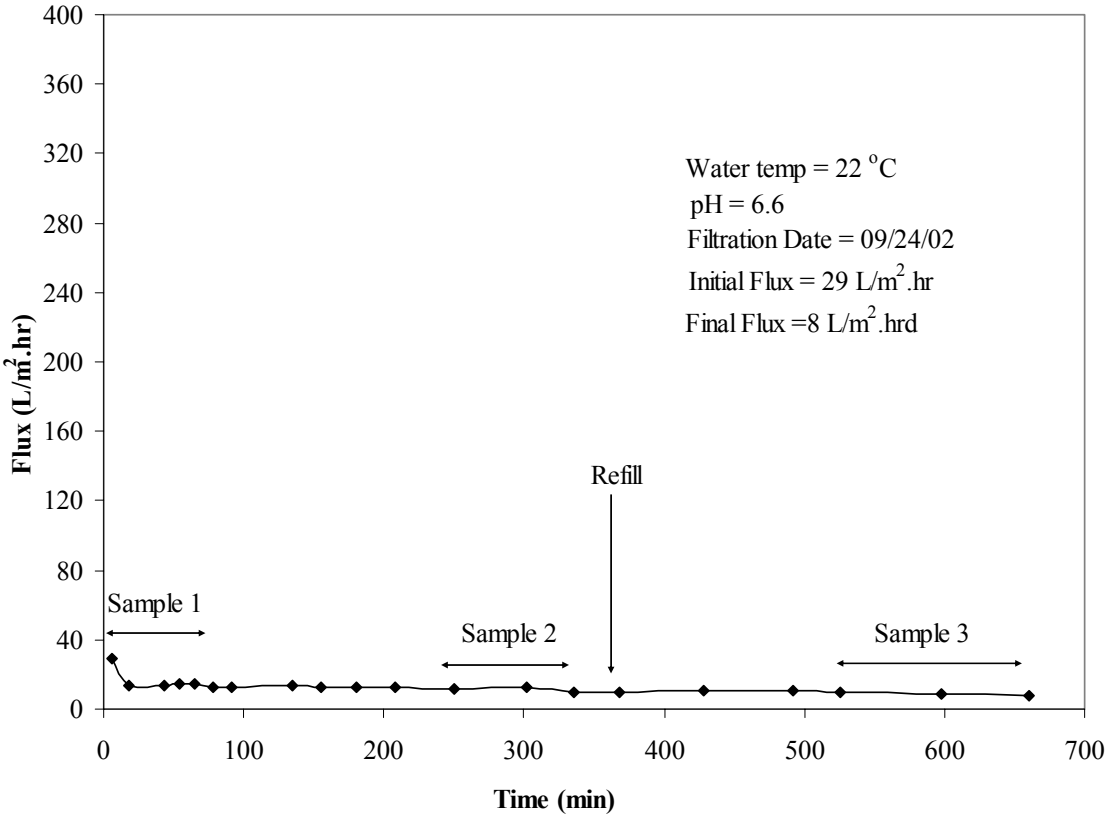

Figure A-28 Variation in permeate flux for AC-0.45 membrane at 1.03 bar

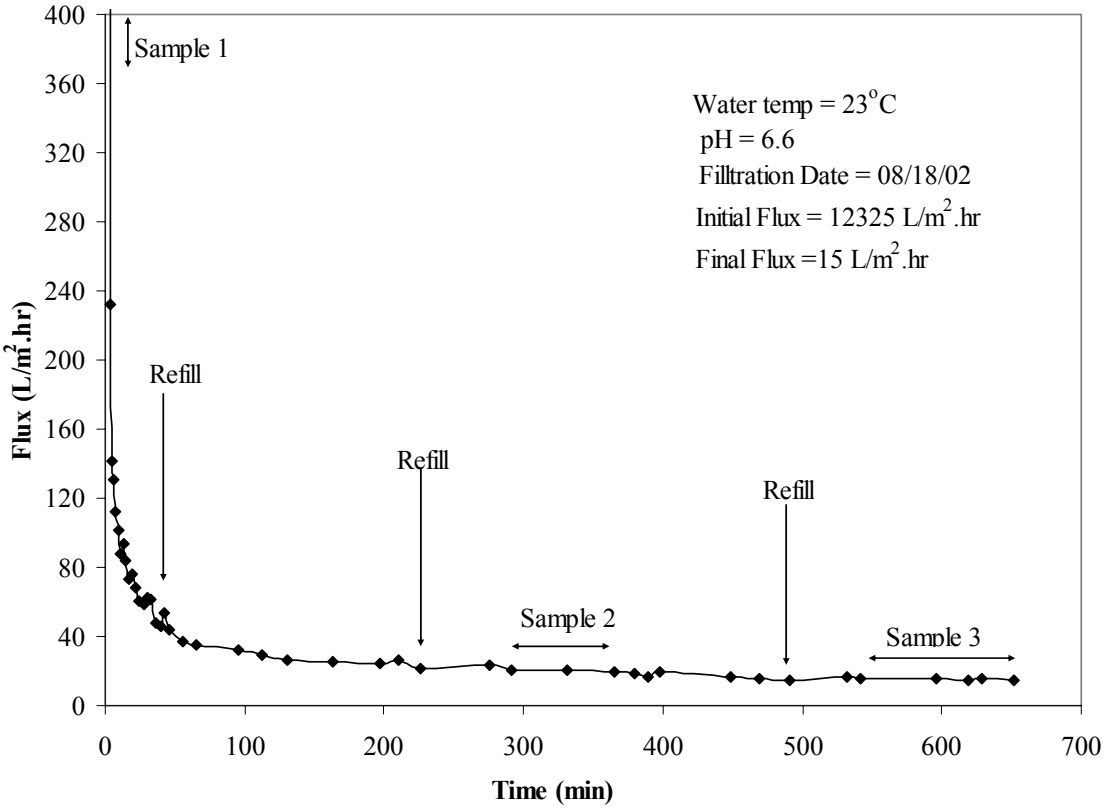

Figure A-29 Variation in permeate flux for AC+0.8 membrane at 1.03 bar

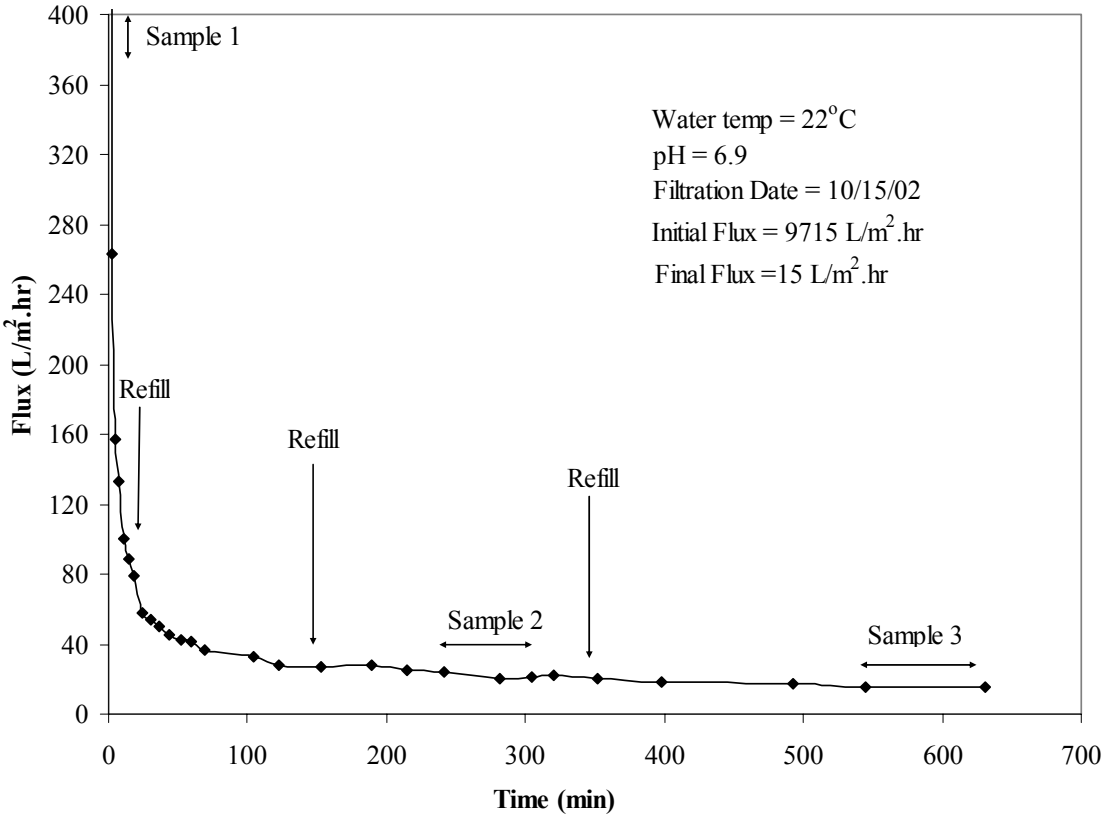

Figure A-30 Variation in permeate flux for PF+0.45 membrane at 1.03 bar

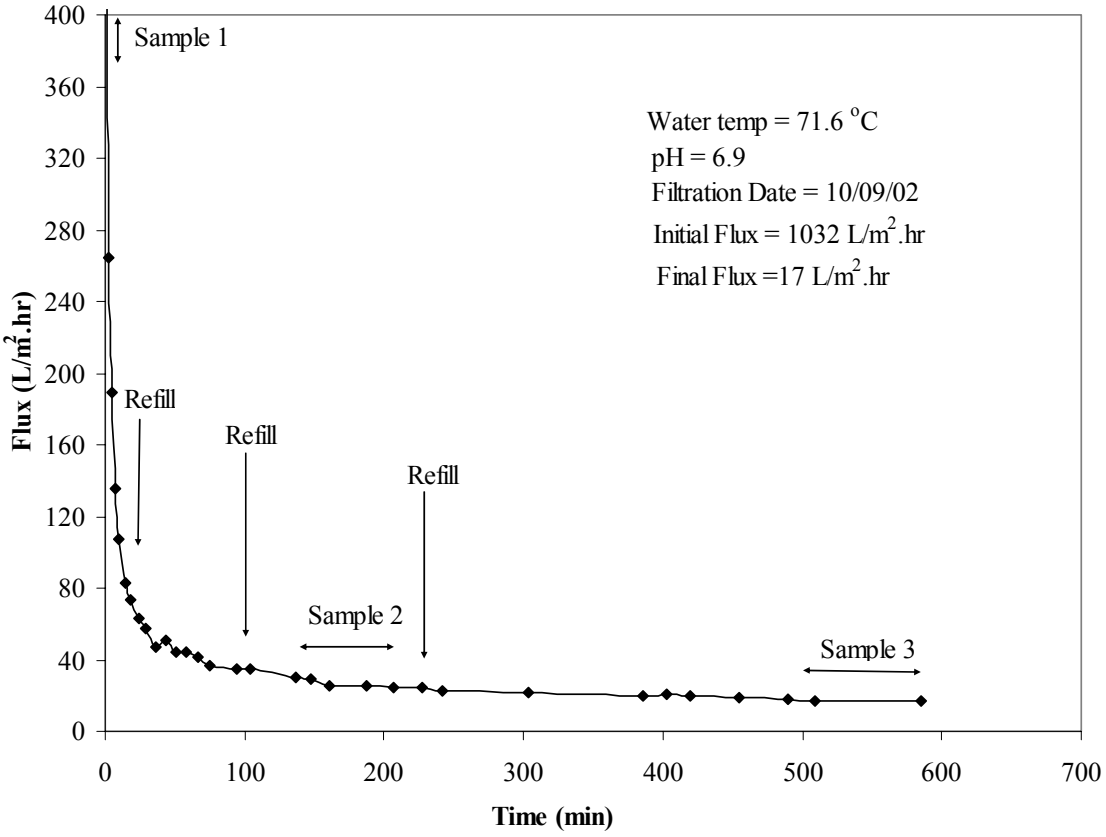

Figure A-31 Variation in permeate flux for PF-0.45 membrane at 1.03 bar

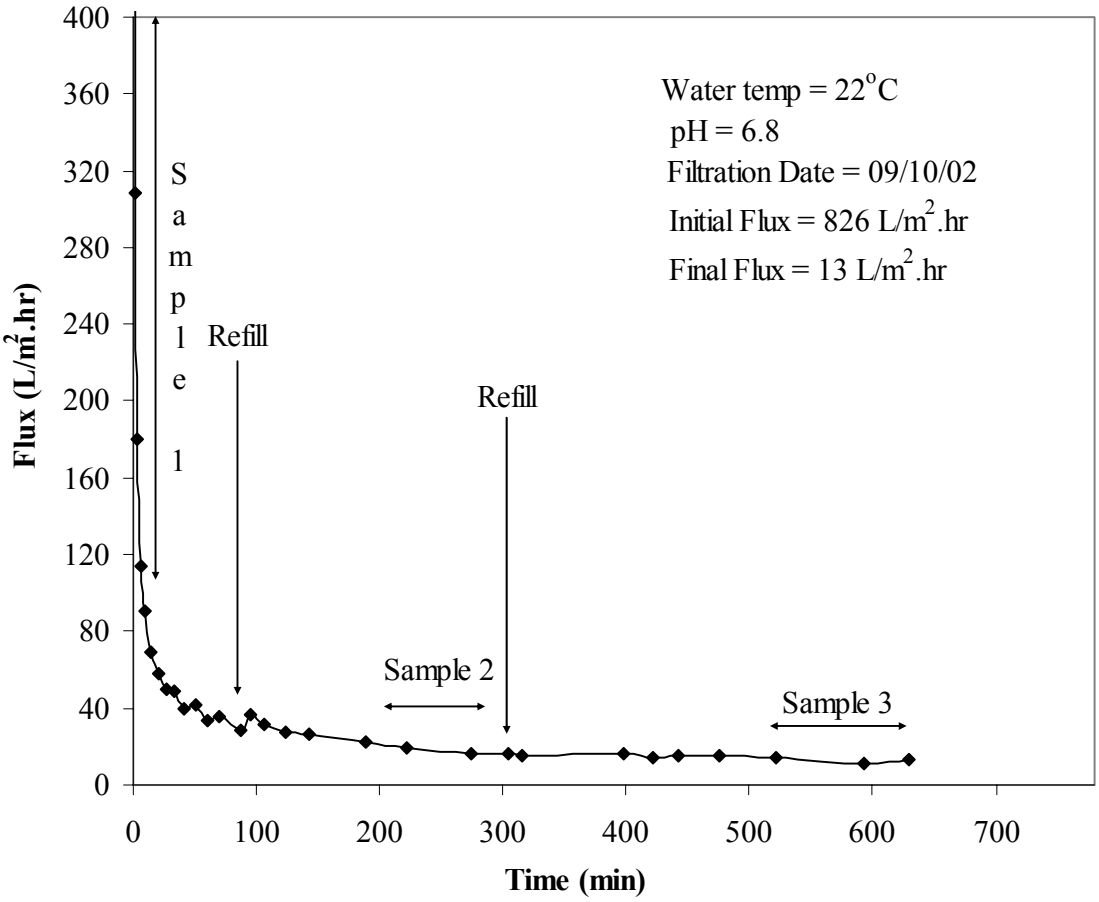

Figure A-32 Variation in permeate flux for PF-0.3 membrane at 1.03 bar

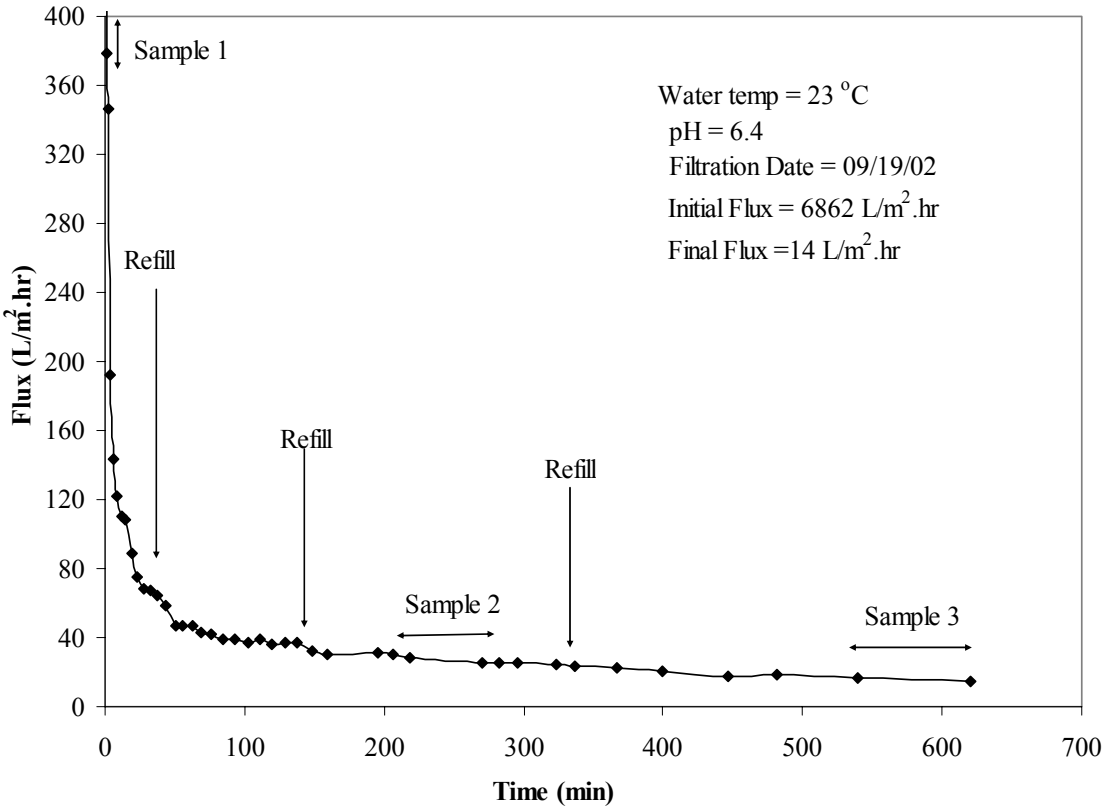

Figure A-33 Variation in permeate flux for AC+0.45 membrane at 2.06 bar

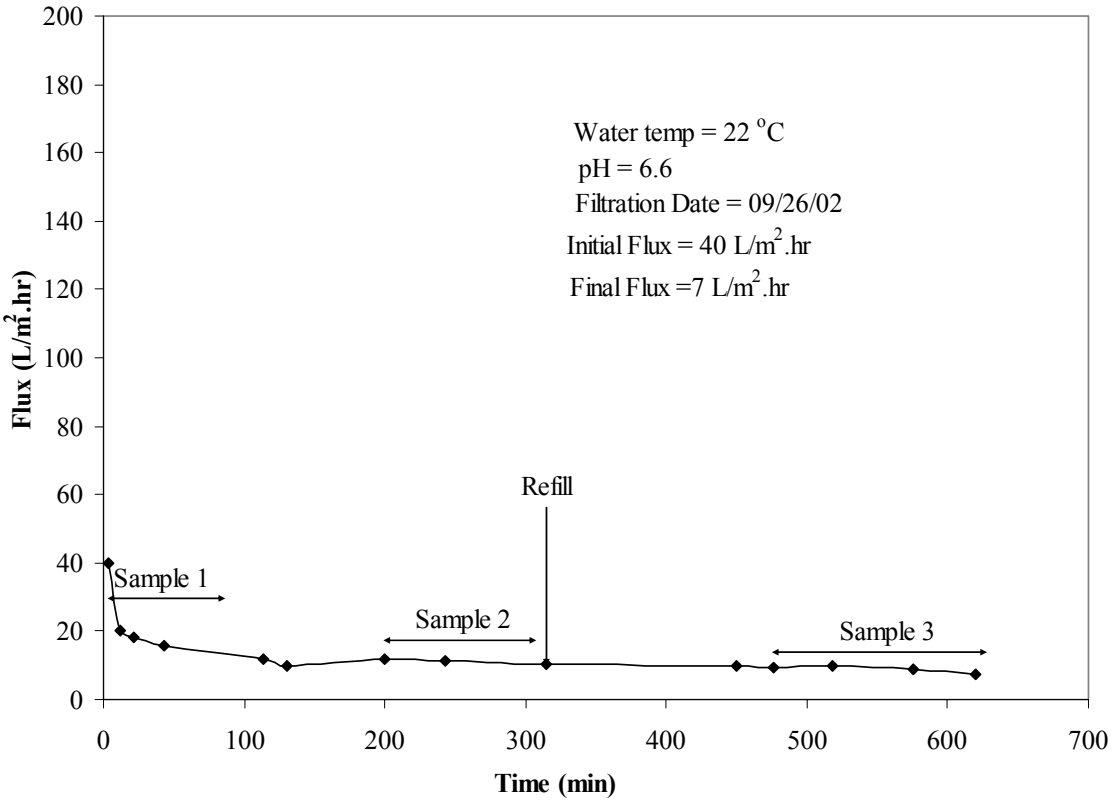

Figure A-34 Variation in permeate flux for AC-0.45 membrane at 2.06 bar

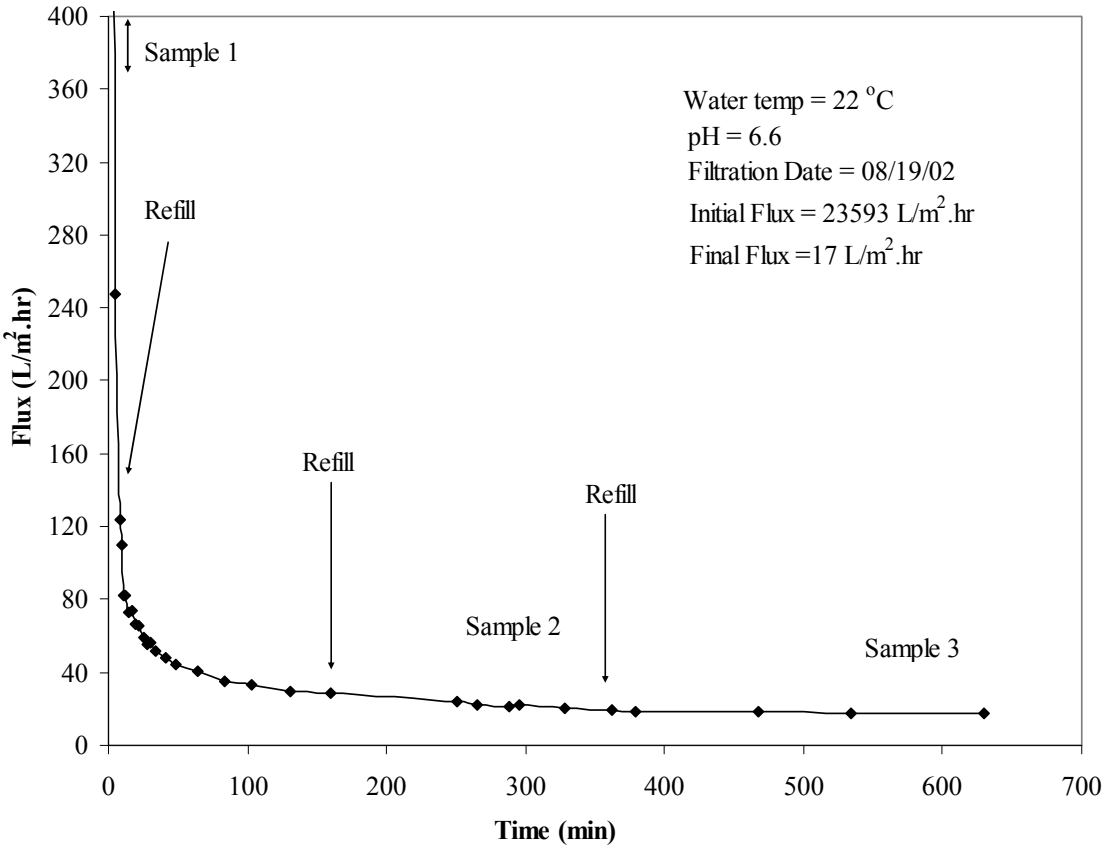

Figure A-35 Variation in permeate flux for AC+0.8 membrane at 2.06 bar

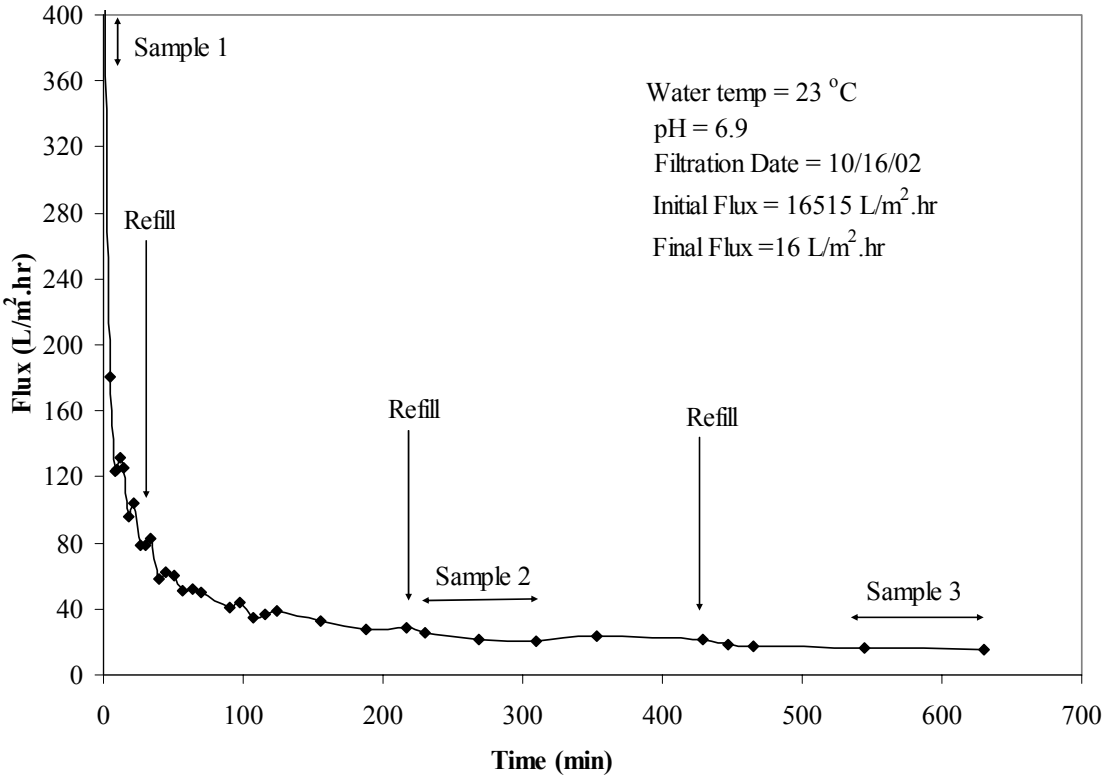

Figure A-36 Variation in permeate flux for PF+0.45 membrane at 2.06 bar

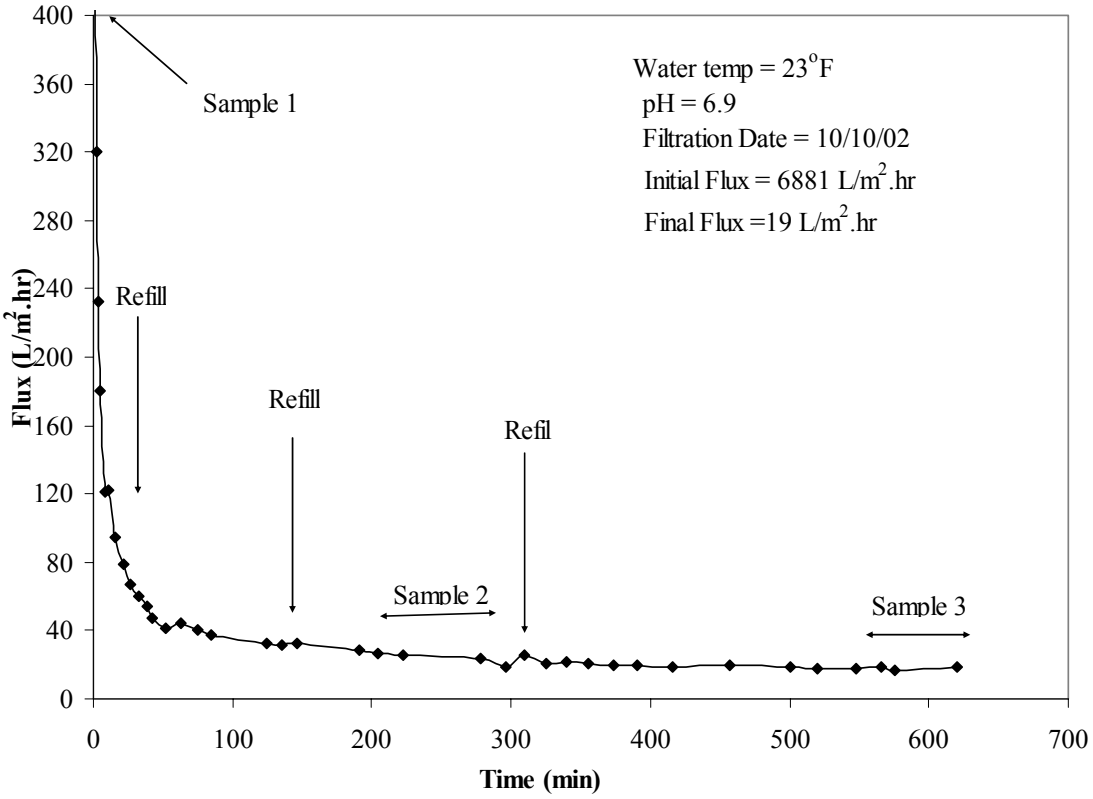

Figure A-37 Variation in permeate flux for PF-0.45 membrane at 2.06 bar

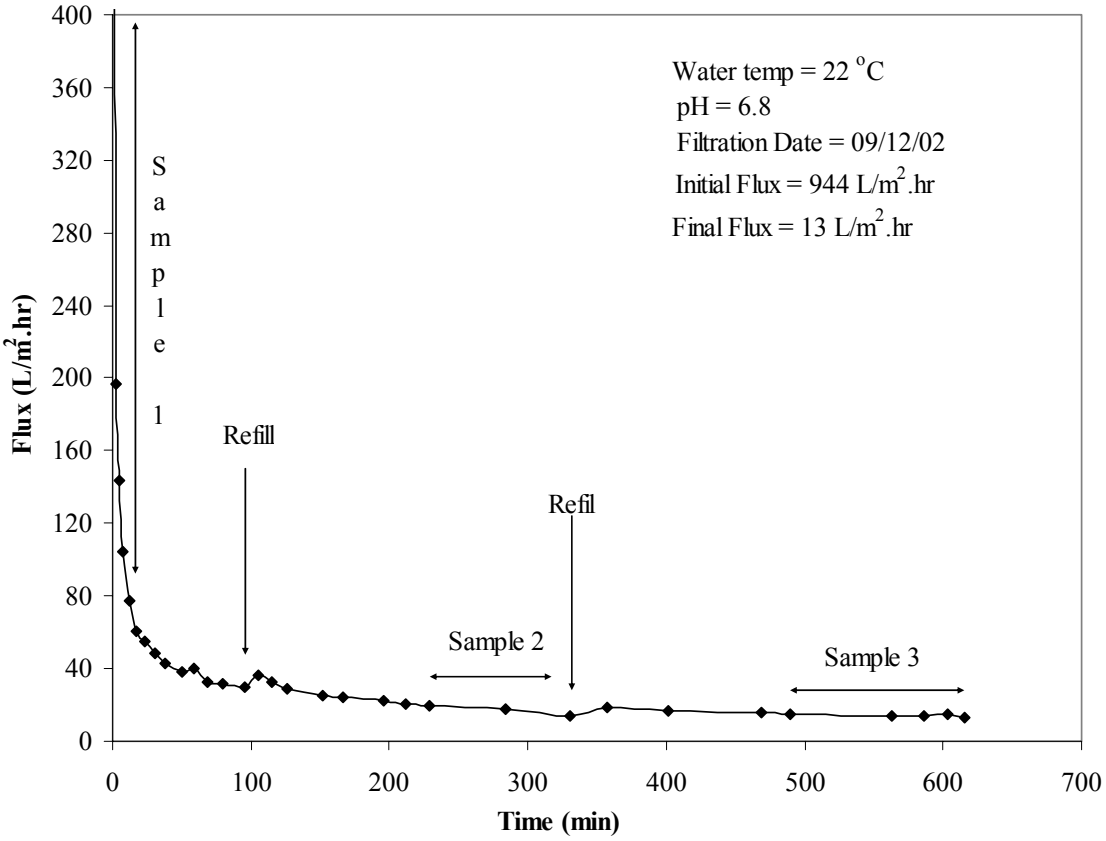

Figure A-38 Variation in permeate flux for PF-0.3 membrane at 2.06 bar

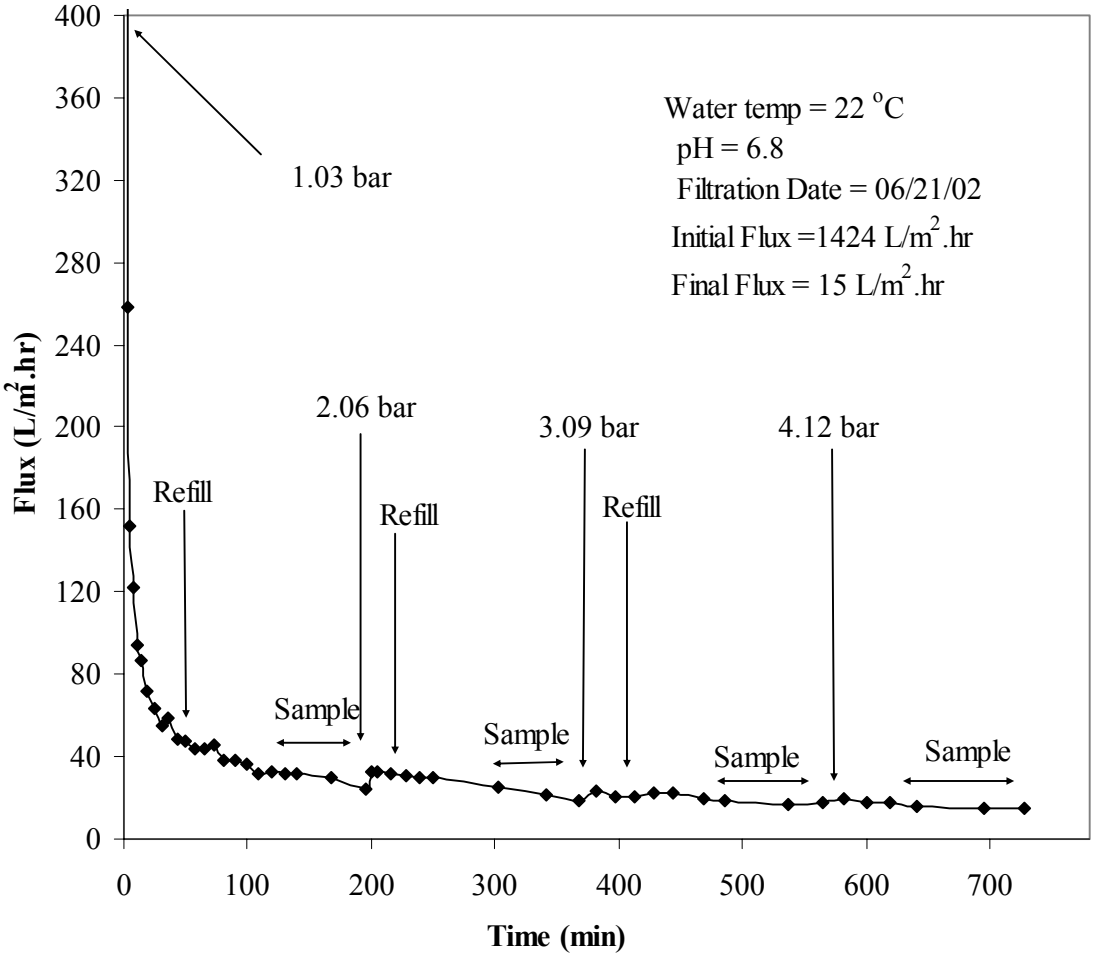

Figure A-39 Variation in permeate flux for AC+0.2 membrane at various pressures

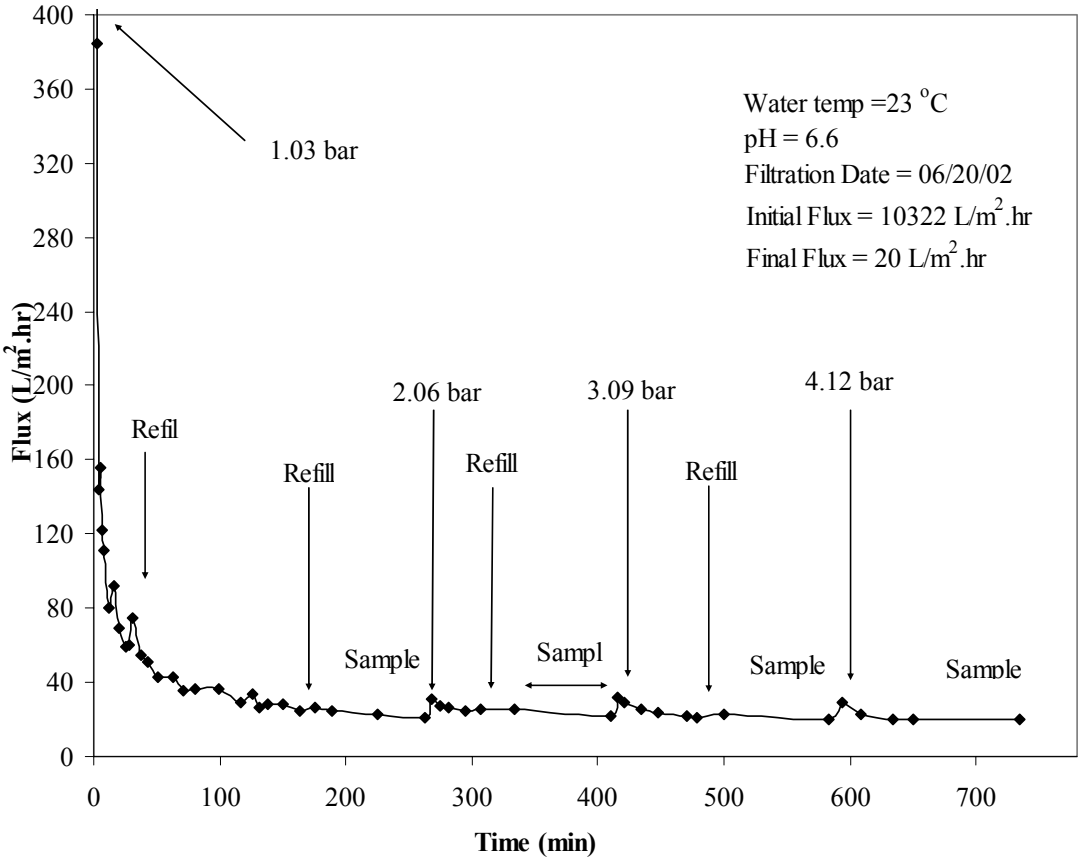

Figure A-40 Variation in permeate flux for AC+0.8 membrane at various pressures

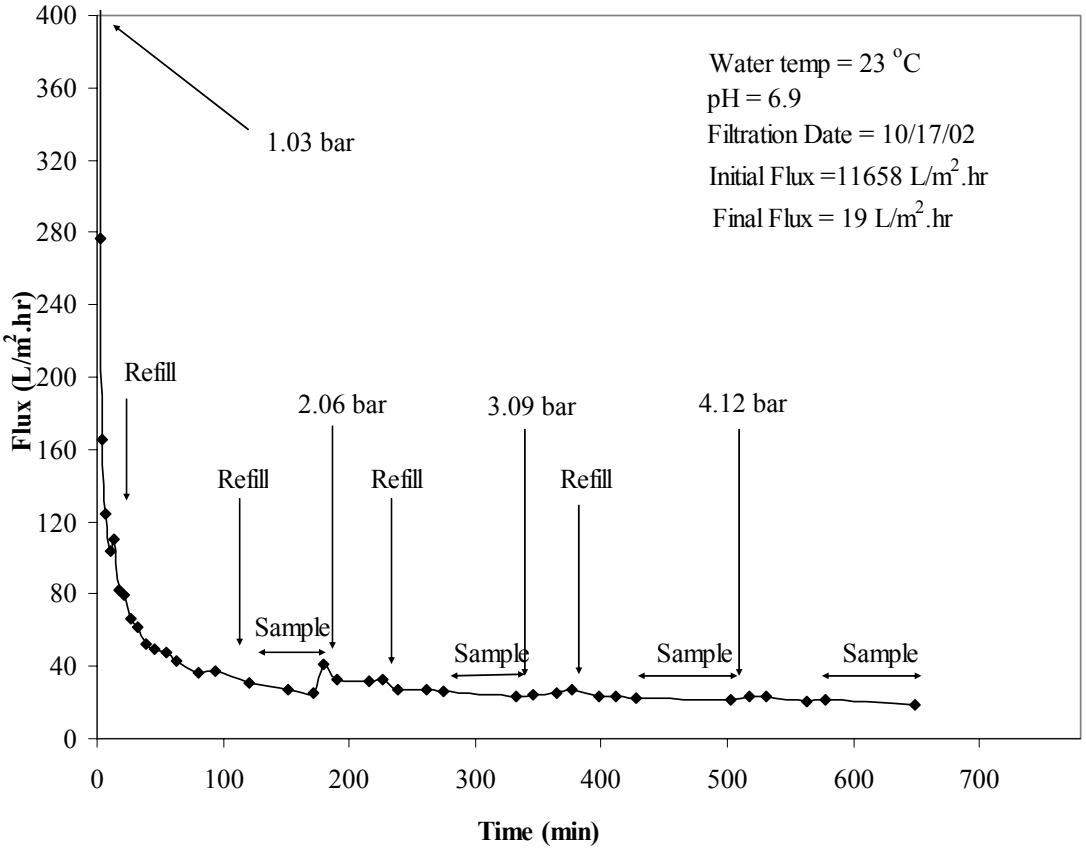

Figure A-41 Variation in permeate flux for PF+0.45 membrane at various pressures

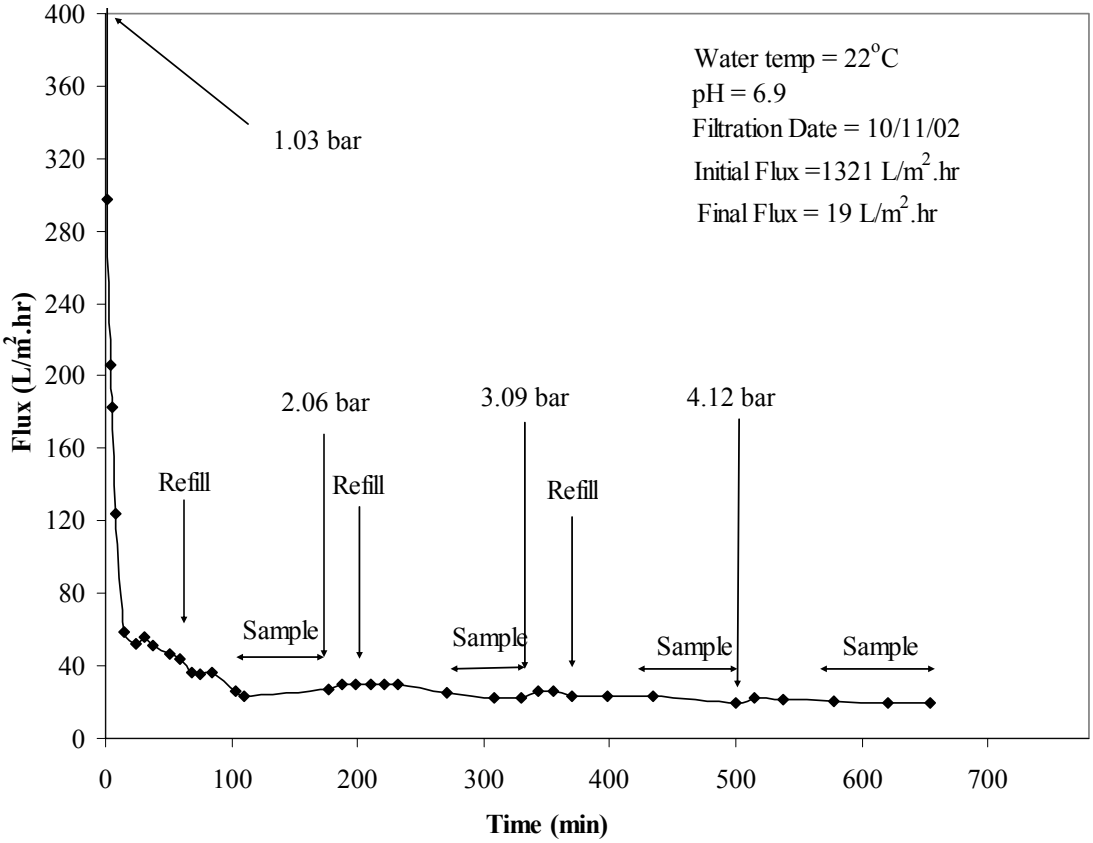

Figure A-42 Variation in permeate flux for PF-0.45 membrane at various pressures

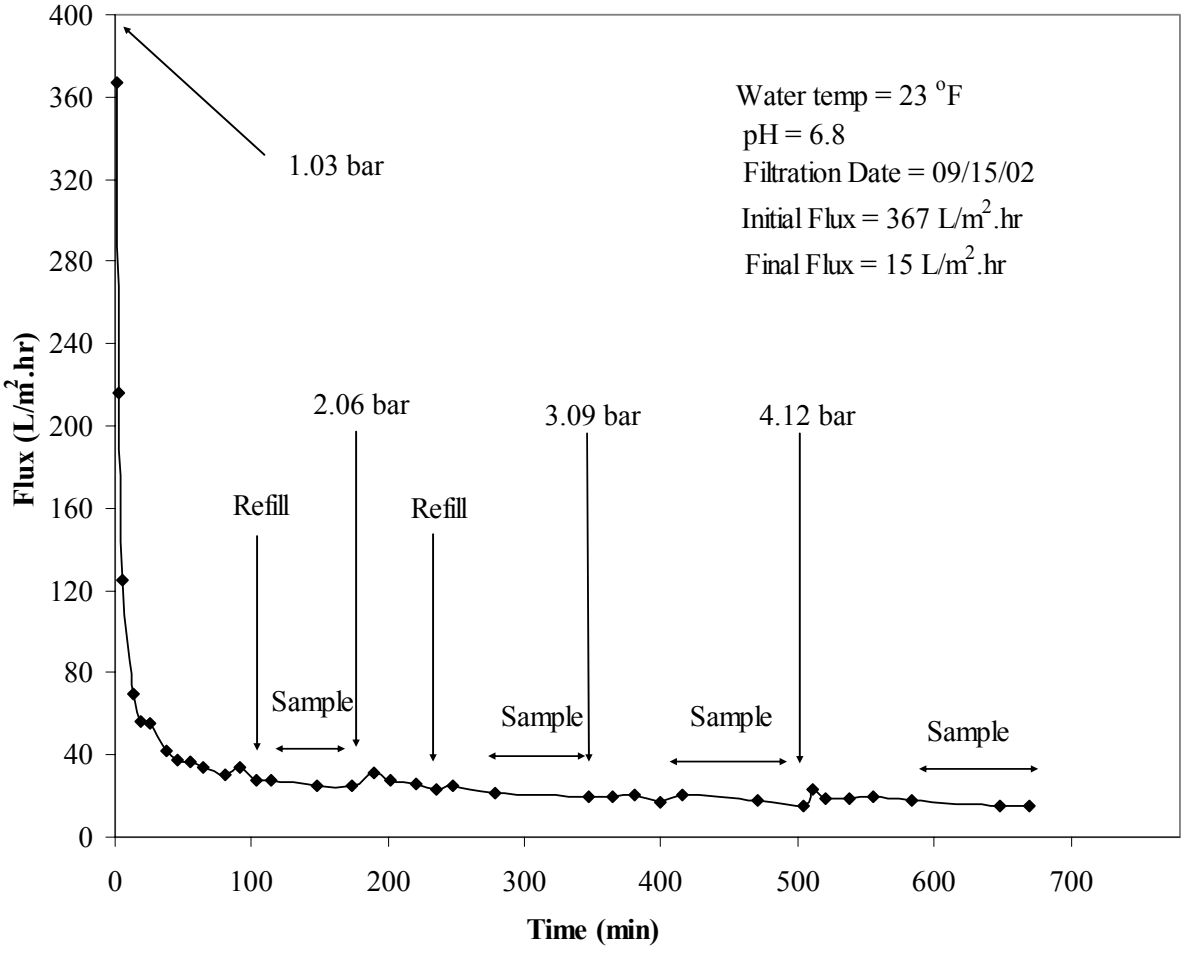

Figure A-43 Variation in permeate flux for PF-0.3 membrane at various pressures

APPENDIX B

COD and Bacterial Permeate Analysis

Table B-21 COD and bacterial permeate analysis for the AC+0.2 membrane

Pressure bar	**Throughput Volume** L/m^2	**Fecal coliforms** cfu/100ml	***E coli*** cfu/100ml	***Enterococci*** cfu/100ml	**COD** mg/l	**Time** minutes
Unfiltered Sample		$2.9x10^6$	$2.5x10^6$	$1.1x10^5$	99.6	-
1.03	0	0	0	0	43.2	0
	200	0	0	0	41.5	285
	281	0	0	0	41.5	540
2.06	0	0	0	0	43.2	0
	220	0	0	0	43.2	273
	303	0	0	0	41.5	517
Various						
1.03	132	0	0	0	43.2	140
2.06	207	0	0	0	41.5	302
3.09	262	0	0	0	41.5	486
4.12	315	0	0	0	41.5	640

Table B-22 COD and bacterial permeate analysis for the AC+0.45 membrane

Pressure bar	**Throughput Volume** L/m^2	**Fecal coliforms** cfu/100ml	***E coli*** cfu/100ml	***Enterococci*** cfu/100ml	**COD** mg/l	**Time** minutes
Unfiltered Sample		$3.3x10^6$	$2.4x10^6$	$1.1x10^5$	39.7	-
1.03	0	0	0	0	30.7	0
	179	0	0	0	28.9	223
	278	0	0	0	25.1	506
2.06	0	0	0	0	30.7	0
	198	0	0	0	27.0	218
	311	0	0	0	25.1	540
Various						
1.03	143	0	0	0	30.7	128
2.06	212	0	0	0	30.7	263
3.09	267	0	0	0	23.1	397
4.12	328	0	0	0	23.1	558

Table B-23 COD and bacterial permeate analysis for the AC-0.45 membrane

Pressure bar	**Throughput Volume** L/m^2	**Fecal coliforms** cfu/100ml	***E coli*** cfu/100ml	***Enterococci*** cfu/100ml	**COD** mg/l	**Time** minutes
Unfiltered Sample		$3.3x10^6$	$2.4x10^6$	$1.1x10^5$	74.7	-
1.03	0	0	0	0	51.5	0
	47	0	0	0	48.3	208
	107	0	0	0	45.0	526
2.06	0	0	0	0	53.2	0
	30	0	0	0	46.6	200
	98	0	0	0	44.9	518
Various						
1.03	8	0	0	0	46.6	52
2.06	43	0	0	0	45.0	292
3.09	127	0	0	0	45.0	481
4.12	198	0	0	0	43.0	623

Table B-24 COD and bacterial permeate analysis for the AC+0.8 membrane

Pressure bar	**Throughput Volume** L/m^2	**Fecal coliforms** cfu/100ml	***E coli*** cfu/100ml	***Enterococci*** cfu/100ml	**COD** mg/l	**Time** minutes
Unfiltered Sample		$3.8x10^6$	$1.5x10^6$	$8.3x10^4$	58.0	-
1.03	0	$2.4x10^5$	$4.5x10^5$	$4.6x10^3$	41.5	0
	204	$3.1x10^4$	$3.1x10^4$	360	41.5	276
	279	$1.7x10^4$	$1.7x10^4$	302	39.7	531
2.06	0	$4.2x10^5$	$2.1x10^5$	$5.2x10^3$	43.2	0
	224	$5.7x10^4$	$2.6x10^4$	800	41.5	250
	315	$4.0x10^4$	$2.5x10^3$	532	41.5	534
Various						
1.03	195	$5.2x10^4$	$1.3x10^4$	228	43.2	189
2.06	253	$9.1x10^4$	$3.3x10^4$	355	41.5	334
3.09	317	$1.3x10^5$	$3.8x10^4$	826	41.5	500
4.12	369	$5.0x10^5$	$5.0x10^4$	992	43.2	651

Table B-25 COD and bacterial permeate analysis for the PF+0.45 membrane

Pressure bar	**Throughput Volume** L/m^2	**Fecal coliforms** cfu/100ml	***E coli*** cfu/100ml	***Enterococci*** cfu/100ml	**COD** mg/l	**Time** minutes
Unfiltered Sample		$2.4x10^6$	$2.0x10^6$	$1.2x10^5$	68.0	-
1.03	0	0	0	0	30.7	0
	195	0	0	0	21.1	242
	289	0	0	0	21.1	545
2.06	0	0	0	0	23.1	0
	227	0	0	0	21.1	230
	332	0	0	0	21.1	545
Various						
1.03	157	0	0	0	21.1	121
2.06	226	0	0	0	21.1	262
3.09	292	0	0	0	19.0	427
4.12	341	0	0	0	19.0	563

Table B-26 COD and bacterial permeate analysis for the PF-0.45 membrane

Pressure bar	**Throughput Volume** L/m^2	**Fecal coliforms** cfu/100ml	***E coli*** cfu/100ml	***Enterococci*** cfu/100ml	**COD** mg/l	**Time** minutes
Unfiltered Sample		$2.4x10^6$	$2.0x10^6$	$1.2x10^5$	70.2	-
	0	0	0	0	35	0
1.03	132	0	0	0	34.4	148
	220	0	0	0	34.4	386
	0	0	0	0	30.7	0
2.06	186	0	0	0	27.7	204
	304	0	0	0	27.7	548
Various						
1.03	102	0	0	0	28.9	110
2.06	176	0	0	0	28.9	271
3.09	240	0	0	0	25.0	434
4.12	289	0	0	0	25.0	578

Table B-27 COD and bacterial permeate analysis for the PF-0.3 membrane

Pressure Bar	**Throughput Volume** L/m^2	**Fecal coliforms** cfu/100ml	***E coli*** cfu/100ml	***Enterococci*** cfu/100ml	**COD** mg/l	**Time** minutes
Unfiltered Sample		$4.9x10^6$	$4.8x10^6$	$2.1x10^5$	85.5	-
1.03	0	331	0	10	58.0	0
	61	30	0	0	54.8	188
	212	10	0	0	52.6	522
2.06	0	700	0	20	54.8	0
	138	17	0	0	53.3	229
	209	0	0	0	51.6	490
Various						
1.03	87	32	0	0	58.0	115
2.06	156	0	0	0	54.8	278
3.09	200	10	10	0	54.8	415
4.12	249	10	10	0	53.3	583

APPENDIX C

Estimation of Cake Thickness and Porosity

Table C-28 Cake thickness and cake resistance for each membrane at 2.06 bar for average suspended particles diameter of 0.1, 0.5 and 1 μm when ψ = 1

Membranes	Final R_c at 2.06bar ($1/m * 10^{10}$)	Final $^1\Delta X_c$(μm) for various particle diameter, d_p (μm)			$^2\Delta X_c$, μm
		0.1	0.5	1	
AC+0.2(PALL)	5766.0	568.0	14208.0	56832.0	17.1
AC+0.45(PALL)	5349.0	526.0	13170.0	52681.0	17.4
AC-0.45(PALL)	8560.0	849.0	21214.0	84857.0	5.9
AC+0.8(PALL)	4527.0	446.0	11151.0	44604.0	18.0
PF+0.45(Millipore)	4975.0	490.0	12259.0	49034.0	18.6
PF-0.45(Millipore)	4109.0	498.0	12444.0	49778.0	17.2
PF-0.3(Osmonics)	6008.0	592.0	14811.0	59243.0	12.5

[1] ΔX_c= calculated cake thickness based on Equation 10, K = 5, ε = 0.4

[2] ΔX_c= maximum possible cake thickness based on a mass balance for suspended solids concentration

Table C-29 Cake thickness and cake resistance for each membrane at 2.06 bar for average suspended particles diameter of 0.1, 0.5 and 1 µm when ψ = 0.1

Membranes	Final R_c at 2.06bar ($1/m * 10^{10}$)	Final $^1\Delta X_c$(µm) for various particle diameter, d_p (µm)			^2DX_c, µm
		0.1	0.5	1	
AC+0.2(PALL)	5766.0	5.7	142.1	568.3	17.1
AC+0.45(PALL)	5349.0	5.3	131.7	526.8	17.4
AC-0.45(PALL)	8560.0	8.5	212.1	848.6	5.9
AC+0.8(PALL)	4527.0	4.5	111.5	446.0	18.0
PF+0.45(Millipore)	4975.0	4.9	122.6	490.3	18.6
PF-0.45(Millipore)	4109.0	5.0	124.4	497.8	17.2
PF-0.3(Osmonics)	6008.0	5.9	148.1	592.4	12.5

$^1\Delta X_c$= calculated cake thickness based on Equation 10, K = 5, ε = 0.4

$^2\Delta X_c$= maximum possible cake thickness based on a mass balance for suspended solids concentration

Table C-30 Required cake porosity at TMP 2.06 bar when ψ = 1

Membrane	Final R_c at ($1/m * 10^{10}$)	$^1\Delta X_c$ (µm)	Porosity, ε_c		
			Diameter of Cake Solids, d_p (µm)		
			0.1	0.5	1
AC+0.2	5766	17.1	0.156	0.057	0.037
AC+0.45	5349	17.4	0.160	0.059	0.038
AC-0.45	8560	5.9	0.100	0.036	0.023
AC+0.8	4527	18.0	0.170	0.063	0.040
PF+0.45	4975	18.6	0.167	0.062	0.040
PF-0.45	4109	17.2	0.173	0.064	0.041
PF-0.3	6008	12.5	0.140	0.051	0.033

$^1\Delta X_c$= calculated cake thickness based on Equation 10, K = 5, ψ = 1

Table C-31 Required cake porosity at TMP 2.06 bar when ψ = 0.1

Membrane	Final R_c at ($1/m * 10^{10}$)	ΔX_c (μm)	Porosity, ε_c		
			Diameter of Cake Solids (μm)		
			0.1	0.5	1
AC+0.2	5766	17.1	0.507	0.232	0.156
AC+0.45	5349	17.4	0.516	0.239	0.160
AC-0.45	8560	5.9	0.367	0.153	0.100
AC+0.8	4527	18.0	0.536	0.252	0.170
PF+0.45	4975	18.6	0.530	0.248	0.167
PF-0.45	4109	17.2	0.541	0.256	0.173
PF-0.3	6008	12.5	0.471	0.211	0.140

[1] ΔX_c= calculated cake thickness based on Equation 10, K = 5, ψ = 1

From Equation 10, $R_c = K(1-\varepsilon_c)^2 S^2_c \Delta X_c / \varepsilon^3_c$

Estimation of cake thickness,

$$\Delta X_c = R_c \varepsilon^3_c / (K S^2_c (1-\varepsilon_c)^2),\ S_c = 6/\psi d_p = 6/(1 \times 0.1 \times 10^{-6})$$

$$= 25 \times 10^{10} \times (0.4)^3 / S^2_c \times 5 \times (1- 0.4)^2$$

$$= 252\ \mu m$$

Estimation of porosity,

$$(1-\varepsilon_c)^2/\varepsilon^3_c = R_c / K S^2_c \Delta X_c,\ S_c = 6/\psi d_p = 6/(1 \times 0.1 \times 10^{-6})$$

$$= 25 \times 10^{10}/(15.8 \times 10^{-6} \times 5 \times S^2_c)$$

Therefore $\varepsilon_c = 0.193$

APPENDIX D

Tables Used for COD Estimation

Table D-32 Low Range Calibration Table 0-150 mg/L COD

MG/L COD VS % TRANSMITTANCE % T, Units										
%T, TENS	**0**	**1**	**2**	**3**	**4**	**5**	**6**	**7**	**8**	**9**
10	--	--	--	--	--	--	--	--	--	--
20	--	--	--	--	--	--	--	--	--	--
30	--	--	--	--	--	0	3.7	7.5	11.3	15
40	18.7	22.2	25.6	28.9	32.1	35.3	38.4	41.4	44.4	47.3
50	50.2	53.0	55.8	58.5	61.2	63.8	66.3	68.8	71.3	73.8
60	76.2	78.6	80.9	83.2	85.5	87.7	89.9	92.1	94.2	96.3
70	98.4	100.4	102.4	104.3	106.2	108.2	110.1	112.0	113.9	115.8
80	117.6	119.4	121.1	122.8	124.5	126.2	127.9	129.6	131.2	132.8
90	134.5	136.1	137.7	139.3	140.9	142.5	144.1	145.6	147.0	148.6

Table D-33 High Range Calibration Table, 0-1500 mg/L COD

MG/L COD VS % TRANSMITTANCE % T, Units										
%T, TENS	**0**	**1**	**2**	**3**	**4**	**5**	**6**	**7**	**8**	**9**
0	--	--	--	--	--	--	--	--	--	--
0	--	--	--	--	--	--	--	--	--	--
20	--	--	1515	1468	1425	1385	1345	1308	1272	1238
30	1203	1170	1138	1107	1077	1048	1020	992	965	940
40	915	890	867	844	821	798	776	754	733	713
50	693	674	655	637	618	599	581	563	545	528
60	512	496	479	463	447	432	417	402	388	374
70	359	345	331	317	303	290	277	264	252	239
80	226	213	201	188	177	165	153	141	130	119
90	108	97	85	74	63	53	42	31	21	10

BIBLIOGRAPHY

1. Al-Malack, M.H., Anderson, G.K., Use of Crossflow Microfiltration in Wastewater Treatment, Water Resource Vol. 31, No. 12, pp. 3064-3072, 1997.

2. Alonso E., Santos A., Solis G.J., Riesco P., "On the feasibility of urban wastewater tertiary treatment by membranes: a comparative assessment," Desalination, Vol. 141(2001), pp 39-51.

3. Asaadi, M., White, D.A., "A model for determining the steady state flux of inorganic microfiltration membranes," The Chemical Engineering Journal, Vol. 48(1992), pp 11-16.

4. Baker, Richard W., Membrane Technolgy and Applications (New York: McGraw-Hill, 2000), pp. 2-7.

5. Barnes G.E., Soil Mechanics; principles and practice (London: Mcmillan Press ltd, 1995).

6. Bungay P.M., Londsdale H.K., de Pinho M.N., ed. Synthetic Membranes: Science, Engineering and Applications, (Dordrecht, D. Reidel Publishing Company, 1983), pp 225-247.

7. Cardew P.T., Le M.S., Membrane process: A Technology Guide(Cambridge: The Royal Society of Chemistry, 1998), pp 7-13.

8. Defrance, L., Jaffrin, M.Y., "Comparison between filtrations at fixed transmembrane pressure and fixed permeate flux: application to a membrane bioreactor used for wastewater treatment," Vol. 152(1999), pp 203-210.

9. Fan L., Harris J.L., Roddick F.A., Booker N.A., "Influence of the characteristics of natural organic matter on the fouling of microfiltration membranes," Vol. 35(2001), pp 4455-4463.

10. Gan, Q., "Evaluation of solids reduction and backflush technique in crossflow microfiltration of a primary sewage effluent," Resources, Conservation and Recycling, Vol. 27,(1999), pp. 9-14.

11. Gan Q., Field R.W., Bird M.R., England R., Howell J.A., McKechne M.T., O'Shaughnessy C.L, "Beer clarification by crossflow microfiltration: fouling mechanisms and flux enhancement," Institute of Chemical Engineers, Vol. 75(1997), pp 3-8.

12. Gary Yakub, Personal Communication, ALCOSAN, April 2003.

13. Greenberg A.E., Clesceri L.S., ed., Standard Methods for the Examination of Water and Wastewater, (18th Edition, Washington D.C., APHA, AWWWA, WEF, 1992).

14. Ho, W.S., Sirkar, K.K., Membrane Handbook, (New York: Van Nostrand Reinhold, 1992), pp 457-477.

15. Hong, S., Faibish, R.S., Elimelech, M., "Kinetics of permeate flux decline in crossflow membrane filtration of colloidal suspensions," Journal of colloid and interface science, Vol.196 (1997), pp 267-277.

16. Judd S.J., Till S.W., "Bacterial rejection in crossflow microfiltration of sewage," Desalination, Vol. 127(2000), pp 251-260.

17. Metcalf and Eddy, Waste Water Engineering; Treatment, Disposal, and Reuse, (4th Edition; Irvin/McGraw-Hill, Boston, Massachusetts, 2003) pp.104-191, pp.1035-1622.

18. Mueller J., Davis H.D., "Protein fouling of surface-modified polymeric microfiltration membranes," Journal of membrane Science, Vol. 116(1996), pp 47-60.

19. Mulder, M., Basic Principles of Membrane Technology, (2nd edition. Dordrecht: Kluwer Academic Publishers, 1991), pp. 206-208.

20. Nunes S.P., Peinemann K.-V., ed. Membrane Technology in Chemical Industry, (Weinheim, Wiley-VCH, 2001), pp 3-7.

21. Parameshwaran, K., Fane, A.G., Cho, B.D. and Kim, K.J., "Analysis of Microfiltration Performance with Constant Flux Processing of Secondary Effluent," Water Resources, Vol. 35, No 18(2001), pp. 4349-4358.

22. Slack J., Nemura A., (2000) Evolving Wet Weather and Water Quality Standards Issues for CSO Communities. WEFTEC 2000: Surface Water Quality and Ecology Symposium I: Wet Weather CSO issues, Water Environment Federation 73rd Annual Conference & Exposition on Water Quality and Wastewater Treatment, Anaheim, CA, October 14-18, 2000.

23. Till S.W., Simon J.J., Mcloughlin B., "Reduction of fecal coliform bacteria in sewage effluents using microporous membrane," Water Resources, Vol. 32, No 5(1998), pp 1417-1422.

24. U.S. Environmental Protection Agency (1986) Ambient Water Quality Criteria for Bacteria, EPA440/5-84-002, Washington, D.C.

25. U.S. Environmental Protection Agency (1994) Combined Sewer Overflow (CSO) Control Policy; Federal Register Vol. 59 No. 75, FR Doc. 94-9295.

26. U.S. Environmental Protection Agency (2001) Report to Congress Implementation and Enforcement of the Combined Sewer Overflow Control Policy; EPA-833-R-01-003, Washington D.C.

27. Vyas H.K., Mawson A.J., Bennet R.J., Marshall A.D., "A new method for estimating cake height and porosity during crossflow filtration of particulate suspensions," Journal of Membrane Science, Vol. (2000), pp 113-119.

28. www.millipore.com

29. www.pall.com

30. Zeman, L.J., Zydney, A.L. Microfiltration and Ultrafiltration: Principles and Applications, (New York: Marcel Dekker, INC. 1996), pp 450.